



**Politecnico
di Torino**

ScuDo

Scuola di Dottorato ~ Doctoral School

WHAT YOU ARE, TAKES YOU FAR

Doctoral Dissertation
Doctoral Program in Architectural and Landscape Heritage (34th Cycle)

Methodological approaches to the condition assessment of reinforced concrete architectural heritage

By

Valerio Oliva

Supervisor:

Prof. R., Ceravolo

Doctoral Examination Committee:

Prof. A., Bovsunovsky, National Technical University of Ukraine, Kiev, Ukraine

Prof. D., Abruzzese, Università di Roma Tor Vergata, Italy

Politecnico di Torino

2022

Declaration

I hereby declare that, the contents and organization of this dissertation constitute my own original work and does not compromise in any way the rights of third parties, including those relating to the security of personal data.

Valerio Oliva

2022

You are unique!

Acknowledgment

I would like to thank my supervisor, Prof. Rosario Ceravolo, for patiently guiding me with his experience throughout my PhD program: this project would not have been possible without your support.

I would also like to thank Giorgia, Gaetano, Stefania, Linda, Erica, Giulia, Giovanni and Marco for the fun moments and the efforts shared together in these years: thanks for always supporting and encouraging me.

I would also like to thank all my dear colleagues I met during these years at Politecnico di Torino, Università di Catania and during the collaboration with the engineering firms EP&S and Kelse Engineering.

I would also like to thank all my friends, in particular Andrea L. B., Cesare, Giulia, Seby, Andrea P., Chiara, Pierluca, Ilenia, Stefano, Flaminia, Gabriele, Ruggero, Caterina, Marcello, Antonio, Giuseppe, Sara, Lorenzo, Arianna, Shahry, Ciccio, Fabio, Gabriel, Gigi, Cristiano: thanks for always being there during the enjoy and the hard times.

Finally, I would like to express my deep gratitude to my family: my brothers Fabio, Andrea and Giuseppe; and my sisters Eliana and Mariella; my brother and sisters in law Maurizio, Maria and Susana; my nephews and nieces; my cousins and my uncles: thanks for being my main motivation.

Abstract

The condition assessment of reinforced concrete architectural heritage represent a question of maximum priority that requires more and more attention from architects and engineers. A significant portion of this heritage is nearing the end of its useful life and, therefore, issues related to its conservation should be addressed. Numerous theoretical and experimental researches has been developed in this field in the last years, in order to provide new methodological approach for the conservation of 20th century concrete heritage buildings. This effort resulted in important documents, including deontological standards, guidelines, and regulations.

The specific challenges posed in preserving historic concrete structures are varied and complex. In fact, the strategies to be implemented must take into account the pioneering nature of both construction techniques and structural forms used at that time. The continuous experimentation that has characterized the construction of these buildings causes a difficult understanding of their structural behavior.

The condition assessment, based on Structural Health Monitoring (SHM) and calibrated FE Models, play a fundamental role in the conservation field of 20th century historic concrete structures, especially in identifying structural damages and degradation states. Appropriate strategies and criteria are needed to meet the preservation and conservation challenges of this heritage. In particular, to pursue the conservation principles, optimal strategies based on a correct maintenance, structural health monitoring and non-destructive techniques are preferable.

Experimental activities are part of the operations aimed at determining the state of conservation of the building and predicting its response to accidental actions. To this aim, structural models calibrated based on the experimental results represent a useful tool. In the case of heritage structures, non-invasive techniques are of paramount interest, especially natural vibration-based monitoring.

However, the condition assessment of reinforced concrete architectural heritage raises several unresolved issues. Moreover, a part of this heritage (including buildings, bridge and other civil engineering structures) has been built with the prestressed concrete technique. In this context, post-tensioned concrete structures are very sensitive to natural deterioration and excessive environmental attacks, which can lead to insufficient safety levels. Unfortunately, the partial rupture or corrosion of pre-stressing tendons may be difficult to detect.

The overall aim of this PhD research is to propose methodological approaches, based on experimentally calibrated models, for the static and seismic condition assessments of reinforced concrete heritage structures. The research focuses on how the information coming from experiments can be integrated into a numerical model, which simulate the behavior of the structure and represent a useful tool for a refined condition assessment. In this context, particular attention is paid to the uncertainties in geometry, material characteristics, details, constraints, and the interaction with the surrounding environment that can significantly increase the complexity of the identification and model calibration of the structures.

Under these premises, an historical prestressed concrete structure has been proposed as a case study. In particular, Pavilion V of Turin Exhibition Center, built by Riccardo Morandi in the late 50s, has been selected for its post-tensioned system characterized by a complex spatial design.

Contents

1. Introduction.....	1
1.1 Focus of the thesis	1
1.2 Structure of the thesis	4
2. XX century reinforced concrete heritage.....	6
2.1 The reinforced concrete: from the first applications to the reconstruction and economic growth	6
2.2 Construction possibilities of reinforced concrete in spatial structures ..	12
2.3 Durability problems of reinforced concrete.....	14
2.4 Diagnosis of reinforced concrete structures	15
2.4.1 Concrete strength	16
2.4.2 Reinforcement strength and disposition	18
2.4.3 Assessment of durability.....	18
3. Prestressed concrete systems: diagnosis and conservation.....	20
3.1 Prestressed concrete: first developments.....	20
3.2 Construction possibilities and different types of prestressed concrete..	25
3.2.1 Pretensioned concrete	25
3.2.2 Post-tensioned concrete	26
3.2.3 The importance of a correct grout injection in post-tensioned concrete.....	27
3.2.4 Unbonded post-tensioned construction.....	29
3.2.5 Circular prestressing	30
3.2.6 External prestressing.....	30

3.3	Grout deficiencies and problems of early prestressed concrete	31
3.4	Diagnosis of post-tensioned concrete structures	32
4.	Preservation, retrofit, and reuse of modern heritage structures and case studies	35
4.1	Conservation of the XX century modern architecture.....	35
4.2	Issues in the conservation of concrete heritage structures.....	37
4.3	Case studies	39
4.3.1	Paraboloide of Casale Monferrato: an outstanding example of historical thin shell concrete structure	42
4.3.2	Example of vibration-based structural health monitoring of a reinforced concrete arch bridge	47
5.	Structural and seismic safety evaluation methods: a critical review for modern heritage structures	52
5.1	Evolution of structural safety codes and regulations.....	53
5.2	Structural safety methods	58
5.2.1	Deterministic method.....	59
5.2.2	Semi-probabilistic method.....	60
5.2.3	Probabilistic method	61
5.2.4	Exact probabilistic method	63
5.2.5	Simplified probabilistic method.....	64
5.3	Safety assessment of modern heritage structures	66
5.3.1	Historical analysis.....	68
5.3.2	Geometry	68
5.3.3	Construction details	69
5.3.4	Materials	70
5.3.5	Level of knowledge and confidence factors	70
5.3.6	Levels of evaluation and performance-based approach for heritage buildings	71
5.3.7	Safety indexes for heritage buildings.....	73

5.3.8	Structural health monitoring of heritage structures	74
5.4	Models for the condition assessment of modern heritage buildings	76
6.	Case study application: Pavilion V of Turin Exhibition Center	81
6.1	Review of available documentation and building's history and identify the structural conception	83
6.2	Preliminary investigation.....	105
6.3	Creation of the preliminary model.....	110
6.4	Structural assessment.....	111
6.5	Preliminary structural analysis	112
6.6	Investigations on the post-tensioned reinforced concrete system	114
6.7	Preliminary sensitivity analysis	115
6.8	Preliminary seismic analysis	118
6.9	Design detailed investigation strategy.....	119
6.10	Analysis and processing of the dynamic tests	121
6.11	Parametric study for modal identification of structures with interacting diaphragms	125
6.12	Corroboration of the FE model.....	137
6.13	Structural reassessment based on the corroborated model	141
6.14	Probabilistic estimation of the safety margin level of the post-tensioned systems	144
6.15	Sensitivity analysis of the environmental effect on the modal parameters	145
7.	Methodological approaches to the condition assessment of reinforced concrete heritage structures	152
7.1	Reinforced concrete heritage structures	152
7.2	Early post-tensioned concrete structures	157
	Conclusions.....	162
	References.....	166

List of Figures

Figure 1: Some early patent reinforcement systems (Jones, 1920).....	7
Figure 2: Calculation scheme for Monier slab proposed by Köenen in 1886: δ is the thickness of the slab; F_e is the reinforcements area; k is the concrete compressive strength, k_t is the tensile strength of bars (Iori, 2001)	8
Figure 3: Hennebique calculation hypothesis in 1892 for a beam with bending moment action (Iori, 2001)	9
Figure 4: Hypothesis of the “homogeneous section” formulated by Coignet and de Tédesco in 1894 (Iori, 2001).....	10
Figure 5: The Risorgimento Bridge in Rome, Italy. (https://en.wikipedia.org/wiki/Ponte_del_Risorgimento).....	11
Figure 6: Exhibition Hall B in Turin, Italy (Levi & Chiorino, 2004)	13
Figure 7: Principle of potential measurement for ongoing corrosion in reinforced concrete structures (Beckmann & Bowles, 2004).....	19
Figure 8: Italian patent n. 283075 by E. Freyssinet and J. Séailles: Processo di fabbricazione di pezzi in cement armato, October 1st 1929 (Archivio Centrale dello Stato).....	21
Figure 9: Prestressing patent by Dischinger in 1934 (Guidi 1947).....	21
Figure 10: Italian patent n. 383586 by G. Colonnetti: Trave armata ad armature preventivamente tesa. December 12th 1939. (Archivio Centrale dello Stato)	22
Figure 11: Italian patent n. 389946 by G. Colonnetti: Dispositivo per la messa in tensione e l’ancoraggio delle armature nelle strutture in conglomerato cementizio, March 3rd 1941. (Archivio Centrale dello Stato)	23
Figure 12: Underground exhibition hall in Turin, Italy	24
Figure 13: Pretensioning process. (a) Steel tensioning. (b) Element cast and matured. (c) Steel cutting (Gilbert, Mickleborough, & Ranzi, 2017).....	26

Figure 14: Tendon layout and detail in a continuous post-tensioned system (Gilbert, Mickleborough, & Ranzi, 2017)	27
Figure 15: General knowledge-based strategy for the study and assessment of Cultural Heritage buildings.....	41
Figure 16: A photo showing the construction of the clinker warehouse named Paraboloid (Santarella, 1926).....	42
Figure 17: Paraboloid of Casale Monferrato: external (left) and internal (right) views	42
Figure 18: Original drawing reported in Santarella’s manual (Santarella, 1926): silos project for clinker warehouse in Casale Monferrato. Designer Eng. Radici.	43
Figure 19: Structural deterioration and damage: (a) water staining and bio growth on the elements; (b) a detail of the exposed bars of a parabolic arch; (c) exposed bars on the arches; (d) exposed bars and detachments of concrete of the roof elements (Lenticchia, Miraglia, Quattrone, & Ceravolo, 2021)	44
Figure 20: Axonometric scheme of the structure showing sensor positioning in Setup 1 (a) and Setup (2) (Lenticchia, Miraglia, Quattrone, & Ceravolo, 2021) ..	45
Figure 21: Horizontal components plots of the main identified modes of the Paraboloid: (a) first mode; (b) second mode (Lenticchia, Miraglia, Quattrone, & Ceravolo, 2021)	45
Figure 22: First two mode shapes from the updated numerical model: (a) first mode; (b) second mode; (c) first mode compared with the experimental identified; (d) second mode compared with the experimental identified (Lenticchia, Miraglia, Quattrone, & Ceravolo, 2021)	47
Figure 23: Lamberti bridge over the Ceno river (a); joint connecting two spans (b).....	48
Figure 24: Mono-axial accelerometers (a); LVDT at joint (b).....	48
Figure 25: Acquisition setups for the dynamic characterization of Lamberti bridge (Ceravolo, et al., 2019)	49
Figure 26: Dynamic characterization of Lamberti bridge with Setup 2-bis: clustering diagram with stable frequencies in blue colour (Ceravolo, et al., 2019)	49
Figure 27: Schematic representation of the first four experimental modal shapes (Ceravolo, 2020)	50

Figure 28: Lamberti bridge: results of the model updating process (Ceravolo, 2020)	51
Figure 29: Reinforced concrete buildings period of construction in Italy - census 2001 - (Elefante, 2009)	66
Figure 30: Turin Exhibition Center, underground Pavilion by Riccardo Morandi: general views	83
Figure 31: Qualitative comparison of the bending moment between simply supported beam (a), balanced beam with lateral cantilevers (b), and balanced beam with subtended tie elements (c)	84
Figure 32: Bridge over the Cerami, Enna, 1953-1954: general view (Boaga, 1984).....	85
Figure 33: Bridge over the Cerami, Enna, 1953-1954: longitudinal half section (Boaga, 1984).....	85
Figure 34: Via Olimpica overpass, Rome, 1958-1959: bottom view (Boaga, 1984)	86
Figure 35: Via Olimpica overpass, Rome, 1958-1959: longitudinal half section (Boaga, 1984).....	86
Figure 36: Post-tensioning cables of the Pavilion V balanced beam (half section) from a drawing in Morandi's documents (Morandi, 1959).....	86
Figure 37: Construction detail of the shorter strut beam connection with rib and retaining wall (Boaga, 1984)	87
Figure 38: Construction details of the inclined longer strut beams and the connection elements with the ribs (Boaga, 1984).....	87
Figure 39: The static scheme of the Pavilion V balanced beam from a sketch inside Morandi's calculation report (Morandi, 1959).....	88
Figure 40: Scheme of the plan of Morandi's Pavilion V showing the division into three block linked by joints	88
Figure 41: Details of the expansion joint: (a) between the roof and the ribs; (b) between the shorter strut beams and the retaining walls	89
Figure 42: Turin Exhibition Center, underground Pavilion by Riccardo Morandi: internal view with ribs arrangement	89

Figure 43: Intersection of the thin ribs creating a dovetail geometry: (a) general section (Bonadè Bottino & Morandi, 1959); (b) detail of the restraints of the shorter strut beams (Boaga & Boni, 1962)	90
Figure 44: Section B-B from the original drawings in Morandi's documents (Bonadè Bottino & Morandi, 1959).....	91
Figure 45: Roof plan from the original drawings in Morandi's documents (Bonadè Bottino & Morandi, 1959).....	92
Figure 46: Generic cross section of the ribs with cables from the original drawings in Morandi's documents (Bonadè Bottino & Morandi, 1959).....	92
Figure 47: Scheme with the sections of the generic rib from the original drawings in Morandi's documents (Bonadè Bottino & Morandi, 1959).....	93
Figure 48: Service area, section B-B from the original drawings in Morandi's documents (Bonadè Bottino & Morandi, 1959)	94
Figure 49: Service area, extract of the foundations plan at -6.68 m from the original drawings in Morandi's documents (Bonadè Bottino & Morandi, 1959) .	94
Figure 50: Disposition of the reinforcement of retaining wall from the original drawings in Morandi's documents (Bonadè Bottino & Morandi, 1959).....	95
Figure 51: Disposition of the reinforcement of service area walls from the original drawings in Morandi's documents (Bonadè Bottino & Morandi, 1959) .	95
Figure 52: View of the closed stiffening box system between for the external pair of ribs (Boaga, 1984).....	96
Figure 53: External ribs, extract floor plan from the original drawings in Morandi's documents (Bonadè Bottino & Morandi, 1959).....	97
Figure 54: External ribs, section P-P with cables and details from the original drawings in Morandi's documents (Bonadè Bottino & Morandi, 1959).....	97
Figure 55: External ribs detail, section T-T from the original drawings in Morandi's documents (Bonadè Bottino & Morandi, 1959).....	98
Figure 56: External ribs, extract floor plan with cables arrangement from the original drawings in Morandi's documents (Bonadè Bottino & Morandi, 1959) .	98
Figure 57: Elevation of Morandi's Pavilion V with a view of the façade along the short side of the structure (Bonadè Bottino & Morandi, 1959)	99
Figure 58: Internal view of the pavilion after the insertion of the fire walls	100

Figure 59: View of the construction site of Pavilion V of Turin Exhibition Center, 1959.....	101
Figure 60: View of the construction site of Pavilion V of Turin Exhibition Center, 1959.....	102
Figure 61: Photography of Pavilion V construction site: longer strut beams	104
Figure 62: Photography of Pavilion V construction site: retaining walls	104
Figure 63: Photography of Pavilion V construction site: retaining walls	105
Figure 64: Pavilion V: Test positions at the underground floor (MASTRLAB DISEG, 2019)	106
Figure 65: Pavilion V: Test positions at the roof level (MASTRLAB DISEG, 2019).....	106
Figure 66: Pavilion V: Extraction of a concrete sample from a longer strut beam (left); carbonation tests on the samples of the ribs (center); view of the static tests with trucks connected to the ribs through jacks (right) (MASTRLAB DISEG, 2019)	109
Figure 67: Pavilion V: normalized vertical displacements measured during the static test on a rib (MASTRLAB DISEG, 2019)	110
Figure 68: Pavilion V: geometric model (left) and detail of the FE model at the ribs (right)	111
Figure 69: Concrete compression strength in a post-tensioned rib of Pavilion V as a results of 2019 campaign: prior and posterior probability density function (PDF) (left) and cumulative density function (CDF) (right)	112
Figure 70: Scheme with vertical offset from Morandi’s calculation report (a) and bending moment (kNm) acting on a rib as resulting from Morandi’s scheme; (b) due to the permanent loads; (c) due to post-tensioning effect of the shorter strut beams; (d) due to the imposed crowd loads (Morandi, 1959)	113
Figure 71: Visual inspection of post-tensioning tendons in the ribs (left), and endoscopy inspection inside a duct of the rib (right) (MASTRLAB DISEG, 2019)	115
Figure 72: Sensitivity analysis conducted on the rib element: the ultimate load multiplier (for bending moment verification) on Morandi’s scheme as a function of corroded post-tensioning steel area in the rib at midspan (a), at the supports (c) and of the positioning error (in percent of the effective depth) in the vertical direction	

of tendons respect to the extrados of the rib at midspan (b), respect to the intrados of the rib at the supports (d).....	117
Figure 73: Sensitivity analysis conducted at midspan of the rib element: the ultimate load multiplier (for bending moment verification) on Morandi’s scheme as a function of both corroded post-tensioning steel area in the rib ($A_{r,corr}$) and corroded post-tensioning steel area in the shorter strut beams ($A_{sb,corr}$).....	118
Figure 74: Critical elements of the Pavilion V: longer strut beams (left) and shorter strut beams (right).....	119
Figure 75: Accelerometers configurations for setup 1 (Ceravolo, Coletta, Lenticchia, Minervini, & Quattrone, 2020)	120
Figure 76: Accelerometers configurations for setup 2 (Ceravolo, Coletta, Lenticchia, Minervini, & Quattrone, 2020)	121
Figure 77: Identified vertical mode of the South block with setup 2: stability diagram with power spectrum density (PSD) curves of the considered signals (left) and clustering diagram (right).....	123
Figure 78: Identified horizontal mode of the South block with setup 1: stability diagram with power spectrum density (PSD) curves of the considered signals (left) and clustering diagram (right).....	123
Figure 79: Identified mainly horizontal modes of the South block: (a) $f=3.20$ Hz: translational mode in transverse direction; (b) $f=3.60$ Hz: torsional mode; (c) $f=5.62$ Hz: translational mode in longitudinal direction	124
Figure 80: Lumped mass model of the interacting i -th diaphragm	127
Figure 81: Lumped mass model of three adjacent interactive diaphragms...	128
Figure 82: Variation of the modes and of the natural frequencies of the system from 1 to 3 as a function of $kvar$	130
Figure 83: Variation of the modes and of the natural frequencies of the system from 4 to 6 as a function of $kvar$	130
Figure 84: Variation of the modes and of the natural frequencies of the system from 7 to 9 as a function of $kvar$	131
Figure 85: Re-ordering of modes: (a) modes 3 and 4; (b) modes 6 and 7	132
Figure 86: Measured acceleration responses for setup 1: (a) time-domain; (b) frequency-domain	133

Figure 87: Stabilization (a) and clustering (b) diagram of the identification performed on the sixth sub-signal of setup 1 of the entire Pavilion V, with evidence of the mode at 2.57 Hz.....	134
Figure 88: Horizontal component of the mode shape identified at 2.57 Hz .	135
Figure 89: Objective function for a variation of $kvar, left$ and $kvar, right$ in the range between 0 and 1.....	136
Figure 90: Objective function for a variation of $kvar, left$ and $kvar, right$ in the range between 0 and 1×10^{-3}	137
Figure 91: Modes of the updated FE model: (a) horizontal (with roof bending) modes; (b) mainly vertical modes; (c) mainly translational modes in longitudinal direction	140
Figure 92: Bending moment diagrams (kNm) on a rib resulting from the updated FE model: due to the permanent loads (a); due to the imposed crowd loads (b).....	141
Figure 93: Sensitivity analysis conducted at midspan of the rib element with the calibrated FE model: the ultimate load multiplier (for bending moment verification) as a function of both corroded post-tensioning steel area in the rib ($A_{r,corr}$) and corroded post-tensioning steel area in the shorter strut beams ($A_{sb,corr}$).....	142
Figure 94: Sensitivity analysis conducted on the considered system composed of 4 ribs: ultimate load multipliers (for bending moment verification) with the updated FE model as a function of corroded post-tensioning steel area in the different ribs at midspan (a) and at the support (b).....	143
Figure 95: Sensitivity analysis conducted on the considered system composed of 4 ribs: ultimate load multipliers (for bending moment verification at midspan) with the updated FE model as a function of both corroded post-tensioning steel area in the ribs ($A_{r,corr,midspan}$) and corroded post-tensioning steel area in the different pairs of shorter strut beams (sb)	144
Figure 96: Flowchart for inspection process of post-tensioned systems.....	145
Figure 97: FEM of Morandi's Pavilion V.....	148
Figure 98: Temperature-frequencies relationships for different scenarios of effectiveness of joints	150
Figure 99: Temperature-frequencies relationships for an intermediate range between two significant magnitude orders	150

Figure 100: Flowchart illustrating the entire concrete conservation process, combining best practices in concrete repair and conservation processes (Macdonald & Arato Gonçalves, 2020)	153
Figure 101: Flowchart illustrating the methodology for the condition assessment of concrete structures	156
Figure 102: Flowchart illustrating the methodology for the condition assessment of early post-tensioned concrete structures	158

List of Tables

Table 1: Evolution of the allowable stress for mild steel structures in the USA (Blockley, 1992)	60
Table 2: Results of concrete compression tests: average depth h , average diameter d , ratio h/d , ultimate load F , compressive strength f_c and average carbonation depth c (MASTRLAB DISEG, 2019).....	108
Table 3: Comparison between ultimate load multipliers (with respect to bending moment verification at midspan and at the supports) calculated: at the design stage ($RD39$); at the design stage with the current standards (EC); at the reassessment stage during construction ($REASS 1959$); at the reassessment stage in 2019 ($REASS 2019$). μ and σ represent the mean and standard deviation assumed for the concrete compression strength	114
Table 4: Comparison between the frequencies (f_{EXP}) identified for the three blocks of the pavilion.....	125
Table 5: Comparison between the damping (ζ_{EXP}) identified for the three blocks of the pavilion.....	125
Table 6: Numerical values of parameters.....	129
Table 7: Identified modes of the entire pavilion	134
Table 8: Values of the elastic moduli as resulting from the mechanical tests	138
Table 9: Values of the elastic moduli before and after the updating based on the results of the dynamic tests.....	139
Table 10: Predicted natural frequencies (f_{FEM}) by the updated FE model. Experimental values are reported in Table 4	139
Table 11: Values of the elastic moduli of the FE model in the sensitivity analysis.....	147
Table 12: Natural frequencies of the FE model used for the sensitivity analysis	148

Chapter 1

Introduction

1.1 Focus of the thesis

According to (Aktan, Lee, Chuntavan, & Aksel, 1994), condition assessment can be defined as the measure and the evaluation of the current state for a constructed facility in terms of indices such as flexibility/stiffness, damping, toughness against fatigue, resistance to deterioration mechanisms and aging, and, the available strength, deformability and energy dissipation capacities under the probable failure modes. Condition assessment includes identifying any design, construction or maintenance errors as well as any local defects, deterioration and damage such that the global state of health, i.e. the structural reliability of the facility may be established for rational management decisions.

The present PhD research is part of the extremely topical line of the condition assessment aimed at the conservation of the architectural heritage of the 20th century; a heritage of great importance but which is threatened by several problems, starting with the difficult recognition of their historical documental value by non-experts. The reinforced concrete architectural heritage consists of a great variety of buildings, bridges and other civil structures, in terms of typology, construction techniques etc.

This fragile legacy is strongly threatened by corrosion phenomena, amplified by the lack of specific knowledge on concrete durability at that period. Moreover, a large part of these structures is designed based on construction standards that did not include any anti-seismic measures. For this reason, seismic risk is certainly a

part of these threats. To this, it must be added the potential decline of the safety levels due to a progressive structural degradation caused by poor maintenance.

Moreover, numerous of these building and bridges have been built with the prestressed concrete technique, in which the tendons constitute the main load-carrying elements. Over time, these structures are increasingly subjected to adverse effects due to corrosion. The deterioration problems raise serious concerns about the long-term durability of these structures with possible sudden and fatal consequences. This is particularly true for early post-tensioned systems, which are becoming part of the concrete architectural heritage, and for which problems of corrosion may be accelerated by the poor quality material and poor constructions practices.

Extensive experimental and numerical researches have been carried out on this subject and it is necessary to consider the clear difficulties in determining the residual prestress force and the level of corrosion in each single cable of a structure. In fact, the partial rupture or corrosion of pre-stressing tendons can be difficult to detect exhaustively, but at most on a statistical basis. Therefore, sensitivity analyses are needed to evaluate possible severe decreases in residual capacity due to the corrosion increase or the stress loss in the prestressing strands.

Despite the increased culturally recognition of the significance of modern architecture thanks to international documents and guidelines, there are still challenges to secure its preservation. Moreover, in actual practice, this cultural awareness clashes with the difficulties involved in adapting recent buildings to current building regulations. In fact, architectural heritage of the 20th century presents numerous issues, related to the materials and the construction techniques used, as well as to the spatial solutions that sometimes were complex and innovative. In fact, the past century architectural and engineering research in all these area has been characterized by the continuous innovations and experimentations. For these reasons, considering a possible restoration and re-functionalization of these buildings, it is fundamental to perform a careful condition assessment, both as regard the level of safety in static and seismic conditions.

For the analysis and conservation of concrete heritage, like for other architectural heritage, a multi-disciplinary approach is required. Anamnesis operations include activities such as historical research, the survey of the artifact, diagnostic, identification and quantification of chemical-physical properties of material. It is a fundamental step to the diagnosis of the structure, which is even

more effective more the information obtained from the various activities dialogues directly with each other. It is essential to acquire a deep knowledge of the structures and the materials used, as well as their characteristics and of the possible presence and causes of damage state. In fact, a correct conservation and rehabilitation of modern heritage structures can be reached only if a diagnosis of the building has been adequately formulated. Experimental investigations are part of those operations that aim to identify the structural characteristics and the state of health of the building. In particular, in order to understand the behavior and the vulnerabilities of these structures, the anamnesis process have to address aspects related to the identification of construction defect, irregularities, deterioration, the damage produced by previous events.

In the light of the above-mentioned concepts, monitoring activities can play an important role in the preservation of concrete architectural heritage, both in condition assessment and conservation process. Indeed, monitoring is not only a method to investigate the past of the structure, but it can play an active role in the conservation of modern heritage influencing decision-making actions. After the collapse of Polcevera Viaduct (2018) the scientific continue to stress the paramount role of maintenance and permanent structural health monitoring (SHM). In order to reconcile conservation principles and new building standards, methodological approaches and guidelines need to be established for this heritage, as well as descriptive and interpretative models for the structure and its health state.

Another important aspect in the assessment procedure is the revision of the standards over the years. In fact, the assessment based on current standards could lead to insufficient safety levels. A possible solution is the application of more refined models, such as the use of finite element (FE) models of the structure. These models can be updated to match the experimental results as closely as possible in terms of mechanical properties, measured displacements, and identified parameters.

This thesis provides, through numerical studies on experimentally calibrated models, methodological approaches and strategies for the static and seismic condition assessments for conserving reinforced concrete heritage structures. Thanks to the model updating techniques, these models can simulate the actual behavior of the structure, so becoming a useful tool for a more refined estimation of the static and seismic safety levels. In fact, the use of corroborated models offers a solid basis for making parametric, or even statistical, assessments of safety levels. Moreover, the model is also a natural tool for fusion of experimental data of a

different nature, or coming from subsequent campaigns, or at the limit of continuous monitoring.

1.2 Structure of the thesis

The thesis is organized in the following order:

Chapter 1 – It contains the introduction of the thesis, with the motivation for the application of the structural health monitoring and calibrated models as useful tools for the analysis and the condition assessment of 20th century concrete heritage structures, identifying the focus of the thesis.

Chapter 2 – It presents the 20th century reinforced concrete heritage features. Starting from the first applications of reinforced concrete in the structures, retracing the rapid spread of this material in the years thanks to its novel construction possibilities, this chapter ends describing the durability problems and the diagnostic techniques of reinforced concrete.

Chapter 3 – It describes the prestressed concrete systems. The chapter starts from the first developments of these systems, and contains the construction possibilities allowed by the different types of prestressed techniques. In this chapter the main durability problems of prestressed concrete structures, especially (but not only) early post-tensioned, and the current diagnostic techniques are reported.

Chapter 4 – It presents an overview of the main issues related to the protection and analysis of the reinforced concrete architectural heritage, highlighting the multidisciplinary approach required for its correct conservation. In particular, the most relevant national and international documents are presented and discussed. The importance of attaining an adequate level of knowledge in this heritage structures is evidenced especially in relation to the accurate static and seismic condition assessments. In the final part, some examples of interdisciplinary approach to concrete heritage structures are reported.

Chapter 5 – It contains a critical review of structural and seismic safety evaluations methods applied to modern heritage structures. Starting from the evolution of structural and seismic safety methods and standards, this chapter presents and analyzes the safety assessment for modern heritage structures. In the final part, is introduced the role of models for the structural analysis and preservation of concrete architectural heritage.

Chapter 6 – It presents the case study of the thesis, used for validating the methodological approaches proposed for the condition assessment: Pavilion V, the historical post-tensioned concrete structure built by Riccardo Morandi in Turin Exhibition Center. It is highlighted the importance of a proper cognitive path, in particular to understand the structural conception of the building. The second part addresses the design and execution of the experimental tests and their use for the corroboration of the FE model with predictive capabilities. For the determination of modal parameters, particular attention is paid to the role of structural joints in the case of structures composed by several interacting diaphragms. In the final part, the numerical analyses and the results of both seismic assessment and structural reassessment with respect to static loads are reported. The final part on structural reassessment compares Morandi's predictions with the results from corroborated model.

Chapter 7 – It describes the proposed methodological approaches to the condition assessment of reinforced concrete architectural heritage. The approaches, based on experimentally corroborated models of the structure, are summarized in a general flowchart. In the last part, methodological approaches are extended to the condition assessment of early post-tensioned systems.

Conclusions – It summarizes the main outcomes of the thesis. Then it describes possible future works that can be carried out thanks to the combination of the outcomes of the thesis, focusing on methodological approaches to the condition assessment of reinforced concrete architectural heritage.

Chapter 2

XX century reinforced concrete heritage

2.1 The reinforced concrete: from the first applications to the reconstruction and economic growth

The twentieth century can be defined as the century of concrete. In fact, although concrete as a building material did appear before 1900, its complete development took place afterward in the progress of the XX century. A wide number of patents protecting conceptual technical innovations, design procedures, and systems for concrete construction have characterized this period, with specific regard, but not solely limited to, reinforcement type and detailing (Levi & Chiorino, 2004).

The chronology of the first applications and patents are reported in the following (Beckmann & Bowles, 2004):

- Joseph Aspdin, patent for Portland cement (1824)
- First reliable Portland cement (1845 approx.)
- Marc Isambard Brunel, reinforced brickwork cantilever (1851)
- William B Wilkinson, flat iron reinforcement (1854)
- Francois Coignet, first (British) patent system (1855)
- Coignet publishes 'Betons agglomerés' (1861)
- Joseph Monier, patent for tanks, pipes, and box culverts (1867)
- Wayss & Freytag (Köenen) publish 'Das System Monier': first design

textbook (1887)

- Francois Hennebique, patent (1892)
- Emperger, Bauschinger, Mörsch and Considère, research (1890–1910)

Some of the early patent reinforcement systems are illustrated in the following Figure (Figure 1).

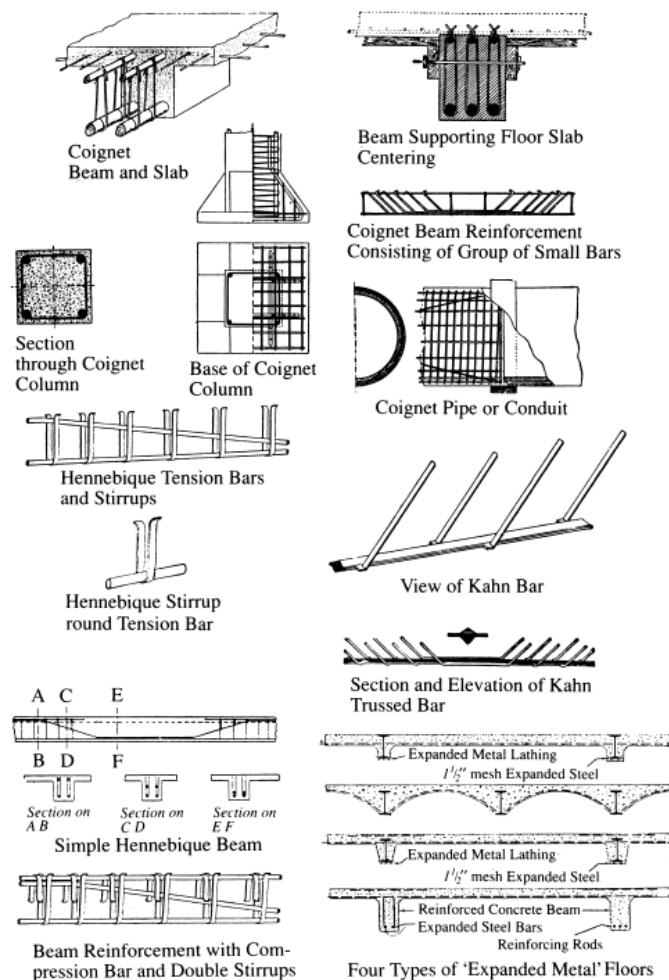
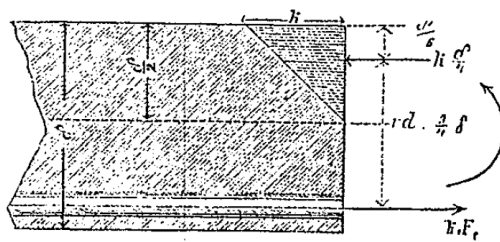


Figure 1: Some early patent reinforcement systems (Jones, 1920)

In 1886, Köenen faced the problem of designing a slab with this new material. In fact, Saint-Venant's principles, based on the mathematical theory of elasticity, was developed during the 19th century for a homogeneous and isotropic material with linear elastic behavior, and were not immediately applicable to reinforced

concrete. Köenen bypassed the problem with some simplifying assumptions: referring to a slab with rectangular section subjected to bending, he imagined that the neutral axis passed through the gravity center divided the section in half, as it happened for homogeneous materials. The compressed concrete above this axis behaved as an ideal homogeneous and elastic material, and in the lower area, only reinforcements resisted. Köenen mistakenly believed that the two material touched their maximum strength at the same time. Therefore, with the two equations of equilibrium, translation and rotations, it was possible to obtain the unknown geometric parameters: height of the section and area of the reinforcements (Figure 2). The simplicity of this method ensured its application for many years, but the passage of neutral axis to the gravity center, the assumptions that the two material worked simultaneously at their ultimate strength and the deformations incongruity between bars and concrete will in any case be the subject of numerous studies in the following years (Iori, 2001).



$$\begin{aligned}
 1. \quad & \dots k_1 \cdot F_s = k \frac{\delta}{4} \\
 2. \quad & \dots k \frac{\delta}{4} \cdot \frac{3}{4} \delta = M_{\max} \\
 & \text{woraus:} \\
 \text{I.} \quad & \dots \delta = 2,31 \sqrt{\frac{M_{\max}}{k}} \\
 \text{II.} \quad & \dots F_s = \frac{1}{4} \frac{k}{k_1} \delta
 \end{aligned}$$

Figure 2: Calculation scheme for Monier slab proposed by Köenen in 1886: δ is the thickness of the slab; F_s is the reinforcements area; k is the concrete compressive strength, k_1 is the tensile strength of bars (Iori, 2001)

However, the real revolution took place in 1892, when Hennebique filed his first patent on the combination of concrete and bars for the creation of beams. This event represent a decisive step in the technical evolution of reinforced concrete, because Hennebique focused its experimentation on linear building elements (the beam and the pillar), constituting the framed structures in reinforced concrete. Some improvements were made to the beam, especially regarding shear solicitation: introduction of *étriers* elements and shaped bars in correspondence of the supports.

With Hennebique the true modern history of reinforced concrete began, also for the entrepreneurial approach given to the problem. He organized the first congress on reinforced concrete in 1897, inviting its dealers but also personalities from the scientific world. In 1898 he published the first volume of the journal *Le Béton Armé*, which contributed significantly to making known the system, its

applications and progressive improvements. The success of Hennebique was also based on the simplicity of the proposed calculation method: concrete and reinforcements counteract the bending moment, sharing the tasks equally. So, in a rectangular section beam, cut from the neutral axis no longer in half (as for Köenen), but in an unknown position, the compressed concrete (above the axis) absorbed half of the bending moment, as well as the reinforcements (below the axis). This arbitrary imposition went well with two successive simplifications: the distribution of compressive stresses in concrete had to be uniform and both materials had to reach the ultimate admissible stress at the same time (Figure 3) (Iori, 2001).

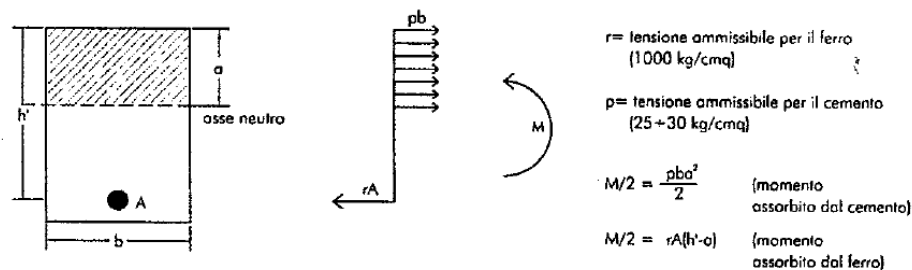


Figure 3: Hennebique calculation hypothesis in 1892 for a beam with bending moment action (Iori, 2001)

In 1894, Coignet and de Tédesco presented some results in which they presented the concept of “homogeneous section” for the first time. In fact, to solve the problem of non-homogeneity that questioned the applicability of the elasticity theory to reinforced concrete, they proposed to amplify the reinforcement’s area in the calculation by an appropriate coefficient, and then to operate as if the whole section was in concrete. The problem then became quantitative about the value to give to this coefficient, later widely called “m” or “n”. By exploiting the principle of planarity conservation of the sections and recognizing, for the first time, the need for deformation congruence between the bars and the concrete, they shown that this amplification coefficient should have been equal to the ration between the elastic moduli of the two materials. As for the numerical value, they noted that the elastic modulus of concrete persisted in changing value depending of many factors (Iori, 2001).

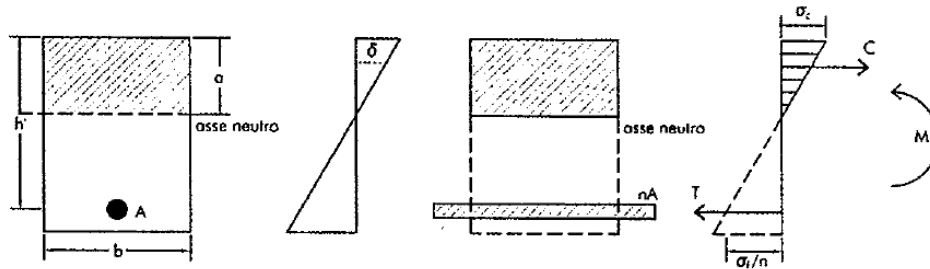


Figure 4: Hypothesis of the “homogeneous section” formulated by Coignet and de Tédesco in 1894 (Iori, 2001)

Many of the scientists of the time, stimulate by the experimental inconsistencies (the method was very conservative and much more loads were needed to bring about the deformations foreseen by the calculations), continued to investigate the theories of calculation applicable to reinforced concrete. In 1889, Considère expounded his theory in which the concrete, after having reached the maximum possible tensile stress, entered in a phase in which the bars forced it to further deformation, without causing it to crack: the tensile stress absorbed by the concrete was considered for bending moment capacity calculation. Only many years later, in the theoretical justifications of his results, the foundations of the theory of plasticity and of the limit state calculation were recognized. Ritter’s and Ostenfeld’s theories were also very rigorous and prelude to modern hypotheses on the behavior of the material. They recognized that the elastic modulus varied, not negligibly, with the load and in the response of the section, various phases could have been identified: fully reacting concrete and, with the increasing of bending moment, a second in which it was possible to neglect the tensile strength (Iori, 2001). The difficulties of reproducing the experiments, which always provided different values, suggested that the characteristics of the material were strongly linked to many factors and, in short, the problem of rigorous calculation had an unexpected complexity.

As the scientific world increasingly advanced into the study of phenomena relating to reinforced concrete, the Hennebique system spread rapidly throughout Europe and the world through a network of subsidiary companies in these early years. In Italy, in particular, the first large industrial structures of reinforced concrete were grain silos, built between 1899 and 1901 in Genoa by Hennebique’s main Italian agent Giovanni A. Porcheddu and the company he established in Turin. In 1911, for the celebration marking 50 years of Italian unification, the company also built the first large reinforced concrete bridge in Italy, the Risorgimento Bridge (Figure 5). Hennebique designed the bridge based on his intuition of the static

behavior of structural concrete incorporating technical innovations such as the high-bond ribbed bars patented by Porcheddu (Iori, 2001) (Levi & Chiorino, 2004).



Figure 5: The Risorgimento Bridge in Rome, Italy.
(https://en.wikipedia.org/wiki/Ponte_del_Risorgimento)

The versatility of this new material technique was demonstrated during the reconstruction of the cities of Messina and Reggio, after the severe 1908 earthquake. In the years before and after World War I reinforced concrete use expanded exponentially, becoming the most wide-spread building technique. Construction companies, assisted by designers and the academic community, competed on the basis of the quality and economy of their projects. Despite the lack of well-defined code, the advancement of reinforced concrete was conspicuous and the progress was driven essentially by experience and intuition of the designers and constructors, especially for large structures (Levi & Chiorino, 2004).

The diffusion in ordinary building and apartment construction was favored by the reconstruction after World War I and the growth of cities. Reinforced concrete was also largely employed during the industrial development occurring in and after World War I. The creation of public works for infrastructure and public building, after the economic crisis of 1929, provided new possibilities for the evolution of reinforced concrete in modern architecture, as debate continued between traditional and more innovative approaches. New opportunities for a wide expansion of reinforced concrete were offered by the reconstruction and economic development after World War II.

Concrete secured the position as the twentieth century's preeminent construction material, providing an economical solution to the large-scale construction challenges in the aftermath of World War II, (Macdonald & Arato Gonçalves,

2020). In fact, in the two decades following the war, modernization of infrastructure, with particular regard to the creation of a national highway system in Italy, was fueled by some important innovations, such as prestressing, prefabrication, and industrialization of the construction process. A post-war generation of new designers emerged who were determined to explore the broad horizons opened by the technical progress being seen in the concrete industry (Levi & Chiorino, 2004).

Therefore, concrete's development, in these 200 years, has produced an extraordinarily big and varied legacy. This heritage is more and more recognized primarily for their cultural significance (Macdonald & Arato Gonçalves, 2020).

2.2 Construction possibilities of reinforced concrete in spatial structures

Many concrete structures designed and built by architects and engineers all over the world and especially in Europe, rival the masterpiece structures of past centuries. The creation of different and innovative forms of spatial structures, especially for buildings requiring large space, has been permitted by the particularly properties of this material. In fact, great architects and structural engineers have designed recognized works of art (Ceravolo & Lenticchia, 2019). These researchers contributed to the birth of a science of spatial architecture with concrete.

First shells in reinforced concrete were built as thin members for spatial structures (Cassinello, Schlaich, & Torroja, 2010). Designers, such as F. Dischinger, E. Torroja, R. Maillart A. Tedesco, exploited the particular benefits of double-curvature structures allowing to build elements with very low thickness. These elements were mainly characterized by membrane stresses, with very low bending and shear ones. The elements in the edges aimed to achieve a membrane behavior as ideal as possible. Analytical expressions defined the shapes of these structures, built mainly between 1920 and 1940. In America, new developments took place following this period, above all on the approach, by the Spanish architect F. Candela. This approach, consisting on carried out simple analyses and combine various sections of previous shapes, led to a wide variety of structural forms (Muttoni, 2014). The engineer H. Isler built also numerous shell structures in Switzerland between the 1960's and 1980's. The unusual shapes was obtained and optimized considering various mechanical analogies, such as pneumatic and gravity-shaped membranes (Chilton & Isler, 2000) (Kotnik & Schwartz, 2011).

In Italy, P. L. Nervi was one of the most outstanding figure in the design of concrete spatial structures during the past century. He combined, for the first time on a big project for a vaulted structure, an significant use of prefabrication system with his personal invention of ferrocement in the Exhibition Hall in Turin (1949), obtaining extraordinary aesthetic results (Figure 6). The same technique was adopted also in other its projects such as the elegant domes of the Palazzetto and the Palazzo dello Sport (1956-1959) for the 1960 Olympic Games in Rome (Levi & Chiorino, 2004).



Figure 6: Exhibition Hall B in Turin, Italy (Levi & Chiorino, 2004)

Due to the high man work required for the positioning of the formwork and the placing of the reinforcement bars, compared to the prices of the construction materials, in the last twenty years of the 20th century, shells structural solutions were rarely chosen. In fact, in that period other structural solutions were usually privileged. In recent years, thanks to the opportunities coming from new concrete types (fibre-reinforced), prestressed technique also used for these types of structures, the automatic cut and position at construction site of formworks, and the new possibility to use software with computer to analyze shells have contributed to the development of a new approach to these structures, allowing more freedom in the shaping choice (Muttoni, 2014).

The experiences on the first reinforced concrete spatial architectures were mostly related to the genius of their designers rather than an evolution in concrete shell theory. Thus, for spatial structures, issues in the concrete conservation are fundamental, regarding both formal and structural engineering aspects.

2.3 Durability problems of reinforced concrete

The wide variety and quantity of concrete architectures built during the past century were not exempt from problems. In some cases, especially in the early structures, an appropriate level of safety checking in design was lacking due to an insufficient development of a modern theory for structural concrete (Levi & Chiorino, 2004). Nevertheless, the problems encountered centered more frequently on limitations in structural durability, which eventually required expensive maintenance and repair. These last issues are related to the delay on the introduction of adequate provisions for durability and quality assurance within technical standards of that time.

For this reason, many failures, in terms of durability and functionality, have characterized not only the residential buildings, but also the structures and infrastructures designed by famous engineers and architects (Coppola, 2015). Reinforced concrete architecture have shown a particular vulnerability to aggressive environmental actions promoted mainly by carbon dioxide in the atmosphere, by chlorides in the sea salts, from sulphates in groundwater and soils. Moreover, the thickness of concrete cover, in the design codes in force at that time, was insufficient by today's codes and were sometimes not adequately maintained. (Beckmann & Bowles, 2004).

Thus, scientific awareness that reinforced concrete, this material so celebrated by modernity for its exceptional properties, presented inevitable signs of its life cycle and, therefore, of the need for maintenance, emerged in the last two decades of the XX century. Numerous monuments of twentieth century architecture have shown signs of degradation in the last decades, that affects their use and safety, even before compromising their aesthetic aspects (Coppola, 2015). On the other hand, these negative experiences have represented an important source of information, which influencing progressive improvement of reinforced concrete standards (Levi & Chiorino, 2004). In fact, one of the issues in the conservation and/or repair of these structures is the lack of specific knowledge and information on degradation mechanisms that affect different types of historic materials (Custance-Baker & Macdonald, 2015).

According to (Beckmann & Bowles, 2004), two different processes can endanger the durability in a reinforced concrete structure:

- Disintegration of the concrete as such.

- Reinforcement corrosion with subsequently spalling and/or cracking.

The causes of these processes can be either attacking of aggressive substances present in the external environment, or chemical reaction due to the presence of deleterious ingredients in the concrete. For the diagnosis phase, a correct methodological approach starts from knowledge of the main phenomena of alterations produced by an incorrect choice of the constituents of the conglomerate, by incorrect installation techniques on site, by environmental aggression, by structural deficiencies or by response to seismic action. In fact, for each of these pathological behaviors, specific diagnostic techniques are recommended for the identification of the cause of the damage (Coppola, 2015).

2.4 Diagnosis of reinforced concrete structures

The diagnosis of reinforced concrete structures needs a methodological approach based on the following different steps (Coppola, 2015):

- Visual inspections aimed at detecting the structural pathologies (cracks, areas with anomalous water stagnation, spalling of concrete, presence of corroded reinforcements, etc.);
- Acquisition of historical-geographical information concerning the structure during its construction, the site where it was built, and the boundary conditions (adjacent building, any excavation carried out after the construction, etc.).

The data collected by visual inspection and the historical-geographical ones are rarely sufficient to issue a definitive diagnosis. In fact, usually, they allow only a diagnostic suspicion to be issued, on the basis of which specific investigations will be performed (in situ or in the laboratory) which allow to broaden the knowledge of the structure and which will lead to the actual diagnosis, useful for both the consequent structural assessment and the definition of the therapies.

A comprehensive structural assessment needs information of the concrete properties: strength and durability, as well as the type, arrangement and strength of the steel (Beckmann & Bowles, 2004). In general, multi-scale approach based on the combination of experimental investigations carried out in situ and in the laboratory is needed in the diagnosis. In the case of concrete architectural heritage, it is highlighted that, as far as possible, non-destructive and non-invasive methods

should be used for the investigations of the condition and deterioration of materials (ICOMOS, International Committee on Twentieth Century Heritage, 2017). In fact, destructive methods in the investigation should be used only to confirm or calibrate the results of non-destructive ones, and to obtain additional important information that cannot be achieved with nondestructive techniques (Macdonald & Arato Gonçalves, 2020). Some of the main diagnostic techniques for reinforced concrete structures are reported in the following, depending on the investigated properties.

2.4.1 Concrete strength

Sometimes, in the drawings or also on other original documents, mix proportion specifications and strength requirements can be found. This information can provide a first indication about the concrete properties. In the absence of specific information from the project, a more tenuous clue may be obtained from the then current building codes and regulations. Within them are often reported mix proportions and the minimum strength resulting from the sample tests. Furthermore, it is worth considered that for structures prior to the 1960s, the specified strengths are normally referred to concrete samples matured at 28 days (Beckmann & Bowles, 2004).

The most direct measure of strength is obtained by taking samples of the concrete from the structure and testing them. The ideal diameter of the cores is 100 mm and the ideal depth-to-diameter ratio is 1. The strength obtained from a test depends from many factors; therefore, multiplications with conversion coefficients are needed so they can be used for any structural calculations. The characteristic influencing the compressive strength core are: size and shape of the test specimen; conservation method before the test, presence of reinforcing bars; extraction direction of the sample; and age of the core at the time of the test (Coppola, 2015) (Beckmann & Bowles, 2004).

There are two ways to use these results as a basis for consequent calculations: (a) identify a strength value for all structural concrete, or (b) identify a strength value for different structural members that are considered most critical. A big number of samples taken in random position from the structure are required for the calculation (a). Specific guidance are given in standards about: (1) sampling and testing methods, (2) use of resulting values for structural assessment, (3) conversion factors to use when initial core strengths are converted into design strengths (Beckmann & Bowles, 2004).

The non-destructive techniques for the strength assessment usually exploit the combination of two tests based on: (i) the velocity of an ultrasonic pulse and (ii) the rebound of an elastic surface.

The velocity of an ultrasonic pulse has been demonstrated to be dependent from the Young's modulus, which is related to concrete compressive strength. With this method, it is better when possible that during the test the probes can reach both the sides of the concrete element for estimating its relative strength. Thanks to a calibration with a few samples, the relative strength can be converted into the absolute strength. The method requires the presence of skilled operators with adequate experience. In fact, the obtained results can be influenced by the presence of reinforcement, which puts in connection two concrete faces, giving a shorter path to the pulse.

The rebound of an elastic surface is evaluated with the Schmidt-Hammer. This instrument has a torpedo shape with a plunger at one end, which allows to measure the surface elasticity of a concrete element and, consequently, its strength. It is worth highlighting that close to the surface the concrete has specific properties that were influenced by:

- type of used formwork;
- curing when the forms were removed;
- subsequent operational environment.

Therefore, the Schmidt-Hammer is not recommended in some cases by the experts. However, this method has some advantages: it is simple and robust, requires access only to one face of the element, can be performed by only one operator (Beckmann & Bowles, 2004).

Once the calibration with compression tests on samples taken from the structures is performed, the relative strength values obtained with non-destructive methods can be converted into the absolute strengths of the members. Therefore, it is necessary to proceed with the extraction of cores to determine the concrete strength, which allows to refine the correlation with the results of non-destructive tests. In fact, to give reliable absolute strengths, the instrumentations for both the ultrasonic pulse velocity and the elastic surface rebound have to be calibrated by doing a measurement in the same position from which the cores will be taken (Coppola, 2015) (Beckmann & Bowles, 2004).

2.4.2 Reinforcement strength and disposition

Notes in the original drawings, in the then current standard specifications and codes can provide a first estimate of reinforcement strength. For the structural assessment, the strength of reinforcement from the specifications are preferable to allowable stresses. In fact, in some early regulations, the safety margins can be more conservative than those of today's one. In any case, it is worth pointing out that early specifications required only a minimum ultimate tensile strength for the steel, not design stresses based on the yield values like in the nowadays regulations. Therefore, is essential to obtain sufficient knowledge on the ratio of ultimate strength on yield stress. This can be done accurately by removing reinforcement samples from the element for a subsequent test (Beckmann & Bowles, 2004).

In-situ hardness test, which only requires the removal of few volume of concrete cover, may be considered for a lower number of bar specimens to be removed. Greater removal of cover, on the other hand, is required to check the bars arrangement, with respect to original drawings (if available). If the original drawings are not available, identify the bars arrangement and sizes constitutes a more challenging work. Electromagnetic devices can be used to detect the bars up to approximately 75 mm of depth. These devices can help in identifying the orientation and the diameter of the reinforcement. However, although a huge use of such tools is recommended, a significant amount of cover openings to check the arrangement and diameter of the effective structural reinforcements is necessary (Beckmann & Bowles, 2004).

2.4.3 Assessment of durability

As previously highlighted, the reinforced concrete elements suffer from durability problems due to disintegration of the concrete as such and to reinforcement corrosion with subsequently spalling and/or cracking of the concrete.

An advantage of samples for strength tests is that the porosity, which represent an important factor for the durability, can be evaluated measuring the density and the weight of samples prior to testing. Moreover, after testing, it can be determined the presence of aggressive substances which could influence the durability (sulphates, chlorides, etc.) by means of some chemical analysis on some parts of the crushed remains of the sample (Beckmann & Bowles, 2004).

The spalling phenomena, due to bar corrosion, is related to carbonated front depth in the element. In general, to determine the advanced front of chlorides, carbon dioxide or sulphates, methods defined as “colorimetric” are used. The areas affected by the penetration of the aggressive substance take a different color than that conglomerate not affected by the penetration, as a consequence of the specific reagents that are sprayed on the surface of the concrete. In particular, one of the most used tests to detect the advanced carbonation front in concrete consists in the application of phenolphthalein to a freshly cut section of the sample, immediately after was taken (Coppola, 2015).

Electrochemical potential or resistivity testing can detect the presence of the corrosion phenomena, in concrete elements not yet suffering from spalling. Potential measurements are performed by reading the voltage, generated between an exposed bar and a copper-copper sulphate electrode. The electrode and the concrete element need to be in contact on some points, which are disposed on a grid (Figure 7).

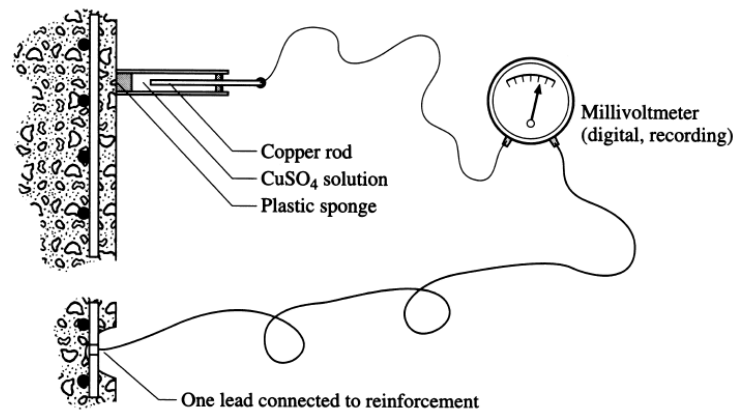


Figure 7: Principle of potential measurement for ongoing corrosion in reinforced concrete structures (Beckmann & Bowles, 2004)

With this method contours of the voltage can be obtained with some indication of the severity of the corrosion (Beckmann & Bowles, 2004).

Chapter 3

Prestressed concrete systems: diagnosis and conservation

3.1 Prestressed concrete: first developments

In 1888 W. Döhring obtained the first patent which provided for the concrete prestress. Afterwards, in 1906 M. Koenen developed the first device for tensioning the bars. The proposed solutions had no real possibility of application because the allowable tensions for the reinforcement of that time permitted small elastic elongations. This small elongation was lost due to shrinkage and slow deformations of concrete, not yet known. However, despite initial failures, this general idea was not discarded (Leonhardt, 1980) (Iori, 2003).

The modern prestressed technique has been introduced by the structural engineer E. Freyssinet. He began building segmental arch bridges from around 1910, with an original technique based on the use of hydraulic jacks, which were positioned at the top and operated in horizontal direction. This prestressing system hinged on this technique and was known as the Systematic Deformation Method (Iori, 2003).

In 1919 K. Wettstein was the first to employ high strength steel under high tension, which was the key prerequisites for the success of the prestressed concrete (Leonhardt, 1980). In 1928, Freyssinet registered a patent in France, and a year later

in Italy as well, on prefabricated members (Figure 8) with straight reinforcing rods, pretensioned before the placement of the concrete. The tension rods transmitted their stress to the cured concrete by means of anchor devices (Iori, 2003). Also F. Dischinger said he was the inventor of prestressed technique for concrete, with a patent registered in 1928. In 1934, another beam's patent for a particular system for build a bridge was deposited by Dischinger (Figure 9). In 1935, Freyssinet licensed his patent to the company company Wayss & Freytag (in Germany). A long experimental phase led to the realization in 1939 of the first bridge in prestressed concrete, with a project by E. Morsch, technical director of the company (Iori, 2003).

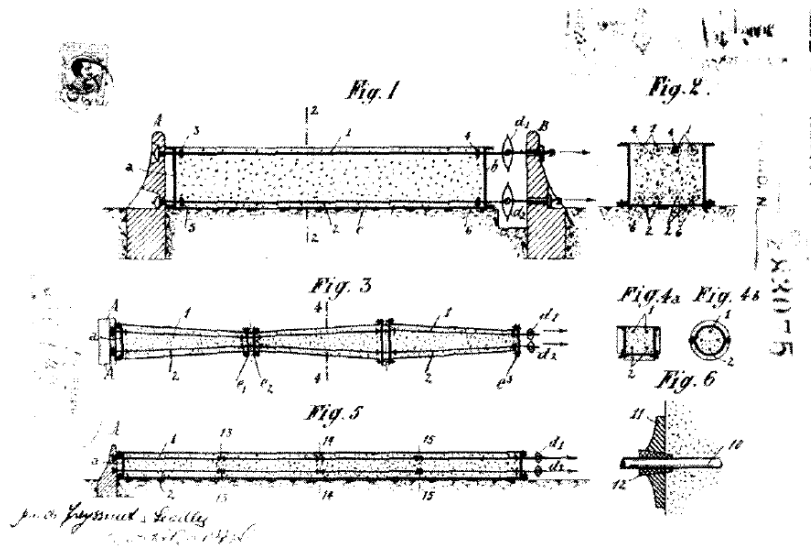


Figure 8: Italian patent n. 283075 by E. Freyssinet and J. Séailles: Processo di fabbricazione di pezzi in cement armato, October 1st 1929 (Archivio Centrale dello Stato)

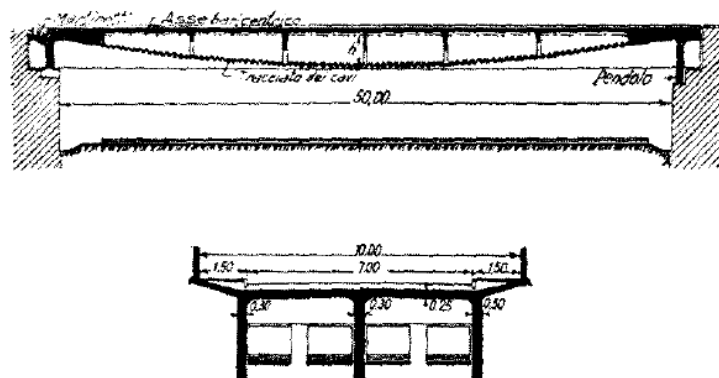


Figure 9: Prestressing patent by Dischinger in 1934 (Guidi 1947)

Italian engineer and mathematician G. Colonnetti brought a notable theoretical contribution to the development of the prestressed concrete technique. Also F. Levi, F. Mattiazzo and C. C. Guidi treated particular problems inherent to the design with this new technique. In 1939, Colonnetti pointed out the potentials of prestressing with his original publications on the Artificial Coaction State Technique (Guidi, 1987). In 1939, he registered the first patent for reinforced concrete with pretensioned systems in Italy (Figure 10), which was distinguished from the ideas already present in the Europe for his particular original solution: the non-adherence between the concrete and the prestressing steel (Iori, 2003).

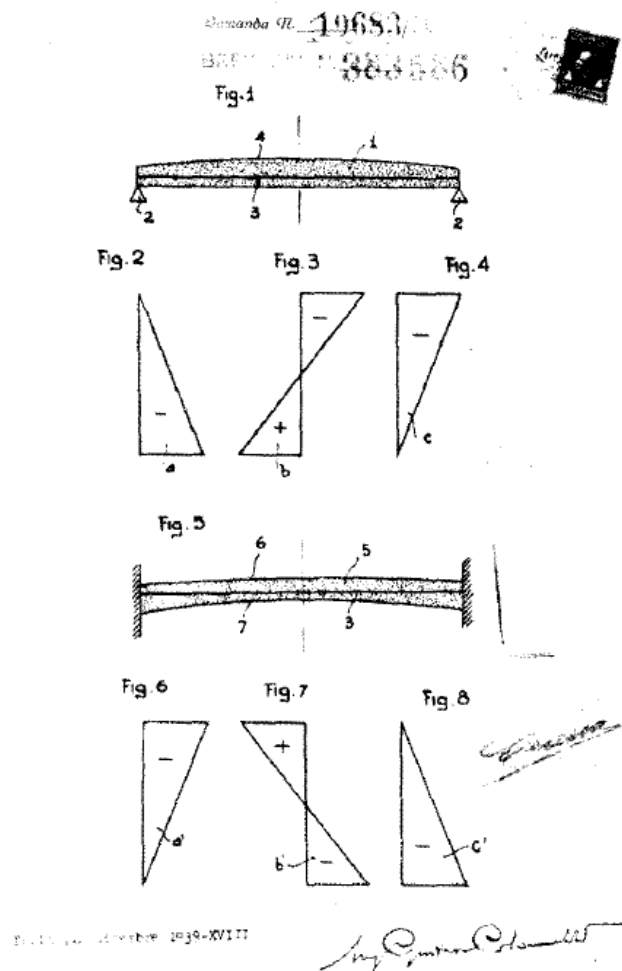


Figure 10: Italian patent n. 383586 by G. Colonnetti: Trave armata ad armature preventivamente tesa. December 12th 1939. (Archivio Centrale dello Stato)

The post-tensioning system with cables inserted in sheaths was patented by Freyssinet in 1940 even if G. Colonnetti had patented the procedure (Giovannardi,

2008). In 1941, Colonnetti introduced a new system (Figure 11) for the tension and the anchor of tendons. The technology of prestressed concrete gave to Colonnetti the chance to promote the elimination of arbitrary design methods for reinforced concrete and a practical application of his elastic coaction theory (Iori, 2003).

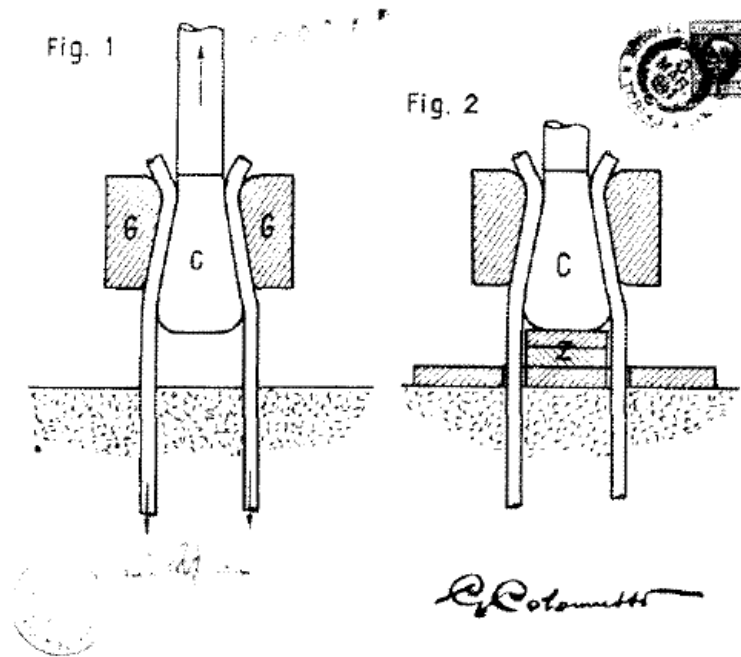


Figure 11: Italian patent n. 389946 by G. Colonnetti: Dispositivo per la messa in tensione e l'ancoraggio delle armature nelle strutture in conglomerato cementizio, March 3rd 1941. (Archivio Centrale dello Stato)

The concrete industry promoted numerous experimentations in Italy, in order to find a solutions to face the crisis due to the laws against the structures in reinforced concrete (Iori, 2001). Moreover, it is worth highlighting that the early period of prestressed concrete is almost entirely related to rearmament and the war effort. For that reason, there was few records of the development of this technique and everything was top secret (Marrey & Grote, 2003).

In 1941, Freyssinet designed a frame bridge with two hinges, on Marne river near Luzancy, which, however, could be completed in 1946 only when the war is over. Five more bridges of the same type followed over the Marne. These bridges constitutes the first true examples of modern prestressing. Further contributions came from German engineers, in particular by Dischinger, who patented the tendons arranged outside the concrete section (Leonhardt, 1980). In few years, the notoriety of prestressed concrete technique has increased, spreading at an

international level, and the works carried out have broken records for costs, execution time and dimensions (Giovannardi, 2008).

In 1944, Italian engineer R. Morandi registered his first patent for prestressing tendons by means of low voltage electricity and, over the following years, he registered many others patents (Iori, 2003). Morandi has made a big contribution in introducing prestressed concrete in Italy, designing many bridges with this technique. Among his numerous projects, characterized by impressive shapes, the Maracaibo Bridge (Venezuela, 1957), and the underground exhibition pavilion in Turin (1959), that utilized prestressed concrete frames (Levi & Chiorino, 2004). Morandi's pavilion of Turin Exhibition Center (Figure 12) will be considered as a case study application in this thesis.



Figure 12: Underground exhibition hall in Turin, Italy

Morandi's approach in the underground pavilion, consisted of combine different elements in balanced relationship, is also found in others his constructions, such as the Via Olimpica bridge in Rome (1958-1960). Despite the different use, the structural conception was the same: balanced beams on supports, whit the beam ends tensioned from below using a tie element (Ingold & Erb, 2018).

Morandi's creations were characterized by the manipulation of internal forces, which are applied in a target manner by means of prestressing within a component. Thus, his technique has a particular influence on the thin forms shaping the concrete on which was applied, without being directly visible (Ingold & Erb, 2018). If Morandi played a key role in the field of structural engineering during the second half of the XX century, is thanks to the creativity he has shown in his research for new types of structures, technologies, and construction process inspired by the

possibilities offered by reinforced and prestressed concrete, a material still recent at the time.

3.2 Construction possibilities and different types of prestressed concrete

Numerous civil engineering structures of the twentieth century have been built with prestressed concrete techniques. The main advantages of this construction technique are reported in the following (Leonhardt, 1980) (Gilbert, Mickleborough, & Ranzi, 2017):

1. Greater spans with beams height and total self-weight lower than the reinforced concrete ones.
2. Reduced execution time, especially in the case of using precast elements standardized and factory produced.
3. Limited cracks and deformation under characteristic loads.
4. High fatigue strength due to the small amplitude stress oscillations in the steel.

As described previously, prestressing forces are transferred to concrete elements by tensioning reinforcements. The steel used can be in the form of wires, strands or bars. In the modern prestressing, the tensioning process is often made by means of hydraulic jacks. These may be actioned before or after the concrete cast. The different types of prestressed concrete, the relative advantages and disadvantages are described in the following.

3.2.1 Pretensioned concrete

Pretensioned concrete is obtained by tensioned and anchored the steel strands between fixed abutments. In this state, the concrete is cast and cured into the formwork (Figure 13). This produces an immediate adherence between the prestressing steel and concrete. When required concrete strengths are reached, the ends of the tendons are cut from the fixed points. In this way, the steel tends to contract and the element is compressed for adherence effects. The tendons are loosened by means of a slow heating or with other suitable system, in order to avoid a sudden transfer of the force of tension to the concrete (Leonhardt, 1980) (Gilbert, Mickleborough, & Ranzi, 2017).

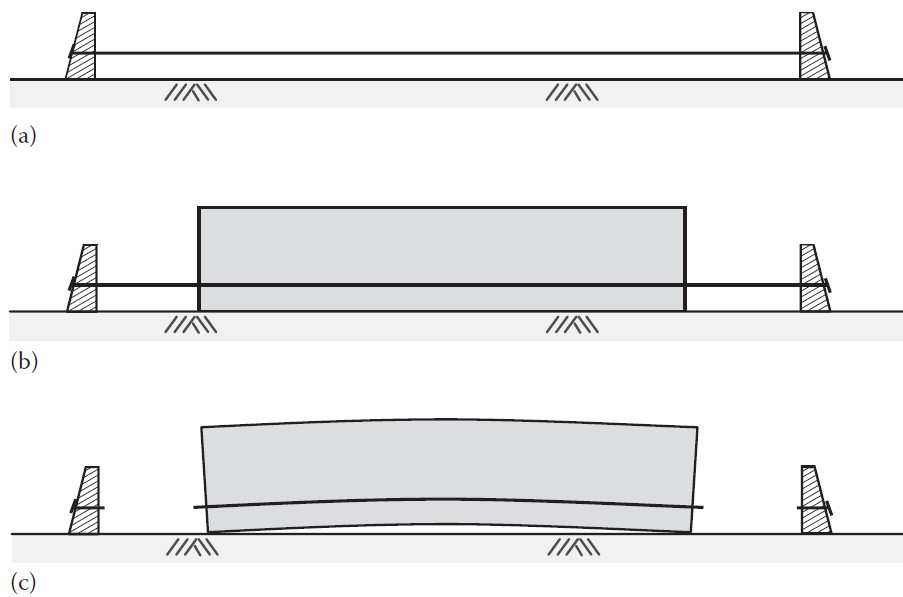


Figure 13: Pretensioning process. (a) Steel tensioning. (b) Element cast and matured. (c) Steel cutting (Gilbert, Mickleborough, & Ranzi, 2017)

In order to reach more quality and production velocity, this technique is performed in specific factories. Moreover, the elements are casted in long beds to produce numerous equal units. To accelerate the process, steam curing is usually employed. The elastic shortening of the concrete as well as the subsequent creep strains tend to be high due to stress application at such an early age. The shortening of the concrete produces a decrease in tensile strain of the steel (Gilbert, Mickleborough, & Ranzi, 2017).

3.2.2 Post-tensioned concrete

Post-tensioned concrete is obtained, with the formwork in position, by casted concrete around hollow ducts, which are fixed to any desire profile. The steel tendons are threaded through the ducts and, when the required concrete strength is reached, they are tensioned and anchored at the ends. Afterwards, in order to bond the tendons to the concrete, the ducts are then filled with pressured grout, which also better protects the steel from corrosion. In this way, the tendons are bonded to the concrete and are more efficient in controlling cracks and providing ultimate strength (Leonhardt, 1980) (Gilbert, Mickleborough, & Ranzi, 2017).

Tendons may be stressed from only one end with the other one anchored, or may be stressed from both the ends. The concrete is compressed with the stressing

operation and, after the tendons are anchored, the prestress is maintained by means of the end anchorage plates bearing onto the concrete (Gilbert, Mickleborough, & Ranzi, 2017). The execution of the injection requires specific procedures and experienced personnel. In fact, a correct injection of the grout is fundamental for the durability of the post-tensioning structure. Many problems occurred because the cables were not perfectly injected (Leonhardt, 1980).

Most in-situ prestressed concrete structures are built with post-tensioned technique. In fact, sufficiently small and manageable hydraulic jacks made this construction technique widely used. Moreover, this method offers significant flexibility in the tendons profiles, which can be adapted to the applied loads and constraints. Post-tensioning technique has been also applied to build large-span bridge girders with segmental construction technique, in which increments of prestress are applied as required as the external loads progressively increase (Gilbert, Mickleborough, & Ranzi, 2017).

3.2.3 The importance of a correct grout injection in post-tensioned concrete

A properly grout injection and a well-designed grout mix are significant for the durability of the structures. For this reason, grouting follows a specific procedure and requires experienced operators. A schematic layout of a post-tensioning tendon in a typical continuous slab or beam is reported in Figure 14. As highlighted previously, the prestressing tendon follows a profile determined from the design loading, and the location and type of supports.

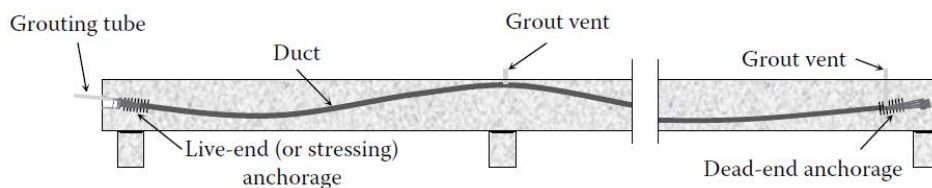


Figure 14: Tendon layout and detail in a continuous post-tensioned system (Gilbert, Mickleborough, & Ranzi, 2017)

The ducts in which prestressing tendons are positioned can be fabricated from corrugated steel sheathing or, in recent structures, plastic ducting. The ducts are sealed to avoid that concrete enters inside during the cast. Grout vents are placed in

different positions of the duct (as shown in Figure 14). In this way, it is more ensures the complete filling of the duct in the grouting phase. The correct positioning of the vents for the injection of the cement based product and the expulsion of the air in the duct affect the success of the filling operation. From one of the tendon end the grout is injected into the duct. At the highest points of the tendon profile, or near these points, some vents are placed. These vents allow to expel the air and water from the crest of the tendon profile.

In order to allow easy positioning of the strands and adequate filling with the grout, ducts with sufficient diameter are necessary. Before the filling, air pressure tests are usually performed to check for any leaks of grout. The cement based product is pumped into the inlet of the duct continuously without interruptions. Only when the grout coming out of the vent reaches the same consistency and viscosity characteristics of the injected cement based product the vent is closed. As the grout reaches its initial characteristics, the intermediate vents along the tendon are closed in sequence. The emission of the grout from the last vent along the tendon indicates the complete filling of the duct. Temporary or permanent grout caps are used to ensure complete filling of the anchorages and to allow the subsequent checks of the grouting.

With the hardening of the grout the effective bonding of post-tensioned tendon to the surrounding concrete is achieved. The purposes of this cement based product are reported in the following (Gilbert, Mickleborough, & Ranzi, 2017):

- higher exploitation of the post-tensioned steel for the ultimate limit state bending conditions;
- better corrosion protection of the post-tensioned steel;
- prevention of collapse of the entire tendon following localized damage at the anchorage or an accidental cutting of the wire.

In the last decade, serious concerns about the long-term durability are raised for some early post-tensioned structures that have been built without a fully awareness of all these important aspects in the construction phase (fib, 2010) (ACI, 2014) (Ministero delle Infrastrutture e dei Trasporti, Consiglio Superiore dei Lavori Pubblici, 2020). In these cases, problems of corrosion may be accelerated by both the poor construction practices and quality materials. Examples of construction problems encountered in structures made with this technique are insufficient duct venting, incorrect filling for wires congestion, or poor consistency with segregation.

3.2.4 Unbonded post-tensioned construction

In unbonded post-tensioned technique, the duct is unfilled with grout. In this case the steel remains always unbonded from the surrounding concrete. In this technique the strand can freely move locally with respect to the concrete element. In fact, there is no strain compatibility between the two materials. The steel is usually coated with lithium grease. Moreover, external plastic sheaths are used for the corrosion protection of the strand. This ensure that each strand is relatively freedom to move within the duct. End anchorages, which allow the transfer of the force from the tensioned strands to the structural element, are considered critical components for this technique (Gilbert, Mickleborough, & Ranzi, 2017).

In some countries, the use of this technique is not permitted, with the exception of slabs on ground. This because the disadvantages are considered more than the benefits.

Durability issues are considered among the main threats for the structures. For this reason, in the case of post-tensioned constructions it is significantly important to actively protect the strands from the corrosion. The alkaline condition around the strands is given by adequate grouting process, which allows the steel passivation. Moreover, to control cracking and to resist to progressive collapse in the vent of localized failure, bonded tendons are better than unbonded ones (Gilbert, Mickleborough, & Ranzi, 2017).

Adjustments of the prestressing forces in the strands can be considered and applied to the element during its life. In particular, inspection, re-stressed or replace of the tendons may be applicated. Sometime the grout filling is not carried out for economic reasons, with the results of having permanently unbonded tendons.

It is worth highlighting that the ultimate strength of unbonded element is usually lower than that of bonded element. This is due to the fact that, in the presence of overloads, the maximum strength of unbounded steel could be not achieved. Generally the reduction of the ultimate strength of an element with unbounded steel is approximately 25% respect the same element with bonded tendons (Gilbert, Mickleborough, & Ranzi, 2017).

3.2.5 Circular prestressing

In the case of circular form structures circular prestressing can be used. Some examples of these structures are tanks for liquid or gas with cylindrical form, silos, tunnels, etc. This technique requires that the force direction of prestressing is always applied in a direction such as to counteract the tensile forces from loads on the structure. This condition is obtained by applying the force in a circumferential direction in any point of the structure. Other cases in which circular prestressing is applied are the external ring beams of shell structures with big span. The prestressing is used to balance the significant tension forces produced by these structural forms.

Structural typology and the process used in the prestressing influence the different forms of this construction technique. In particular, individual tendons with multiple anchorage or continuous wrapping single tendon can be used to wrap the structural circumferences. The construction of buttresses in the walls of tanks and silos can be used to facilitate the insertion and the stress of tendons (Gilbert, Mickleborough, & Ranzi, 2017).

3.2.6 External prestressing

Another technique of imposing prestress, applicable to both new and existing elements, consists in the use of external tendons. In fact this methodology is based on the application of tendons or cables positioned externally to the concrete members. For this reason the two materials (the concrete and the steel) are not in bond with each other. External tendons are widely used in the case of some particular forms of structural elements. In case of box beams tendons or cables are usually positioned inside the structure.

One of the advantages of this technique is that the tendons may be removed and replaced throughout the life of the element. Many reinforced concrete bridge decks with box-section beams were built using external prestressing. Concrete diaphragms within the section are used for anchoring the tendons. While appropriate saddles are designed for deviate the tendons. These saddles are usually positioned at the bottom part of the box section in case of elements at mid-span elements or at the top part of box-section in proximity of the supports.

Another advantage deriving from the external position of the tendons is the lack of voids in the web due to the absence of internal cables. Therefore, the

thickness of the web can be optimized and the casting of concrete is facilitated. Furthermore, the prestress losses are generally smaller for the external tendons. External cables can be also applied for the strengthening or retrofitting of existing members. The main disadvantages of this technique, on the other hand, are related to the reduction of the effective depth of tendons positioned within the box section and the extra costs for the supply of anchorages and deviation saddles for the tendons (Gilbert, Mickleborough, & Ranzi, 2017).

3.3 Grout deficiencies and problems of early prestressed concrete

The large number of building and bridges built with prestressed concrete technique are very sensitive to natural deterioration and excessive environmental attacks. This is particularly true for the early prestressed concrete structures built in the past century. Over time, these structures are increasingly subjected to adverse effects due to corrosion such as pitting, stress corrosion cracking, and hydrogen attack (Bertolini, Elsener, Pedferri, Redaelli, & Polder, 2013). Corrosion is particularly favored by the following agents: nitrates favor stress corrosion cracking, sulphides favor hydrogen embrittlement. Chlorides are particularly harmful, as shown by the damage caused by de-icing salts on concrete constructions (Leonhardt, 1980).

These deterioration problems due to the mentioned phenomena raise serious concerns about the long-term durability, above all for early post-tensioned systems, which may suffer possible sudden and fatal consequences (fib, 2010) (ACI, 2014) (Ministero delle Infrastrutture e dei Trasporti, Consiglio Superiore dei Lavori Pubblici, 2020). For these structures, problems of corrosion may be accelerated by the poor quality materials and poor construction practices, possible at that time (Botte, Vereecken, Taerwe, & Caspeele, 2021). These issues are related to the lack of adequate procedures for the grouting phase, adequate provisions for durability and quality assurance within technical standards of that time.

Furthermore, these structures were built with experimental techniques at their time basing on design rules that did not take in account earthquake actions. Moreover, it must be added the potential decline of the residual capacity due to a progressive structural degradation caused by poor maintenance. In this context, for the prestressed concrete buildings that are part of XX century architectural heritage, the difficulties of adapting these structures to current building regulations increase.

As regards corrosion problems, it is important to avoid the entry of water, air, carbon dioxide and hydrochloric acid (Cl^-) by means of adequate sealing of the ducts. In addition, filling with a cement based product with a $\text{pH} > 13$ ensures a good corrosion protection of the steel. Another significant aspect in the protection of the strands is the concentration of Cl^- which must be below a critical value. This avoids the transition of the steel from a passive state to an active one. Cl^- can be present both as a background contaminant of the grout and coming from the outside (Theryo, Hartt, & Paczkowski, 2013).

The grout deficiencies which are of concern according to (Theryo, Hartt, & Paczkowski, 2013) are reported in the following:

- Cl^- concentrations higher than the limit set by current regulations.
- Grout segregation resulting in grouts (some unhardened) and free water which can lead to high concentrations of corrosive ions (hydrochloric acids and sulfates) in proximity of tendons or at high tendon elevations that can facilitate the corrosion.
- Grout subsidence which can lead to exposed wires in the resultant airspace.

In some cases, although Cl^- concentrations were below the specified limit, corrosion-induced tendon failures occurred soon after construction with respect to the expected service life. This indicates that incomplete duct filling (resulting in air voids), segregation and subsidence are major issues for post-tensioned structures and accelerate corrosion affecting the durability of the elements (Theryo, Hartt, & Paczkowski, 2013). Grout segregation problems are concentrate generally at the highest elevations of the tendons, and this indicates that gravimetric forces affect segregation.

3.4 Diagnosis of post-tensioned concrete structures

Post-tensioned systems generally require an extended and systematic program of inspection and diagnostic investigations to be performed as the basis for the subsequent analyses, in terms of assessments of durability and residual service life. Starting from the review of the as-built plans, the post-tensioned drawings, the specification and construction procedure, the program should incorporate accurate visual inspections and the most advanced diagnostic techniques, preferably in terms of non-destructive tests, or, where needed, of partially destructive tests.

Investigations should necessarily include traditional physical-chemical tests aimed at determining the strength of the materials, the geometric characteristics, grouting defects, carbonation front, steel corrosion and other chemical attacks (Breysse, 2012). Moreover, vibration based SHM can be exploited to guide local non-destructive methods to be used (endoscopies or radiographies).

Among the usual diagnostic objectives for prestressed concrete structures, the inspection and diagnostic investigations sometimes must face particularly challenging problems: for instance, accurately diagnosing corrosion or detecting grouting defects in post-tensioned cables in remote positions. Even greater criticalities are found when investigating the durability structural elements constructed with materials, technologies and patents that have not seen a great diffusion.

The partial rupture or corrosion of pre-stressing tendons may be difficult to detect exhaustively. In fact, it is difficult to diagnose any grout voids, as well as the level of severity of this phenomena. The most sensitive points are the higher parts of the cables in correspondence of the vents as well as immediately behind the anchorages. Where the cables are arranged vertically, radiography can help, but where the cables are arranged parallel horizontally, the masking effects make this technique impractical. Furthermore, if the sheaths are made of metallic material, even the pulsed radar can be ineffective. Even when gamma-rays or radar techniques are practicable, investigate the possible corrosion level requires a careful opening of the ducts. Another situation in which corrosion can occur is if the anchorages located outside the structure have not received adequate protection from atmospheric agents (Beckmann & Bowles, 2004).

The main non-destructive diagnostic techniques for post-tensioned concrete structures are: Impact-Echo method; Magnetic flux leakage method; X-Ray diffraction method; Ultrasonic pulse velocity; Acoustic emission; and Radiography. On the other hand, partially destructive diagnostic techniques are based on direct inspection (eventually accompanied by endoscopic investigations) of the post-tensioned elements which allow to locally verify: presence of voids, presence of corrosion, tendons defects; grout segregation and consistency; grout discoloration. As reported in (Theryo, Hartt, & Paczkowski, 2013), statistical grout sample collection and evaluations represent a useful technique to identify chemical or physical grout deficiencies. Detensioning techniques, X-Ray diffraction method, and Hardness tests can be used to evaluate the residual prestressing and strength.

Extensive experimental and numerical studies are present in the literature about the diagnosis of post-tensioned concrete structures. In many of these, the corrosion of pre-stressed concrete beams and the loss of prestress have been investigated through changes in the properties such as stiffness and ductility or vibration response such as natural frequencies and mode shapes (Kim, Ryu, Cho, & Stubbs, 2003) (Jeyasehar & Sumangala, 2006) (Capozucca, 2008) (Maas, et al., 2012) (Limongelli, et al., 2016). In other, magnetic flux leakage, radiography, guided ultrasonic waves and acoustic emission techniques have been used ((Ghorbanpoor, Borchelt, Edwards, & Salam, 2000) (Bartoli, Salamone, Phillips, Lanza di Scalea, & Sikorsky, 2011) (Moustafa, Niri, Farhidzadeh, & Salamone, 2014) (Appalla, ElBatanouny, Velez, & Ziehl, 2016).

Although each of these techniques has its advantages and disadvantages depending on the specific case, it is necessary to consider the clear difficulties in determining the residual prestress force and the level of corrosion in each single cable of a structure. Therefore, a statistical approach is required and sensitivity analyses are needed to evaluate possible severe decreases in residual capacity due to the corrosion increase or the stress loss in the prestressing strands.

Chapter 4

Preservation, retrofit, and reuse of modern heritage structures and case studies

This chapter presents the multidisciplinary approach required in the conservation of modern heritage structures, highlighting the main issues in this field. Particular attention is dedicated to of condition assessment activities, structural monitoring and preservation of this heritage, with emphasis on spatial architectures. In the final part, some examples of interdisciplinary approach to concrete spatial structures are reported.

4.1 Conservation of the XX century modern architecture

In the last decades, the XX century modern architecture appeared more at risk than during any other period. At the end of the 1980s, many modern masterpieces had already been demolished or had changed beyond recognition. This was mainly due to the fact, that many were not considered to be elements of heritage, that their original functions have substantially changed and that their technological innovations have not always endured long-term stresses (DOCOMOMO International).

The interest in the conservation of the XX century heritage works is growing. However significant buildings of this period are underrepresented on heritage registers from local inventories to the World Heritage List. In fact, many of these significant heritage architectures are unrecognized or undervalued, and are thus at risk and in need of deep analysis and protection. Several factors have caused this vulnerable situation. While heritage professionals and scholars have taken notice, general public awareness and appreciation has lagged. It can be difficult to overcome the perception that recent structures don't qualify as heritage, a notion that is reinforced by some national and local registers which include an age threshold for listed structures. This threshold typically range from fifty to seventy years from the time a building is constructed. This time is sufficient for many XX century works to fall into disrepair or to the wrecking ball (Macdonald & Ostergren, 2011).

Furthermore, concrete heritage structures have been made further vulnerable to changes that could compromise their significance values by the use of experimental or new construction materials that have not aged well, less durable materials, and experimental construction techniques (Macdonald & Ostergren, 2011). Moreover, there are many issues influencing the deterioration of the XX century heritage architectures. Some of the issues are the lack of recognition for its material values and reluctance to apply the accepted conservation methodologies, levels of investigation, and diagnostic and repair approaches, all of which can be seen as more expensive than standard repair approaches (Custance-Baker & Macdonald, 2015).

In fact, concrete repair is a large and well-established professional activity, which researchers, practitioners and industrialist have constantly fueled with new knowledge, products, and techniques. The same is not true for the conservation of concrete, which is still a relatively new but rapidly emerging field. In most places, architects, engineers, conservators, and contractors have little experience in concrete conservation, with limited specific information available to guide them. As the conservation of concrete draws on knowledge from both the concrete repair and conservation fields, there is a need for basic principles, founded on current best practices from both of these areas, to guide concrete conservation practice and to enhance outcomes for concrete heritage around the world (Macdonald & Arato Gonçalves, 2020).

A significant aspect is related to the execution of the investigations that aim to define the conditions and deterioration of the materials. These investigations should be undertaken by suitably qualified professionals. Moreover non-destructive and carefully considered non-invasive techniques should be preferred, in order to limit to the absolute minimum destructive analysis. Careful study into the aging of of the XX century materials' may be needed (ICOMOS, International Committee on Twentieth Century Heritage, 2017). Better decision-making and informed choices in concrete conservation will be achieved as the focus is shifted toward long-term repair and conservation solutions that incorporate long-term maintenance, and a progression in knowledge of the many challenges facing this material's conservation (Custance-Baker & Macdonald, 2015).

Another central theme in the field of conservation revolves around the concept of stratification of time and on its possible preservation, as well as on the readability of previous phases (Carbonara, 1996). The latter aspect, as an example, calls into question the issues of modification of some geometries for the structural and seismic improvement and/or alteration of surfaces following the use of cleaning, cortical and protective treatments. Regarding this, it is worth highlighting that, as far as the architecture of the 20th century is concerned, questions related to readability and reversibility are, as matter of fact, still open (Ceravolo, 2020).

Concrete provided an economical solution to the challenges of large-scale construction in the aftermath of World War II. In this way, concrete secured the position as the XX century's preeminent construction material. This is confirmed by the extraordinarily rich and diverse legacy of works provided by concrete's material, structural, and architectural development over the last two centuries. These works are increasingly recognized for their cultural significance (Macdonald & Arato Gonçalves, 2020). The obligation to preserve and manage these heritage places and sites is as important as our duty to conserve the significant cultural heritage of previous eras (ICOMOS, International Committee on Twentieth Century Heritage, 2017).

4.2 Issues in the conservation of concrete heritage structures

Despite increased recognition of the cultural significance of concrete heritage, there are still challenges to secure its conservation (Prudon, 2008). In recent decades, the concern has been widened by the efforts of DOCOMOMO (Documentation and Conservation of the Buildings, Sites and Neighborhoods of Modern Movement), an

independent international initiative, with an emphasis on the products of modern architecture. Addressing these challenges requires a convergent contribution from experts in Social Sciences and Humanities and Structural Engineering.

In fact, many of the features of XX century heritage - such as the application of advanced construction methods and materials, the role of architecture in social reform, and the development of new building types and forms - challenge traditional conservation approaches and raise new methodological and philosophical issues (Normandin & Macdonald, 2013). Concrete spatial structures were built with very limited seismic criteria, due to the lack of specific seismic regulations at the time of their construction. The need for an accurate condition assessment of these buildings arises for their restoration and renewal, particularly for those located in a seismic risk area.

General issues and gaps to be filled for the conservation of concrete heritage are (Custance-Baker & Macdonald, 2015) (Lenticchia, 2017):

- lack of data on deterioration mechanisms affecting historical materials (concrete and reinforcement) and construction techniques, and related implications for their conservation and/or repair;
- requirement for non-destructive testing of concrete structures to obtain reliable results from the investigation;
- lack of long-term and evidence-based data on the efficacy of treatment methods;
- Lack of agreements and standards on basic procedures and methodologies for concrete repair and conservation, oftentimes resulting in poor repairs or interventions that alter appearance;
- repair products are constantly being adapted, so information on their efficacy/use is not always available;
- lack of a robust body of literature on the conservation of concrete;
- the expected long term societal spill over effects on the rehabilitation, restoration and final use/reuse of XX century spatial structures requires analysis.

A significant starting point for preserving this kind of legacy that has been highlighted by different institutions and documents is the anamnesis phase. Work that is based on a deep understanding of a building's history, heritage significance, the state of health and current potential risks is essential for a good conservation. In

this context, a fundamental aspect is the use of the techniques and tools which allow to obtain as much information as possible with the least physical impact on the buildings. Unlike the historical architectures of previous centuries, for the XX century works it is usually possible to find some original documentation, models, and original material specifications. Moreover, in order to identify deterioration and develop proposals for conserving and repairing is fundamental to follow a thorough investigation and condition assessment. An accurate and detailed investigation campaign can be generally done thanks to available different diagnostic tools. For the development of a conservation strategy is also fundamental the prediction, or at least the understanding of the ongoing deterioration as well as the possible effects of different repair approaches.

In order to preserve this threatened architectural heritage the Madrid-New Dheli Document was developed by members of the International Scientific Committee on Twentieth-Century Heritage during 2017. This is a publication issued by the ICOMOS International Committee on Twentieth-Century Heritage (ISC20C) which contributes to provide some benchmark guidance about how to practically conserve and manage the XX century architectural heritage. In this text, as in the other documents about conservation of this heritage, it is underlined how the knowledge phase, maintenance programs and an interdisciplinary approach are important for the preservation of buildings.

Adequate research, documentation and analysis of the historic fabric are needed to guide any change or intervention. The integrity of the architectural heritage of the twentieth century should not be impacted by unsympathetic interventions. In this view SHM techniques may play a key role for the conservation of this kind of legacy.

4.3 Case studies

In this part of the thesis few case studies are discussed to demonstrate a correct approach in the condition assessment, monitoring and preservation of concrete architectural heritage. To this aim, in the following, some significant experiences that were obtained at the Politecnico di Torino on the condition assessment of iconic XX century heritage buildings are described. It is worth to highlighting the multidisciplinary skills required when dealing with this heritage.

In order to investigate with a multi-disciplinary approach the behavior and the criticalities of this heritage, historical research, surveys, diagnosis, and preliminary structural and dynamic analyses are required. The steps of an adequate path of knowledge for heritage structures can be the following: general identification of the structure and its environment factors; collection of geometric and structural data; identification of the materials and survey of their state of conservation, historical documentation; mechanical characterization of the materials by means of different investigation techniques; soil and foundation analysis, and relevant monitoring activities (Ceravolo, 2020). The documentation process, in particular, is useful for addressing aspects such as construction defects, irregularities, deterioration, damage caused by previous events, and in general any factor that makes each of these structures unique and involves a higher degree of complexity in the structural behavior interpretation (ICOMOS, ISCARSAH Committee, 2003). ICOMOS standards also emphasize the importance of periodic building controls as a primary tool for conservation.

In this context, monitoring activities play a key role for architectural heritage, both in assessment and preservation processes. Indeed, monitoring is not only a method to investigate the past of the structure, but it can play an active role in the conservation of historical buildings and influence decision making. After the collapse of Polcevera Viaduct by Morandi, the scientific community has once again stressed the paramount role of maintenance and continuous structural health monitoring (SHM) (Ceravolo & Lenticchia, 2019). The SHM approach in terms of structural assessment and retrofitting of Cultural Heritage buildings can be summarized in four steps: inspection, monitoring, modelling (or structural analysis) and intervention. The general strategy is represented in Figure 15 (Lorenzoni, 2013).

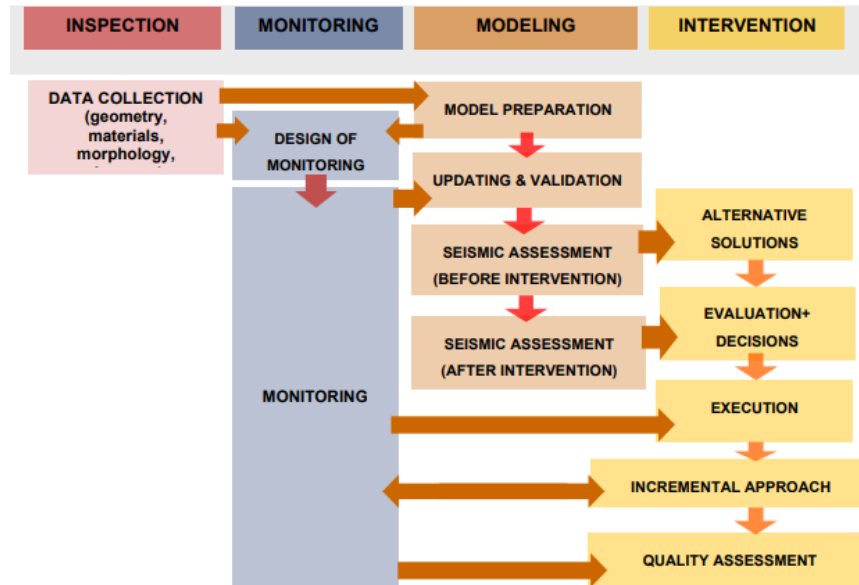


Figure 15: General knowledge-based strategy for the study and assessment of Cultural Heritage buildings

The case studies described in the following are reported in:

- Lenticchia, Erica; Miraglia, Gaetano; Quattrone, Antonino; Ceravolo, Rosario. “Condition Assessment of an Early Thin Reinforced Concrete Vaulted System.” *International Journal of Architectural Heritage*, 1-19, (2021).
- Ceravolo, Rosario. “Conditions assessment, monitoring and preservation of some iconic concrete structures of the 20th century. (Keynote lecture) *IABSE SYMPOSIUM Wroclaw 2020 – Synergy of Culture and Civil Engineering – History and Challenges*, (p. 58-82). Wroclaw, Poland, (2020).
- Ceravolo, Rosario; Lenticchia, Erica. “Diagnosis and preservation of 20th Century architectural Heritage: from the first thin shell solutions to the iconic structures built by Pier Luigi Nervi and Riccardo Morandi in Turin. (Keynote lecture) *7th Structural Engineers World Congress*, (p. 165-179). Istanbul, Turkey, (2019).
- Ceravolo, Rosario; Coletta, Giorgia; Lenticchia, Erica; Li, Lili; Quattrone, Antonino; Rollo, Simone. “In-Operation Experimental Modal Analysis of a Three Span Open-Spandrel RC Arch Bridge.” *In International Conference on Arch Bridge*, (pp. 491-499). Springer, Cham, (2019).

4.3.1 Paraboloide of Casale Monferrato: an outstanding example of historical thin shell concrete structure

(Lenticchia, Miraglia, Quattrone, & Ceravolo, 2021) have recently presented the structural condition assessment of a historical thin shell concrete structure in Casale Monferrato (in Italy). The “Paraboloide” of Casale Monferrato is a former clinker warehouse built in 1922 for the Italcementi factory (Figure 16).

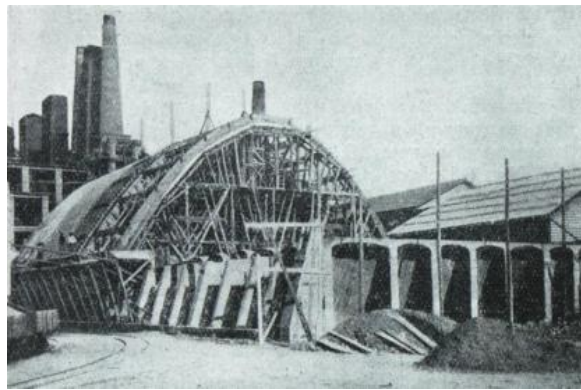


Figure 16: A photo showing the construction of the clinker warehouse named Paraboloide (Santarella, 1926)

The Paraboloide is the first structure in Italy to be built with a thin concrete shell parabolic-shaped. This structural typology subsequently spread throughout the whole country (Modica & Santarella, 2015). The building has a rectangular plan with a tower in concrete positioned on the north-east side. Parabolic arches supported by concrete buttresses constitute the principal structure. Reinforced concrete tie-beams counteract the thrusts coming from parabolic arches. Reinforced concrete pillars contrast the deflection of the ties. The arches support a system of ribs on which thin shell elements rest (Figure 17).



Figure 17: Paraboloide of Casale Monferrato: external (left) and internal (right) views

Some drawings of the Paraboloid were illustrated in the popular construction textbook of Santarella (Santarella, 1926). These drawings report interesting details of the main structural elements as well as their reinforcements (Figure 18).

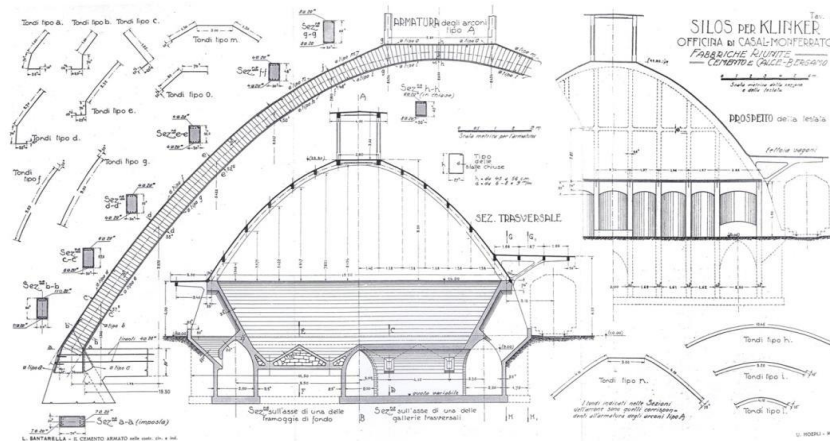


Figure 18: Original drawing reported in Santarella’s manual (Santarella, 1926): silos project for clinker warehouse in Casale Monferrato. Designer Eng. Radici

Due to the particular structural configuration and the lack of original drawings, a metric survey using laser scanner technology was carried out (Invernizzi, Spanò, & Chiabrando, 2019) (Cestari, Chiabrando, Invernizzi, Marzi, & Spanò, 2014), in order to made an accurate 3D model. The Municipality of Casale Monferrato is considering to rehabilitate the Paraboloid for a possible transforming in a “cultural pole”. Both mechanical and dynamic investigation tests were carried out to assess the current state of the building as well as the compatibility with the foreseen uses. This accurate and detailed testing campaign constitutes the initial step in the conservation and rehabilitation process of the Paraboloid.

In particular, the results of the mechanical tests were used to inform a numerical model of the building. This model allowed to carry out the structural condition assessment. The tests have greatly helped in the identification of the dynamic and mechanical performances regarding both local aspects (quality of the materials and connections) and global aspects (dynamic behavior). The connection level between the macro components has been analysed exploiting the dynamic tests and the corroboration of the FE model.

A widespread deterioration and marked damage phenomena affect the structure (Figure 19). The aging phenomena and the degradation due to the lack of durability specification in that period influenced the poor state of conservation. Moreover,

although the historical value of the building has been recently recognized, unfortunately, it has been in a state of neglect for many years.

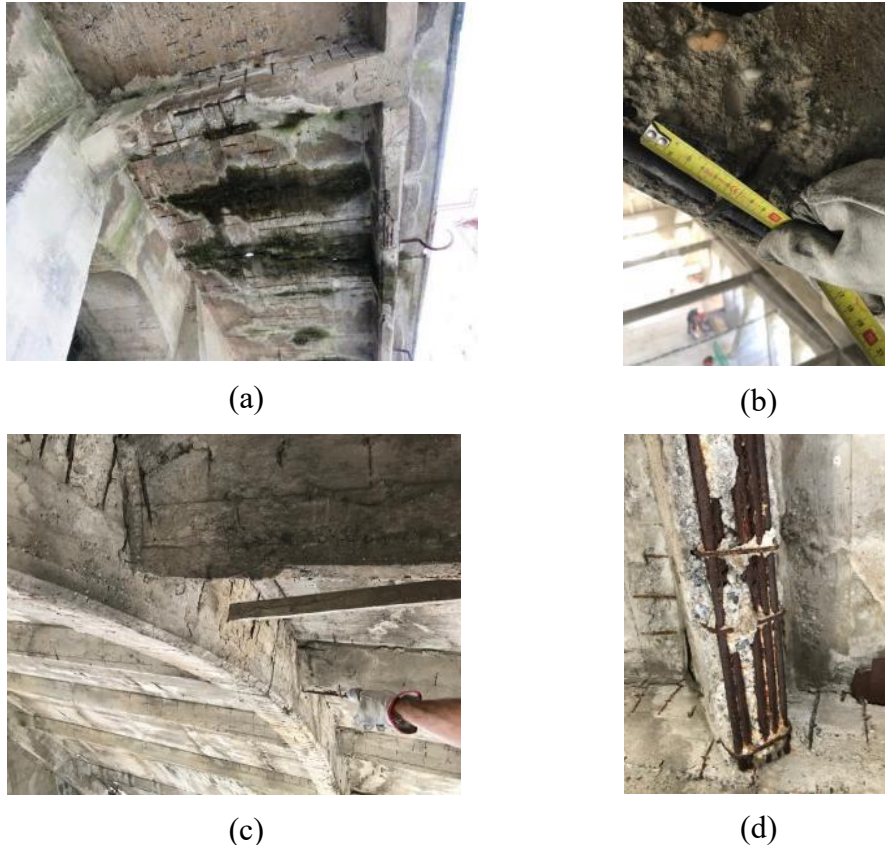


Figure 19: Structural deterioration and damage: (a) water staining and bio growth on the elements; (b) a detail of the exposed bars of a parabolic arch; (c) exposed bars on the arches; (d) exposed bars and detachments of concrete of the roof elements (Lenticchia, Miraglia, Quattrone, & Ceravolo, 2021)

Mechanical tests have included non-destructive, semi-destructive, and destructive tests on the main structural elements: core extractions, pull-out tests, ultrasonic tests, and cover meter scans. The results of compressive tests on the cores have revealed an uneven picture of concrete mechanical properties: modest for the reinforced concrete elements (joists, tie-rods and arches); poor in the lower part of the building (edge beam and buttresses). Then, the consistency of these results has been confirmed comparing them with the mechanical properties of the concrete of the period reported in literature. Moreover, it has been noticed that elements without reinforcement have bigger aggregates than the reinforced ones.

Dynamic tests have been designed to capture the main vibrational modes of the parabolic roof as well as to reach the following goals: investigate the interaction between the main hall and the tower with specifically designed setup; complete the information on mechanical characteristics obtained with mechanical tests; clarify the nature of the connections between buttresses and arches. The results of the dynamic tests have been then used to corroborate the FE model. In particular, Setup 1 has been designed to measure the vibrations of the central portion of the main hall (Figure 20a). Whereas, Setup 2 (Figure 20b), designed to investigate the connection between the hall and the tower, allowed to understand that the mutual influence by the macro-components is negligible.

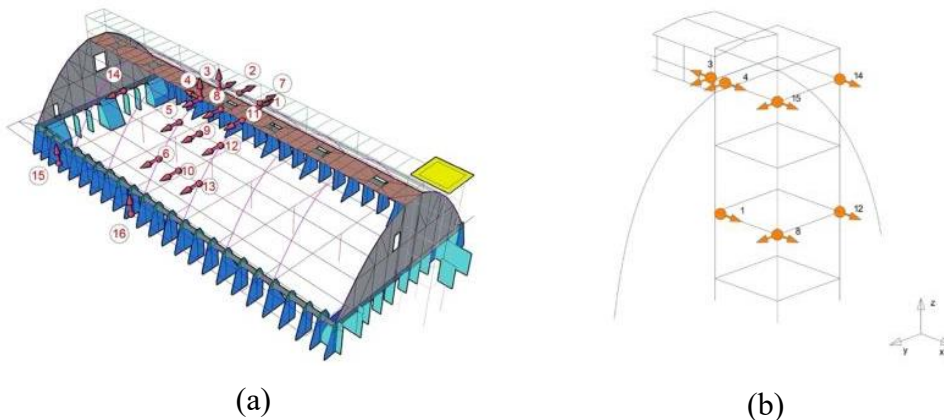


Figure 20: Axonometric scheme of the structure showing sensor positioning in Setup 1 (a) and Setup 2 (b) (Lenticchia, Miraglia, Quattrone, & Ceravolo, 2021)

The first two main modes identified with Setup 1 are reported in Figure 21.

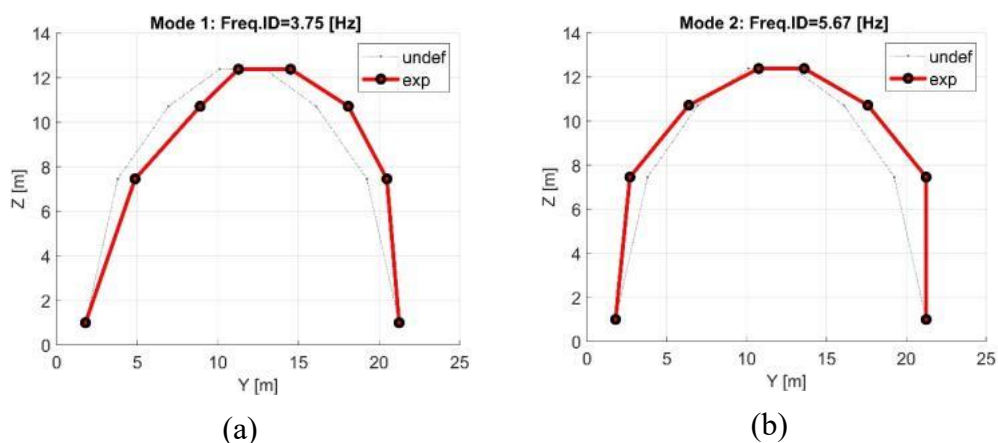


Figure 21: Horizontal components plots of the main identified modes of the Paraboloid: (a) first mode; (b) second mode (Lenticchia, Miraglia, Quattrone, & Ceravolo, 2021)

The first attempt FE model, obtained considering the mechanical properties according to current standards and regulations, has shown a good accordance only for the first modal shape. The second model has been corroborated using the information acquired both from the mechanical tests and the dynamic test campaign (Setup 2). In particular, for the macro-elements for which tests were available, the experimental Young's moduli, appropriately treated, have been used. Moreover, the model was modified as the tower has been omitted from the main structure of the Paraboloid. This modification in the FE model led to a better correlation in the first mode shapes of the structure with first experimental one.

From the experimental investigation, main criticalities are emerged about the behavior of the buttresses/tie-rods nodes connection (due to a lack of reinforcements) and the consistency of the tie-rods. In fact, while the global dynamic response of the structures is not importantly affected by the tie-rods, the static and seismic assessment performed with current standards has shown that a removal of these elements would result in a significant reduction of the safety levels, due to excessive shear force in the buttresses.

In conclusion, the degree of connection between arches, buttresses and tie-rods has been assessed with Model Updating techniques, basing essentially on natural frequencies and mode shapes. In particular, the optimization algorithm reported in (Ceravolo, De Lucia, Miraglia, & Pecorelli, 2020) has been adopted and the main five modes identified have been used to update the Young's moduli in the model by minimizing the difference in natural frequencies and modal shapes (Ceravolo, Pistone, Zanotti Fragonara, Massetto, & Abbiati, 2016). Both the actual material state and the macroscopic condition such as widespread or localized cracks have been considered in updating the parameter values. The used strategy was constituted by two phases: (i) a single multiplying factor acting on the Young's moduli of all the model elements was updated; (ii) reduce the number of variables to be updated, considering the knowledge acquired by the in-situ inspections and pay particular attention on the components with greater uncertainties (nodes connections). The first two mode shapes from the updated model are depicted in Figure 22. The Modal Assurance Criterion (MAC) has been used for the comparison between numerical and experimental mode shapes.

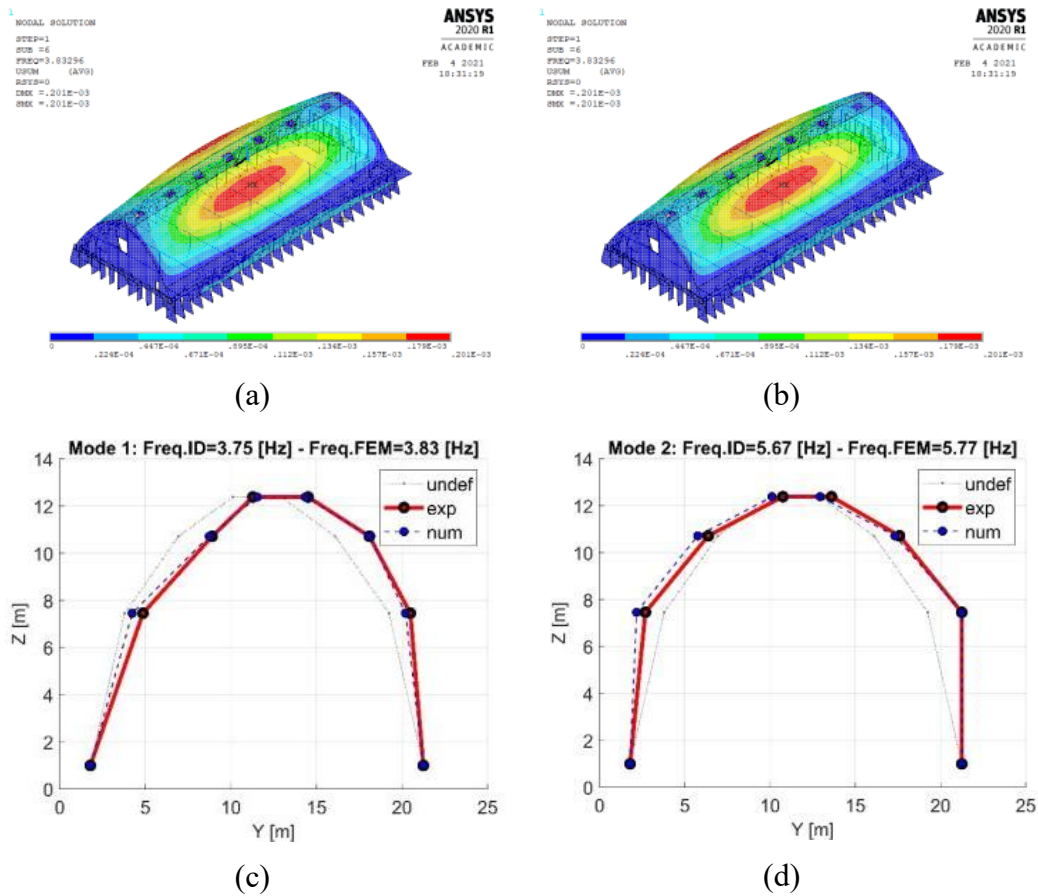


Figure 22: First two mode shapes from the updated numerical model: (a) first mode; (b) second mode; (c) first mode compared with the experimental identified; (d) second mode compared with the experimental identified (Lenticchia, Miraglia, Quattrone, & Ceravolo, 2021)

One of the most important conclusion is that in this kind of structures non-monolithic behavior and material dislocations lead to appreciable stiffness reductions, which can be detected even under ambient excitation.

4.3.2 Example of vibration-based structural health monitoring of a reinforced concrete arch bridge

(Ceravolo, et al., 2019) have presented the vibration-based condition monitoring resulted from a testing campaign conducted on a historical reinforced concrete arch bridge, the Lamberti bridge. The Lamberti bridge was built in 1933 in the Tuscan-Emilian Apennines over the Ceno river (in Italy). The bridge is constituted by three spans of 38 m long each, which are supported by three arches each (Figure 23a).

The spans are disconnected by joints at the level of both the deck and the vertical elements (Figure 23b).



Figure 23: Lamberti bridge over the Ceno river (a); joint connecting two spans (b)

The dynamic tests were performed on November 2018 with an acquisition system consisted of mono-axial piezoelectric accelerometers and Linear Variable Displacement Transducers (LVDT) for dynamic displacement measurements (Figure 24). LVDTs are highly sensitive electromagnetic devices adopted to measure slight displacements over time.



Figure 24: Mono-axial accelerometers (a); LVDT at joint (b)

Figure 25 reports the layout of the two main setups used to investigate the global behavior of the bridge, aiming to maximize the spatial resolution of the experimental modal shapes. In the Setup 1, in order to measure the relative displacements between the arches, the LVDTs were positioned at the joints between the different spans in both the horizontal directions of the deck. The signals were acquired at 512 Hz for 45 minutes during the regular flow of vehicular traffic.

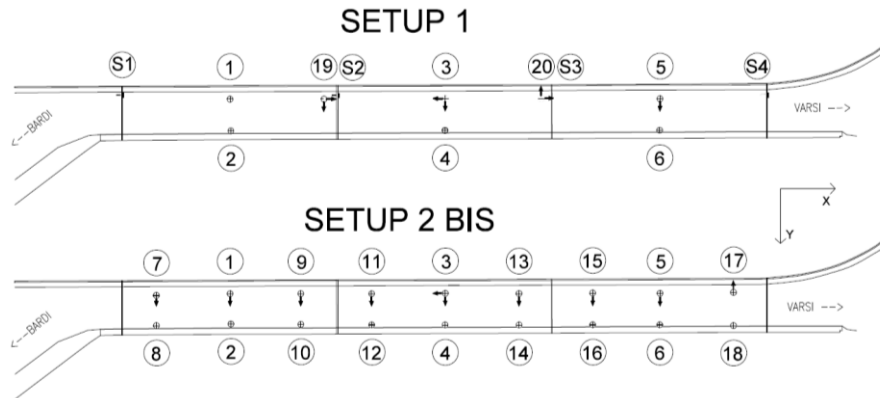


Figure 25: Acquisition setups for the dynamic characterization of Lamberti bridge (Ceravolo, et al., 2019)

A time domain algorithm of the Stochastic Subspace Identification (SSI) family has been adopted, corresponding to the third algorithm considered by the unifying theorem of Van Overschee and De Moor, known as “canonical variate analysis” (CVA) (Van Overschee & De Moor, 2012) (Ceravolo & Abbiati, 2013).

The complexity of dynamic behavior of the Lamberti bridge, resulted in the high density modes (Figure 26), has been ascribed to several factors: i) local dynamics due to the presence of multi-connected elements; ii) presence of joints between the arch spans; iii) presence of compliant restraints and connections; iv) degradation state of the materials.

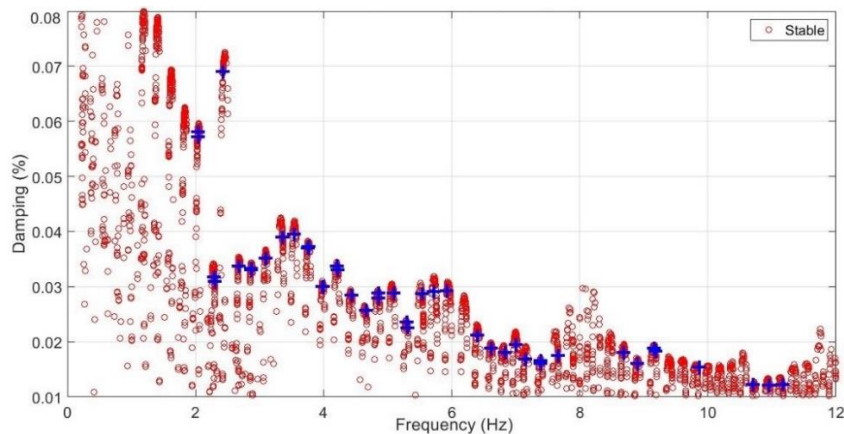


Figure 26: Dynamic characterization of Lamberti bridge with Setup 2-bis: clustering diagram with stable frequencies in blue colour (Ceravolo, et al., 2019)

The vibration modes (Figure 27) appear to be affected by the deformability of the joints, which separate the transverse dynamic behavior of the deck in three blocks, corresponding to the three arches. Some concerns about the transverse response of the bridge are raised from the disconnection at the deck, confirmed also

by the transverse displacements measured under the passage of heavy vehicles by LVDTs.

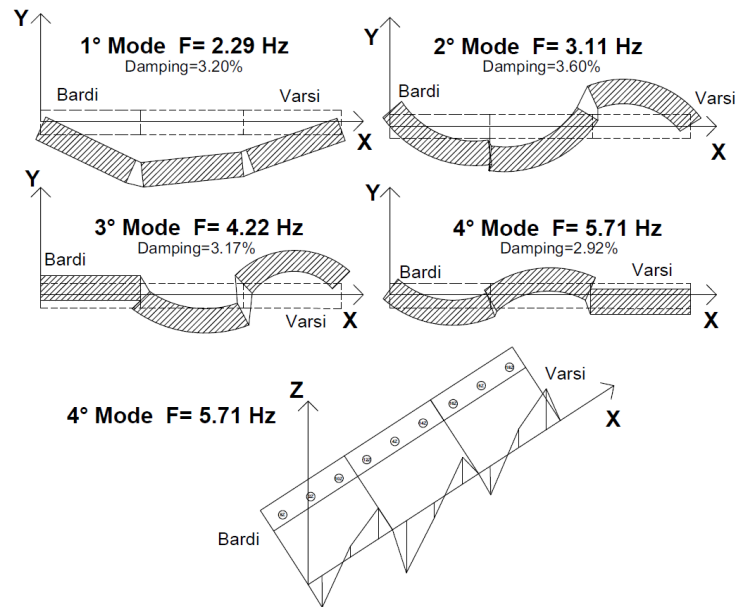


Figure 27: Schematic representation of the first four experimental modal shapes (Ceravolo, 2020)

The model corroboration has been obtained starting from the preliminary one with a standard indirect (penalty) method (Friswell, Mottershead, & Ahmadian, 2001), referring to the experimental modes (main modal frequencies and shapes). The spatial distribution of mass and stiffness has been taken into account in the FEM subdividing into portions considered homogeneous. A homogeneous material was attributed also to the joints, to simulate a degree of connection. The Modal Assurance Criterion (MAC) has been used for the comparison between numerical and experimental mode shapes. Figure 28 reports the values of the Young's moduli resulting from the calibration and the comparison between the identified frequencies and the frequencies of the FE updated model, also in terms of MAC.

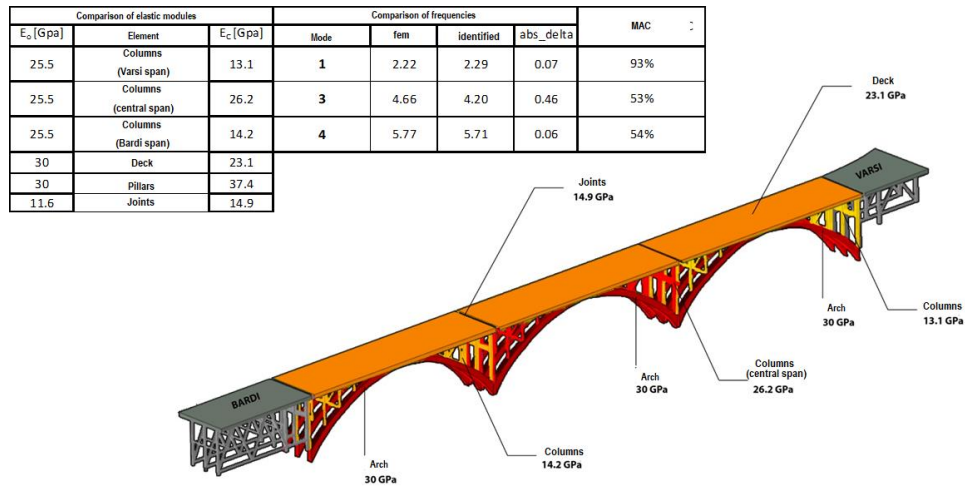


Figure 28: Lamberti bridge: results of the model updating process (Ceravolo, 2020)

The updated model has confirmed the inhomogeneity between the different elements of the bridge. The deformability of pillars has been associated to degradation phenomena in the external spans. The arches appear to be in relatively good conditions from the updated model, consistently with their important static function and with the fact that they are mainly compressed.

Chapter 5

Structural and seismic safety evaluation methods: a critical review for modern heritage structures

This chapter presents a critical review of structural and seismic safety evaluations methods applied to modern heritage structures. Starting from the evolution of structural and seismic safety standards and methods, this chapter presents and analyzes the safety assessment for modern heritage structures. In the final part, is introduced the role of models in the structural analysis and preservation of modern heritage structures.

The main goal of this chapter is to describe the methodological aspects in the safety assessment of concrete heritage structures, and the inevitable interaction between these aspects and those of conservation field for this heritage, which were described in the previous chapter.

As pointed out in the previous chapter, when dealing with the study of this heritage, multidisciplinary approaches are required, involves historical research, surveys, diagnosis, and preliminary structural and dynamic analyses in order to understand the behavior and the vulnerabilities of these buildings. In detail, it has

been described the path of knowledge articulated into various steps that a heritage structure requires. This path of knowledge is described in deep in the following, considering the current codes and standards implications, such as the levels of knowledge, the confidence factors and modelling techniques.

5.1 Evolution of structural safety codes and regulations

Regulations and codes are instruments with the scope of protect the safety, health and welfare of people and the environment from losses of various kinds due to specific events and conditions that may occur. The general terms “regulations” and “codes” includes different typologies of documents, ranging from legal ones at one end to recommendations at the other end such as legal acts, by-laws, regulations, codes, specifications, standards, codes of practice, recommendations and guidelines. Building codes have a long recorded history: the Code of Hammurabi, dating from about 1750 B.C., defined what happened to a builder if the building collapsed causing death, injury or loss of property. This Code was a purely legal instrument with no technical criteria (Blockley, 1992).

In addition, other civilizations, such as the Roman, also had building regulations. Generally, these design methods were based on predetermined proportions and dimensions according to the spaces defined by the structural elements. Some of these were recorder in the manuals of that time or by authors. In the middle ages, however, the rules were often transferred often in the trade guilds in the form of verbal rules (Beckmann & Bowles, 2004). The history of building codes in London represent a model for the modern building regulations development. It started in 1189 with the first technical requirements because of devastating fire frequently occurred. Additional specifications introduced at that time included the fixing of joists in walls. In 1666, after the great fire that swept through the city, the development of comprehensive regulations for the reconstruction of London began. These codes, which also included structural requirements on masonry walls thickness and sizing of wood framing, provided the basis for modern building standards (Blockley, 1992).

The first rules-of-thumb for structures were developed also by trial and error, some of the great medieval cathedrals suffered collapses, especially when their builders crossed the frontiers of technology. These rules-of thumb were still based on criteria in the form of span-to-size ratios for floor beams and height-to-thickness ratios for walls. As mentioned, early building codes gradually incorporated and

recorded most of these rules-of thumb. In particular, some of these early regulations survived until the middle of the nineteenth century (Beckmann & Bowles, 2004).

Thanks to the subsequent theory of elasticity came the possibility, under certain assumptions, to evaluate stresses in structural elements. An initial method, which led to the first definition of Factor of safety, was based on testing prototypes or on reduced scale models of entire structures subjected to a force slightly greater than its working force and checking its deflections. Another main method to define the Factor of safety was based on the comparison between the calculated stresses and the material strengths, evaluated with specific tests on standard samples and indicated in building regulations. In particular, in order to define a comprehensive design methodology, allowable stresses were introduced. Allowable stresses were derived from the tested strengths (indicated in standards specifications) by division by Factors of safety. These factors were agreed by committees composed of experts, design practitioners and representatives of vested producer interests. Factors of safety were intended to take account of the variability of the material, the inaccuracies in the design assumptions as well as other variables affecting the strength of the element. Sometimes the Factor of safety was incremented to cover serviceability considerations, e.g. to limit deflections (Beckmann & Bowles, 2004).

The first Italian building regulations for reinforced concrete structures appeared in 1907 due to the contributions from Guidi and Canevazzi. These buildings regulations dealt mainly with construction requirements, but did provide some guidelines for design. As mentioned, these guidelines adhered to the trend emerging at the time in Europe, based on the works developed by Coignet and de Tédesco in France and by Ritter and Mörsch in Switzerland, adapting the theory of elasticity to the new heterogeneous material. As in most European countries, Italian building code requirements for structural concrete evolved gradually between 1920 and 1940 into a system of more detailed technical recommendations, but still founded on the same conventional adaptation of the theory of elasticity to reinforced concrete (Levi & Chiorino, 2004).

Italian researchers, particularly in the last half century, have made significant contributions to the progress of the technical culture and to development of a real science of building with concrete. During this period, the need to master the extraordinary possibilities deriving from technical advances in concrete, particularly in the area of prestressing, promoted the development at the international level, with significant contributions of Italian specialists, of a

renovated scientific approach to structural concrete. Many researchers have contributed to the establishment of an internationally harmonized system of codes. Eventually, as cooperation within the European technical community arose, a harmonization between countries as to the conceptual basis of national standards was achieved (Levi & Chiorino, 2004).

Subsequently, the allowable stress design method was substituted from the limit states design method. Moreover, although convenient for the designers and for the checking authority, the application of a single factor of safety could be unnecessarily restrictive for one structure, while for another it could provide an inadequate level of safety. This unsatisfactory aspect over time led to the development of the 'partial factor' approach. With this approach separate partial factors were applied to the strength of the material, to the inaccuracies in design and construction, and to the loads. Many efforts have been invested for the determination and the calibration of these partial safety factors for the new design codes (Beckmann & Bowles, 2004).

A brief summary of the structural safety methods has been reported in the following (Beckmann & Bowles, 2004):

- Until XVIII century: Rules-of-thumb such as "the thickness of a wall should be equal or greater than its height divided by a certain number".

- First half of XIX century:

$$\text{Factor of safety} = \frac{\text{failure load of prototype in test}}{\text{working load on component in structure}}$$

- Second half of XIX century - 1970s:

$$\text{Factor of safety} = \frac{\text{strength of standard test specimen}}{\text{calculated stress in structural member}}$$

- 1970s: The strength of the structural member divided by the partial 'strength' factor ' γ_M ' must be greater than the load effects multiplied by the partial 'load' factor ' γ_L '.

It is interesting to highlight that in 1992 Blockley recognized the materials deterioration as one of the most serious concern of structures. In fact, structural

engineers, who are called to evaluate deterioration and recommend repairs, must be able to understand deterioration with a high level of professional competence (Blockley, 1992). This has required education and the development of limit states criteria also for durability in construction codes. The introduction of durability as well as estimated life into structural engineering has meant that maintenance and repair have become essential aspects for the structures.

Another aspect to pointed out, as shown in paragraph “5.3 Safety assessment of modern heritage structures”, is that many existing reinforced concrete structures have been designed mainly considering the vertical loads with very few or non-existent seismic provisions. The first introduction of some seismic zones in Italy happened in early 900, after the destructive Messina and Reggio Calabria earthquake (1908). Consequently, the cities hit by the earthquake were placed on a list. This list was updated by adding new cities after the occurrence of other strong earthquakes. The first standard that established a national classification of seismic hazard with special requirements for seismic zones, with the drafting of technical regulations, is the Legge 2/2/1974, n. 64 (Legge n. 64, 2 febbraio 1974), “*Provvedimenti per le costruzioni con particolari prescrizioni per le zone sismiche*”. The national seismic classification of this standard was obtained by the evolution of the knowledge of seismic phenomena. The DM 3/3/1975 (Decreto Ministero per i lavori pubblici, 3 marzo 1975) enacted the first seismic provisions, subsequently supplemented by a series of successive decrees. These decrees were accompanied by ministerial circulars containing some relevant technical information.

Significant seismological characterizations was conducted after the earthquakes of Friuli Venezia Giulia (1976) and of Irpinia (1980). In fact, an increase in knowledge on seismicity and an updated seismic classification of the national territory followed these two events. This led to the issue of various decrees approved between 1980 and 1984, defining the Italian seismic classification. After the earthquake of 2002, which has interested the territories on the border between Puglia and Molise, the Department of Civil Protection (DPC) has adopted the OPCM (Ordinanza del Presidente del Consiglio dei Ministri n. 3431, 2005), to provide a response to the need for updating the seismic zonation and seismic provisions (Elefante, 2009).

The main innovations in this legislation were: i) the replacement of the allowable stress method in favour of the limit state method, with particular attention to proper structural modelling analysis, ii) the extension of the seismic zonation throughout the entire country. In fact, in the OPCM, the entire national territory has been classified as seismic and is divided into 4 zones, characterized by decreasing seismic hazard. These zones have been identified by 4 classes of peak ground acceleration with a probability of exceedance of 10% in 50 years. In this new identification of seismic hazard, were provided the seismic design standards with different levels of severity (Ordinanza del Presidente del Consiglio dei Ministri n. 3431, 2005). The OPCM was the first regulation in Italy with a close link with Eurocode 8 (CEN, EUROCODE 8, 2005), the system of codes already established in Europe. This new generation codes have substituted the conventional design and purely prescriptive approach with a performance-based approach. Moreover, with the OPCM, for the first time the problem of appraisal of existing structures was explicitly addressed and an entire chapter was dedicated to it (Elefante, 2009).

With the DM 14/09/2005 (Ministero delle infrastrutture e dei trasporti, 2005), the “Technical standards for construction” have been published. These standards constitute the first attempt towards unification in one text of the design and assessment criteria for different construction types. This uniform code contains both the mechanical materials properties and the definition of loads, which are fixed base on the level of safety to be achieved and the minimum performance expectations for structures. Subsequently, with the DM 14/01/2008, the “New Technical standards for construction” (NTC2008) (Ministero delle infrastrutture e dei trasporti, 2008) are approved, resulting from the revision of standards approved in 2005. Finally, with DM 17/01/2018, the current “Updating of Technical standards for construction” (NTC2018) (Ministero delle Infrastrutture e dei Trasporti, 2018) are approved. These standards are accompanied by the ministerial circular (Ministero delle Infrastrutture e dei Trasporti, 2019), which contains some relevant technical information.

The new standards, which in general pursue the basic approach of the 2005 codes, introducing some changes. The main changes are:

- the consideration of the coordinates of the location and class of use of the building for defining seismic intensity parameters;

- slight variations in load factors and their combination;
- redefinition of the shear capacity assessment for reinforced concrete members;
- definition of design rules for performance-based design and the parameters to achieve a high or low ductility;
- redefinition of some parameters in the check of the load-bearing capacity of foundations;
- slight changes in the structural behavior factor q expressions.

Definitely, the function of a design code is to regulate design so that the resulting artefact is safe, serviceable, economical and ensures uniformity of all designs for a certain type of construction. A design code, then, is a common standard against which all constructions of the same type are to be measured. By this very definition the code must be a 'minimum' standard (Blockley, 1992). Gibson defined the performance based approach in (Gibson, 1982) as “the practice of thinking and working in terms of ends rather than means. It is concerned with what a building or a building product is required to do, and not with prescribing how it is to be constructed”. Therefore, the approach aims at the required performance for the construction.

Nowadays, most of the national structural engineering codes across the world use performance based design. Anyway, new constructions account for only a small percentage of the total building inventory, and this is particularly true for developed countries. The application of the codes developed for new buildings to existing buildings could be misleading and inappropriate. In fact, in the case of existing buildings the situation is extremely more complicated due to the high individualities and the huge differences with respect to the age of construction, the condition of the existing building and also with respect to the social environment (IRCC, 2008).

5.2 Structural safety methods

One of the main aspects about structural safety concerns the delicate balance between cost and safety. In fact, as the knowledge of structural systems behavior develops, it is clearly desirable to use that knowledge to reduce the cost of an artefact, being able to predict with greater certainty how that artefact will behave in use. As a consequence, the need to consider this balance has led to the developments of reliability theory. On the other hand, the introduction of new approaches in structural design, such as the concept of limit state design implemented in many

codes worldwide, provoked initially controversy, causing much concern and debate in some professional engineering circles (Blockley, 1992). For example, some of the common criticisms, in particular concerning the use of partial factors, seem to be that limit state design:

- results in long and complicated regulations;
- depends upon an inappropriate use of statistics and probability;
- is more complicated than previous methods;
- removes the need for engineering judgement;
- cannot deal with the fact that uncertainty is different and prescribed factors are not appropriate when uncertainty varies from site to site.

Numerous sources of uncertainties arise in the analysis and assessment process. Uncertainties can arise from randomness inherent in nature or from a lack of knowledge and ignorance. Being equally important, both types of uncertainty must be considered in structural safety problems (Wen, Ellingwood, Veneziano, & Bracci, 2003). Conservative assumptions (worst-case scenario postulation and factors of safety application) are used by engineers to deal with risk and uncertainty. Such approaches provide an unknown margin of safety against the failure state, however it is defined. In recent decades the use of reliability and risk analysis, based in the mathematics of probabilistic and statistics, has grown in order to support decision making in the presence of uncertainties.

A brief review of different methods to solve engineering safety problems is reported in the following.

5.2.1 Deterministic method

The design approach, which evolved from the application of elasticity theory, is called the allowable stress method. This method computes the stresses σ by linear theory for the maximum loads that can be expected during the life-span of the structure, and it compared these stresses to allowable stresses σ_{all} , which are obtained from the limiting stresses σ_{lim} , divided by a factor of safety FS. σ_{lim} represents the stress levels where linear elastic theory ceases to apply, that is where the material yields or the structure becomes unstable. The magnitude of factor of safety has been one of the crucial issued in design codes and it evolved historically, from high values when a technology is just starting to gradually lower values until a lower ceiling, dictated by common sense and by successful and unsuccessful

experience, is reached. According to (Blockley, 1992), Table 2 reports an example evolution of the allowable stress evolution for mild steel in the USA.

Table 1: Evolution of the allowable stress for mild steel structures in the USA (Blockley, 1992)

Year	Minimum yield stress (MPa)	Factor of safety	Allowable stress (MPa)
1890	197	2.00	98
1918	190	1.72	110
1923	228	1.83	124
1936	228	1.65	138
1963	248	1.67	149

Many civil engineering structures of the twentieth century have been designed with this method.

5.2.2 Semi-probabilistic method

Current codes and standards allow the assessment of structural safety using the semi-probabilistic method, which is based on the definition of the limit states. As defined by Ditlevsen and Madsen (Ditlevsen & Madsen, 1996), “the concept of limit state related to a specified requirement is defined as a state of the structure including its loads at which the structure is just on the point of not satisfying the requirement. Often the requirement is verbally formulated. However, usually the requirement will be interpreted and formulated within a mathematical model for the geometric and mechanical properties of the structure and for the actions on the structure.”

The semi-probabilistic method, also known as the first level approach, is closer to the probabilistic one (described later), with the difference that are introduced partial safety factors to the characteristic values of the load and resistance. According to this method, the structural engineer has to ensure that:

$$\gamma_S S_k \leq \frac{R_k}{\gamma_R} \quad (1)$$

where the characteristic values S_k and R_k are defined as an upper and a lower percentile p , respectively (with p usually equal to 0.05).

$$P[S > S_k] = p \qquad P[R < R_k] = p \qquad (2)$$

The coefficients γ_S and γ_R represent the partial safety factors, which are greater than 1 and come from probabilistic and statistical considerations. It should be highlighted that safety factors are not a protection against gross human error, inexperience, lack of judgement, greed, carelessness and other unfortunate events, which cause the predominant share of the known structural failures (Blockley, 1992).

5.2.3 Probabilistic method

The traditional interpretation of deterministic method (allowable stress design) is:

- The behavior of all the elements of the construction is linearly elastic at service loads.
- If the service loads are selected to be high enough so as to have a small chance of being exceeded and if the allowable stresses are chosen to be a small enough fraction of a limiting stress then the structure will have an excellent chance of serving out its allotted time without experiencing damage or distress.

Various objections arises from this way of approaching to the design safety problem from economic, probabilistic and scientific standpoints (Blockley, 1992):

- If all the constructions designed by allowable stress method have a consistently good record of performance, then there must be many members of this set that are overdesigned; therefore some structures are too expensive.
- Strain and stress are not always linear, e.g. the stress-strain curve of concrete is non-linear even for small stresses.
- Time effects (creep and shrinkage of concrete) and loading rate effects represent a non-linearity in time and space.
- Load effect and deformation are not always linear.

- The load-deformation behavior past the theoretical limit of linear response may be brittle or ductile (with a different reserve of post-yield capacity).
- In some circumstances, it is necessary to use the energy absorption capacitance of the non-linear range to resist seismic actions.
- The possibility of exceeding the limit state of the onset of non-linearity depends on the statistical characteristics of the materials, the loads, the idealizations used to devise a computational model, etc. The reliability of the elements within the structure or the reliability of different structures can thus vary considerably.
- New construction materials and design techniques must undergo years of trial and error until an acceptable safety factor can evolve.

These discrepancy between the real behavior of constructions and the safety problem analyzed with the deterministic approach, as well as the uncertainties regarding the allowable stresses approach, led the engineers to try to deal the structural safety problem by defining probabilistic approaches. According to these methods, the resistance of the structural elements and the loads are modelled through aleatory variables describing the intrinsic uncertainty of these parameters. This uncertainty is caused by a very large number of phenomena that cannot be modelled in a deterministic framework (Ditlevsen & Madsen, 1996).

Probabilistic method is based on the definition of the limit states. In particular, the safety problem can be expressed by the following equation:

$$S \leq R \quad (3)$$

where S is the demand expressed in performance terms and R is the available capacity. The threshold of the limit state corresponds to the equality in the previous equation.

For each limit state it is possible to define the relative limit state function and identify a domain of significant variables (an R - S space). This domain is divided in a "safe domain" where inequality is verified and a "failure domain" in which it is not. The probability of failure and reliability of the system can be determined, respectively, as the probability that the limit state function is less than zero or not:

$$\begin{aligned} P_{failure} &= P[R - S < 0] \\ P_{success} &= 1 - P_{failure} = P[R - S \geq 0] \end{aligned} \quad (4)$$

5.2.4 Exact probabilistic method

Introducing the joint probability density function (JPDF) $f(X)$ of the vector X representative of the random variables characterizing the problem under consideration, the probability of collapse (failure) can be defined as:

$$P_{failure} = \int_{\Omega} f_x(X) dx \quad (5)$$

where Ω is the failure domain.

Moreover, can be defined a limit state function $G=G(X)$ as:

- $(G(X) > 0) \rightarrow (success)$
- $(G(X) < 0) \rightarrow (failure)$

The limit state can be written as $G(R,S) = R-S$ where S and R represent the two random variables (load and resistance). With this assumption, can be written:

$$P_{failure} = \int_{G(X) < 0} f_x(X) dx \quad (6)$$

The problem is apparently reduced to the solution of this multidimensional integral. However, the solution in closed form of this integral is possible only under very restrictive circumstances and in very rare cases. In particular, to solve this structural reliability problem with the total probabilistic method is necessary: determinate the JPDF for X ; define the functional form of the limit state function; and solve the multiple integral.

The determination of the JPDF for X is substantially based on the statistical independence hypothesis between the variables. The determination of the limit state function is a specific problem of reliability theory. Integration of equation is a purely computation problem with multidimensional integration domains defined in implicit form. In general, the integral can be solved only numerically with computationally expensive simulation methods.

However, a closed form solution of the equation 6 can be find in the case of the two-dimensional problem of independent load and resistance variables and linear limit state function. For example in the case of the formulation of structural reliability problem based on the limit state function defined as $G(R,S) = R-S$, where R and S are independent variables for which the functions of probability density

PDFs (Probability Density Functions), $f_R(r)$ and $f_S(s)$, are known, equation 6 can be written as follows:

$$P_{failure} = P_f = \iint_{[R-S<0]} f_{R,S}(r, s) dr ds \quad (7)$$

The assumption on independence of the variables allows to write:

$$f_{R,S}(r, s) = f_R(r) f_S(s) \quad (8)$$

and by substitution in equation 7, it can be obtained:

$$P_f = \int_0^{\infty} f_S(s) \left[\int_0^s f_R(r) dr \right] ds = \int_0^{\infty} f_S(s) F_R(s) ds \quad (9)$$

and then the probability of failure is given by the convolution integral of two functions of s , where $f_S(s)$ is the PDF of S and $F_R(s)=P[R<S]$ is the CDF (Cumulative Distribution Function) of R .

In general, situations in which the integral is solved analytically arriving at the exact solution are extremely rare. However, the problem of calculating the probability of failure can be solved with numerical methods. These simulation methods sample the variables in the safety-checking problem from their JPDF and for each realization of these variables, the result of the limit state function is checked. The easier and best known simulation method is the Monte Carlo method (Elefante, 2009). The accuracy that characterized these procedures is inversely proportional to the number of simulations. Since the probability of collapse in structures is generally very small and each simulation requires a complete structural analysis, the computational effort can be prohibitive even for computer and therefore alternative simulation methods, called *smart simulation methods*, have been developed.

5.2.5 Simplified probabilistic method

As stated previously, the main problems to solve the integral in equation 5 are summarized in the following (Casati & Roberts, 1996):

- the integration domain is known only in implicit form;
- the integration domain is generally "far" from the mean of the vector X ;

- the integrand may have a high slope in the integration domain.

For these reasons, various experts have proposed the idea of assess the reliability with an index β , called *reliability index* (Cornell, 1967). The *reliability index* measures the distance between the average value of the vector X (*design point*) and the boundary of the domain of failure (limit state function $G(X)=0$) in units of standard deviation. Therefore, the evaluation of this index is a constrained minimization problem. Once this index has been calculated, it is possible to calculate the probability of failure and compare it with the reference values to assess the degree of reliability of the structure. The greater the value of β , the lower the probability of failure.

In the case of the load-resistance model, assuming that the vector of random variables R and S is normally distributed, the function $G = R-S$ is still normally distributed. Assuming that R and S are also independent, the mean and standard deviation of G are obtained as:

$$\begin{aligned}\mu_G &= \mu_R - \mu_S \\ \sigma_G &= \sqrt{\sigma_R^2 + \sigma_S^2}\end{aligned}\quad (10)$$

In this case the probability of collapse can be calculated by recalling the Gauss integral:

$$P_f = \frac{1}{\sqrt{2\pi}\sigma_G} \int_{-\infty}^0 e^{-\frac{1}{2}\left(\frac{g-\mu_G}{\sigma_G}\right)^2} dg = \Phi\left(-\frac{\mu_R - \mu_S}{\sqrt{\sigma_R^2 + \sigma_S^2}}\right) = \Phi(-\beta) = 1 - \Phi(\beta) \quad (11)$$

where β is the value at which the Gaussian function is calculated in order to obtain the probability of failure.

This calculation is exact in the cases in which the limit state function G is a linear combination of the random variables that influence the structural behavior, characterized by a jointly Gaussian distribution. However, this method can also be adopted if the described conditions are not fully satisfied. In fact, in these cases an approximation of the probability of failure is obtained that depends on the shape of the limit state function, the nature of the random variables involved and the possible correlation between the variables (i.e., FORM and SORM methods (Cornell, 1969)).

5.3 Safety assessment of modern heritage structures

Figure 29 shows reports the period of construction of the existing reinforced concrete buildings in Italy, obtained from the data provided by the 14th census of Italian population and buildings (2001). From these results, it is possible to have a clear idea regarding the percentage (35%) of reinforced concrete structures that have been built before 1972. These structures, corresponding to one million of building units (Elefante, 2009), have been designed before the first code with seismic provisions, as well as the diffusion of the limit state method and durability criteria in the standards.

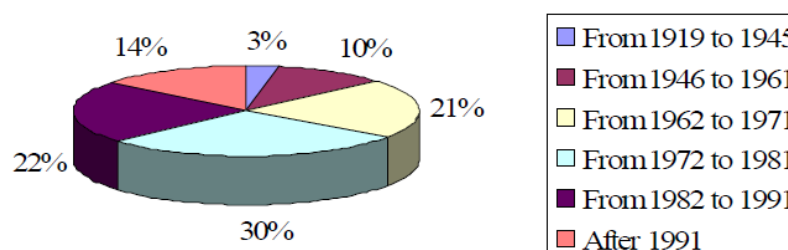


Figure 29: Reinforced concrete buildings period of construction in Italy - census 2001 - (Elefante, 2009)

This is valid also for many other European countries in which the buildings have an average service life greater than that of regions like the United States. Therefore, management of existing buildings represent one of the major concern in such countries. In fact, particular attention to the existing structures assessment is paid by recent European and Italian guidelines (e.g., EC8, OPCM, NTC2008, NTC2018). These guidelines distinguish the assessment of existing structures from that of the new buildings by lack of information about both the original features and the current state of building in consideration. Several documents stating the guidelines for protection of heritage structures were formulated in Italy:

- Italian Guidelines for Evaluation and Mitigation of Seismic Risk to Cultural Heritage (Cecchi, Calvi, & Lagormarsino, 2006),
- Directive PCM 9/2/2011 (Recommendations PCM, 2011).

In the international context, PERPETUATE (Performance-based approach to the earthquake protection of cultural heritage in European and Mediterranean countries) programme, supported by the European Commission, formulated the

European Guidelines for the Seismic Preservation of Cultural Heritage (Lagomarsino, et al., 2010), (Lagomarsino, Cattari, & Calderini, 2012).

Numerous sources of uncertainty affect the assessment of existing structures. In addition, these construction may have been affected by past earthquakes or other accidental actions whose effects are not easily evident. For these reasons, the assessment of existing buildings results highly sensitive to uncertainties. In fact, the most recent seismic regulation for cultural heritage structures, the Directive PCM (Recommendations PCM, 2011), encourages the achievement of an adequate “level of knowledge” obtainable only through extended tests and investigations. An accurate level of knowledge presumes several researches that can be carried on with traditional or modern technologies:

- recognition and localization of the structure (associated with risk areas);
- geometric data gathering;
- historical analysis survey of the materials and their state of preservation;
- mechanical characterisation of the materials;
- monitoring activities.

The condition assessment of heritage buildings is more complex than the ordinary structures. Nowadays, the uncertainties associated with the materials properties, and the structural behavior, are covered with partial safety factors corresponded to a specific safety level. Standard approaches for condition assessment are inappropriate for heritage structures because could be very invasive. When dealing with safety assessment of these structures, a more flexible approach should be used. In particular, safety for the users and reduction of the intervention to the minimum possible should be pursued. Therefore, in heritage structures, lower safety levels may be justified in some cases, because it is possible to reduce the risks associated to the use of the building by limiting the access in certain areas of the building, or because of continuous or periodic monitoring programs etc. (Zanotti Fragonara, 2012). In fact, the partial safety factors used for new structures, which take in account uncertainties related to strength of materials, can be reduced thanks to an adequate level of knowledge on the structure.

The actions that should be undertaken to reach a right knowledge of a reinforced concrete building belonging to architectural heritage are reported in the following.

Data collection is one of the main aspects in the knowledge path for heritage buildings. This consists in the retrieval of all possible information and in the more deepening of investigations regarding to history of the structure (including historic events and building transformations), survey of geometric arrangement and constructive material, constructive details and material properties. The information can be acquired during cognitive surveys and direct analyses on the building. Archive documentations and analysis of the sources are useful together with direct analyses to define the material constructive texture, the building dimensions, the state of preservation, the transformation interventions, the health state, the crack patterns and possible (local or global) mechanisms of collapse. Then, the deepening of this knowledge consists in determining the strength of the materials by means of experimental tests.

5.3.1 Historical analysis

The historical analysis of a cultural heritage building represents the first step towards a full understanding of its structural state. Historical analysis is therefore a fundamental step to retrace the feedback process that generated heritage architectures, and this process cannot be generalized, because of the inevitable absence of immutable and univocally identifiable construction rules. In this context, the first step is represented by the collection of documental information. To unravel the history of a construction it is necessary to research into site conditions and the building technology of the construction period. All the other relevant historic and archival evidences should be found and recorded. To understand a building, it is necessary to know the story of its gradual construction and the entire history of the ground upon which it stands, and have information about any external environmental changes. Obtaining this information is not always easy. The second step is represented by the direct analysis of the building. In particular, when dealing with constructions that underwent turbulent building process or successive modifications, historic analysis can prove to be very helpful. Historic analysis can also be useful if a particular traumatic event has occurred to the building during its lifetime. In fact, in this case, a qualitative behavior model can be deduced from the building response to that specific event.

5.3.2 Geometry

The geometric data represent fundamental quantities, also for the definition of a model capable of representing the real structure in an acceptable way. There are

countless technologies to support these investigations aimed at collecting geometric data. In a broad sense, it is possible to classify geometric data as follows:

- Spatial geometric dimensions of structural and non-structural elements;
- Estimates for loads on all structural elements;
- Identification of the typology and dimensions of the foundations;
- Definition of the possible crack pattern (in terms of the size of the cracks and the typology) and of the existing failures or of evident deformation conditions that may arouse suspicion or represent pathological conditions for structure.

Visual inspection in situ must always accompany the collection of these geometric data. During data gathering, it should be remembered that from a structural point of view the survey accuracy should not be too high. In such a case, one would risk introducing too much meaningless information, which would actually result in adding noise to the survey rather than an increase of the level of knowledge.

5.3.3 Construction details

For the definition of a reliable structural model and an accurate condition assessment of the building, the acquisition of a good level of knowledge of construction and structural details is important. The details commonly represent very sensitive parts of the structure. Among the countless of details that can be collected, one should always focus his attention on:

- nature and quality of the connection between structural components;
- presence of elements with high vulnerability;
- presence of interventions capable to decrease the vulnerability of the structure;
- amount and arrangement of reinforcement in beams, pillars and walls;
- amount and details of transverse reinforcement in critical areas and beam-column joints;
- constraint conditions of the horizontal elements;
- thickness of the concrete covers;
- length of the overlapping of the bars and their anchorage.

5.3.4 Materials

For the condition assessment of a modern heritage building, a mechanical characterization of materials is required. This characterization strongly depends by the level of knowledge that one wants to achieve. To achieve adequate knowledge of the material, one can rely on the documentation already available, on visual checks in situ and on experimental investigations. The design values of the mechanical properties are assessed starting from the investigations and tests on the structure, taking justifiably into account the extent of the dispersions. For the material characterization, the data collected in the experimental campaigns may concern the following tasks:

- characterization of strength and elastic modulus of the concrete;
- yield stress, failure stress and elongation of steel;
- chemical analysis to distinguish chemical composition of structural material or grout;
- etc.

The experimental campaign should combine destructive, partially destructive and non-destructive techniques. As indicated in current standards (Ministero delle Infrastrutture e dei Trasporti, 2018), in the case of buildings subject to Italian Code of Cultural Heritage and Landscape (2004), must be considered the impact of the investigation campaign in terms of conservation.

5.3.5 Level of knowledge and confidence factors

According to NTC2018 (Ministero delle Infrastrutture e dei Trasporti, 2018) and the ministerial circular (Ministero delle Infrastrutture e dei Trasporti, 2019), there are three levels of knowledge (LK):

- LK1 - *Limited*;
- LK2 - *Extended*;
- LK3 - *Comprehensive*.

The levels of knowledge are defined by the aspects reported in the previous paragraphs: *geometry* (i.e., the geometric characteristics of structural elements); *structural details* (the quantity and the disposition of the reinforcements, including the stirrups); and *materials* (i.e., the mechanical properties of materials). According to Italian Guidelines for Evaluation and Mitigation of Seismic Risk to Cultural

Heritage (Cecchi, Calvi, & Lagormarsino, 2006) and to Eurocode 8 (CEN, EUROCODE 8, 2005), once the level of knowledge has been defined it is possible to assign a confidence factor FC (ranging from 1.00 to 1.35). This FC grades the reliability of the structural analysis model and the evaluation of the seismic safety index. Larger amount of information corresponds to a lower value of the confidence factor.

Although the confidence factor is applied to the materials properties, the uncertainties in modelling are not limited to them but include also other detailing structural parameters affecting the seismic assessment such as reinforcement detailing, cover thickness, etc. In fact, one of the most challenging aspects of the seismic assessment of existing buildings is represented by the characterization of structural modelling uncertainties. Current regulations synthesize the effect of these uncertainties in confidence factors, which are applied to mean material property values. In fact, according to the discrete levels of knowledge achieved with specific in-situ tests and inspections, the confidence factors are classified and tabulated in current regulations.

5.3.6 Levels of evaluation and performance-based approach for heritage buildings

The Italian codes (Recommendations PCM, 2011) (Ministero delle Infrastrutture e dei Trasporti, 2018), distinguish between three different levels of evaluation for the analysis methods:

- LV1: this level can be applied for the seismic assessment at territorial or urban scale on the entire protected architectural heritage;
- LV2: is applied in the case of local intervention on the structure;
- LV3: is the most detailed level that is required in the presence of interventions that modify the structural behavior of the building or in the case that a seismic assessment of the building is required.

The performance-based approach is used also for architectural heritage structures. In particular, according to the Directive PCM (Recommendations PCM, 2011), the safety and protection when dealing with seismic risk is obtained considering two limit states. These limit states are motivated by the intention to safeguard the occupants from danger in case of a high intensity earthquake, and to limit economical and functional damage in the event of low intensity quakes.

Moreover, reasons for protecting specific works of art may exist where it is advisable to establish a special limit state. The limit states considered are:

- Ultimate limit state (SLU): under the effect of a reference seismic event which is characterized by a probability of exceeding 10% in 50 years. The structure even when submitted to severe damage, maintains a residual resistance and stiffness with respect to horizontal actions and the full load capacity to vertical loads.
- Damage limit state (SLD): under the effect of a seismic event, characterized by a probability of exceeding limits by 50% in 50 years. The building, on the whole, is not greatly damaged in a way that justifies the interruption of use following the earthquake.
- Artistic limit state (SLA): works of art contained in a building (decorated walls, etc.) which during an earthquake of a certain level are undamaged or slightly damaged but still recoverable without significant loss of their cultural value. The reference earthquake can usually be the same of the Damage limit state.

The European research project PERPETUATE (Lagomarsino, et al., 2010) (Lagomarsino, Cattari, & Calderini, 2012) approaches the problem considering two different assets: architectonic assets (historic buildings or architectonic elements that can be analysed independently from the rest of the building) and artistic assets (statues, stucco-works, frescos, etc.). In one of the several deliverables (Abbas, et al., 2010) (Lagomarsino, et al., 2010), some criteria for the choice of target performance levels for the seismic retrofit of heritage buildings are suggested, with even more detailed than into the Directive. In particular, three levels of performance are proposed: Use and human life, Building conservation, and Artistic assets conservation. Target performance levels can be also associated to damage levels. The damage level is usually obtained with a non-linear static analysis which produces a curve showing sequence of four phases of damage: Slight, Moderate; Heavy; and Complete. In the research project PERPETUATE the definition of more specific levels to be achieved for target performance, based on some of these damage levels, is proposed. Regarding the definition of the project earthquake and the seismic hazard, different return periods can be used. In particular these return period can vary from 50 to 2475 years, in relation to the different damage levels and performance criteria.

5.3.7 Safety indexes for heritage buildings

For the seismic assessment the Directive PCM (Recommendations PCM, 2011) and the Italian building codes (Ministero delle Infrastrutture e dei Trasporti, 2018) define a seismic safety index as the ratio between acceleration that brings the building to a limit state and the expected acceleration of the site, which corresponds to a determined probability of exceeding the limit in 50 years.

The level of seismic protection is differentiated based on the importance and use of the building. Therefore, the consequences may be ascertained more or less important in the event of seismic damage. The following categories are recommended by (Recommendations PCM, 2011):

- Three diverse “importance categories” (limited average, and elevated) which may be defined on the basis of the knowledge of the work by way of methods developed by the Ministry of Cultural Heritage and Activities, by way of an interdisciplinary procedure;
- Three diverse “use categories” (infrequent or unused, frequent, very frequent).

According to its established category, each protected building shall be assigned a probability of exceeding acceptable limits to the corresponding actions for both the verification of SLU and SLD.

For the structural assessment the Italian building codes (Ministero delle Infrastrutture e dei Trasporti, 2018) define a structural index $\zeta_{v,i}$, in this thesis indicated as α , which can be considered as a variable load multiplier. This index is defined as the ratio between the ultimate vertical variable load that a part of the building can bear and the value of variable load that would be used in the design of a new construction.

Preserve a modern heritage building without invasive retrofitting interventions or important permanent changes is another key aspect highlighted in the Directive, in order to follow the principle of “minimum intervention”. The difficulty of finding adequate compromises between safety and conservation assumes important implications also in terms of the responsibility of the different subjects involved in the designing and execution of the work according to law. It is worth highlighting that the definition of “acceptable” safety levels, as well as the concept of “safety”, still represents an open issue for monumental buildings (Lagomarsino, Cattari, & Calderini, 2012).

In the condition assessment, it is necessary to proceed with an evaluation of seismic behavior of the total structure with proper models. According to (Recommendations PCM, 2011), a path of knowledge and analysis is indicated in which judgment on the level of risk for a structure emerges comparing the structural capacity and the seismic hazard. Such a comparison is not meant as a compulsory verification in which capacity must result superior to the demand subsequent to the seismic action, but as a quantitative element to be considered along with others in a qualitative judgment of the whole which considers the needs of conservation.

5.3.8 Structural health monitoring of heritage structures

The effects of aging inevitably affect heritage buildings, the preservation of which requires expensive maintenance acts and surveillance against accidental events. For these buildings an essential method to assure an adequate level of reliability and safety is the availability of a permanent assessment of the structural conditions. For this reason, in addition to the traditional methods, new experimental procedures have been developed in the last three decades. These new approaches aim to provide widespread and accurate information about the structural performance and integrity (Ruocci, 2010).

Farrar and Worden (Farrar & Worden, 2007) define structural health monitoring (SHM) as a process which involves the periodic monitoring of a structure through measurements, the extraction of features symptomatic to the phenomena under investigation and their statistical analysis to determine the actual state of the system.

A diagnostic monitoring system is therefore the result of the integration of several sensors, devices and auxiliary tools, like: a measurement system, an acquisition system, a data processing system, a communication/warning system, an identification/modelling system, and a decision making system.

SHM is based on innovative techniques of measurement, analysis, modelling and communication. However, it shares the same goals of traditional methods. In fact, the diagnostic monitoring tries to overcome the limitations of traditional visual inspections and, since it integrates its novel technologies into a single smart system, it can be considered as an extension of the well-established investigation practices.

An automatic monitoring system operating in real or at least nearly-real time is preferable to periodic investigations for several reasons. First of all, it is a matter of economic convenience. Traditional inspections must be performed by high

qualified personnel with a periodic recurrence which is not related to the actual state of the building. Sometimes, in order to carry out the inspections, are necessary expensive service equipment and the complete closure or, at least, the partial limitation of the building usability. A permanent monitoring system is much more cost-effective over a long period of time because of the amortization of the initial costs of ideation, design and execution. Therefore, this is particularly true in the case of the historical buildings because, differently from ordinary ones, they do not have a very limited life-cycle.

A large series of technical drawbacks affect traditional investigation methods. Among these drawbacks, certainly the fact that visual inspections are generally carried out with a periodicity too spaced in time which can affect their predictive nature. Furthermore, both because they do not allow the identification of hidden defects or the invisible effects of an on-going damage process and because the estimation is related to the subjective judgement of an expert who can be fallible, they are neither exhaustive nor objective. More specific and accurate non-destructive testing techniques (Shull, 2002) are performed off-line and usually only after the damage has been localized. This means that in the meantime an excessive level of degradation could have been reached. Nevertheless, non-destructive estimations are performed locally and therefore can provide useful information referring to a limited portion of the building.

Modern diagnostic monitoring systems aim to overcome these limitations easing the plan of maintenance and restoring interventions thanks to an exhaustive depiction of the structural health state. The damage assessment with vibration-based tests has proved its potentialities in different fields and applications. In several cases, modal properties have been useful for the damage identification in modern heritage buildings. Once the main parameters that influence the structural response of the asset have been identified, the investigation can be finalized on a few important points, reducing the amount of destructive tests as well as costs and time. In fact, ambient vibration tests can be very useful for identifying the overall dynamic behavior of heritage structures (structural identification), providing an essential contribution in improving the knowledge of the building, for the purpose of a more reliable modelling and assessment (Lagomarsino, Cattari, & Calderini, 2012).

5.4 Models for the condition assessment of modern heritage buildings

ICOMOS Guidelines report the “diagnosis and safety evaluation” step in the guidance criteria for the structural conservation of heritage. In structural analysis this step has a crucial role because defines the identification of meaningful models that accurately reproduce both the structure and the associated structural behavior with all their complexity as the central point of the structural diagnosis, in order to apply the available theories of the existing buildings. The fundamental role of mathematical model is expressed in the following text:

“mathematical models are the common tools used in structural analysis. Models describing the original structure, if appropriately calibrated, allow comparison of the theoretical damage produced by different kinds of action with the damage actually surveyed, providing a useful tool for identifying the causes of such damage. Mathematical models of both the damaged and the reinforced structure will help to evaluate present safety levels and to assess the benefit of proposed interventions”. (ICOMOS, ISCARSAH Committee, 2003)

Models are essential for identifying the elements that, while defining the building’s character, can influence its structural behavior. Models can play a role also in detecting the relationships between structural elements and architectural outcomes, both in the project and in the transformations that occurred over time. In particular, great attention is required for the effects of degradation on concrete works and their actual performance, taking into account both the construction techniques and the actions that affected the building over the years.

The design of large structures in concrete was often based on physical models, which can represent complex behaviors, especially when they are reproduced on a scale very close to the actual one. For example, most of Nervi’s projects were tested through scale modelling during their final design phase, an approach that he had used since his early important works. A cooperative testing effort was established, in fact, between Nervi and G. Oberti, a professor at Politecnico di Torino and director of ISMES (Istituto Sperimentale Modelli e Strutture). At ISMES, also a reduced-scale model of Maracaibo Bridge by Morandi was tested (Levi & Chiorino, 2004).

However, modern numerical tools are in general cheap and lend themselves to generalizations. An advantage of numerical models is that they can be corroborated to become realistic, because reality is continuously evolving and so do experimental measurements, since the system, as well as the surrounding environment, undergo changes. Therefore, a numerical model is typically able to assimilate new information (Ceravolo, Pistone, Zanotti Fragonara, Massetto, & Abbiati, 2016).

Continuous or periodic monitoring activities can detect changes in the system properties or surrounding environment. For instance, a change in ambient temperature is reflected in the deviations of the system's natural frequencies. If this change is small, periodic (e.g., daily or seasonal), and persistent, it is said to be physiological. When using a mathematical or numerical model to predict a particular response, all physiological phenomena that bring some variability, and therefore uncertainty, should be incorporated, allowing a reliable comparison between the prediction of the model and the measured structural response. If assimilating the system's physiological behaviors into the model is important, incorporating pathological behaviors is fundamental. Pathological behavior typically corresponds to a permanent or temporary change in an environmental condition that produces a permanent change in structural properties. An example of pathological behavior is a permanent reduction in the natural frequencies of a structure after a seismic event or due to the progressive degradation of materials. If such pathological behaviors occur, they must be considered in the models by updating the materials constitutive laws or even geometric and topologic properties. In the end, this approach leads to a sort of digital twin of the structure, where experimental data are released as a part of an ongoing updating and condition assessment process.

ICOMOS standards point to the importance of periodic controls of the construction as the primary tool for the preservation of architectural heritage (Ceravolo, De Lucia, Lenticchia, & Miraglia, 2019) (ICOMOS, ISCARSAH Committee, 2003) (ICOMOS, International Committee on Twentieth Century Heritage, 2017). Usually, the inspections of buildings, useful to improve the knowledge level and reduce the uncertainties, can be executed on a one-off basis or periodically, and most observations and measurement methods provide only local information.

As previously mentioned, modern SHM techniques, which are typically applied to inspect the global structural behavior, try to overcome the limitations of

traditional and visual inspections (Farrar & Worden, 2007). Vibration-based SHM has been successfully used for damage detection and quantification in existing buildings. Vibration tests provide information about the whole-body response, and allow extending to the whole structure the outcomes of the local inspections and measures. These techniques are particularly useful in the architectural heritage field because of their usual non-invasiveness and non-destructiveness and because they provide direct information about the dynamic response and indirect information about structural integrity (Ceravolo, De Lucia, Lenticchia, & Miraglia, 2019) (Ceravolo, Pistone, Zanotti Fragonara, Massetto, & Abbiati, 2016). Moreover, the dynamic test setups can be easily installed and removed.

In the light of their advantages, vibration-based SHM techniques are particularly suitable to understand the dynamic response of complex structural systems, such as the one represented by 20th century architectural heritage: which not only present specific issues, connected to their complex and innovative spatiality, but also by the continuous experimentations of designers and engineers in the material employment, which are characteristic features of this heritage (Croft & Macdonald, 2019).

Since in typical structural engineering problems, the safety assessment is based on mechanical models, the engineer tends to base any final evaluation, prognosis, or decision on the results of an updated model (Miraglia, 2019) (Ceravolo & Lenticchia, 2019). However, in the field of applications to the architectural heritage, uncertainties translate into great difficulties in defining fairly general modelling methods. In reinforced concrete buildings, for instance, infill walls and expansion joints may strongly affect the dynamic behavior of the structure and, consequently, should be accounted for accurate numerical reproduction. In this respect, a damage scenario-driven optimal sensor placement can be an efficient tool (Lenticchia, Ceravolo, & Chiorino, 2017) (Pachón, et al., 2020). For all these reasons, the results of the numerical analysis need to be reconciled with: i) historical information and survey documentation; ii) experimental data (coming from both vibration-based techniques and classical tests).

Contrary to traditional architectural heritage, for 20th century architectural heritage buildings, a large number of documents of various nature are available; in fact, the calculation assumptions and models of safety employed by the designers are often available, as well as safety levels prefigured at the time of their construction. Under these conditions, the experimental corroboration of a model

offers indications on the possible decay of safety margins of the structure and allows for “a posteriori” evaluations in the Bayesian sense.

In particular, when new information of an existing structure becomes available, can be applied the solution methods for the reliability updating. In fact, the assessment of an existing buildings can be updating when (Ditlevsen & Madsen, 1996):

- damages are observed;
- deviations from the project descriptions are observed;
- the life time is up to extension beyond what is planned;
- when inspection schedules are planned to be revised;
- etc.

Compared to the information available at the design phase, new information may come from concrete reception control, steel and reinforcement certificates, actual geometry measurements, collection of load data, proof load testing, inspection and damage assessment. This additional information is usually considered for the purpose of verifying that the structure is reasonably built as prescribed. Therefore, this information is used for detecting possible mistakes that have occurred during the construction. Sometimes this check reveals mistakes that concern the model assumptions or the calculations. In connection with this verification of the calculation assumptions, the information can be used for reliability updating (Ditlevsen & Madsen, 1996). Following these principles, collection of information after the realization of the structure allows to calculate an updated reliability or safety index. Sometimes an updating effect can be obtained by revising the mathematical model used in the design phase to represent the verbally formulated limit-state requirement, especially if the applied mathematical limit state is “on the safe side”.

Chapter 6

Case study application: Pavilion V of Turin Exhibition Center

The reference case study for this thesis is presented in the following. In particular, in this chapter, are reported the results obtained from the condition assessment experience of a real post-tensioned structure. The analysed post-tensioning concrete system is Pavilion V of Turin Exhibition Center, conceived by Riccardo Morandi in the late 50s.

Methodological approaches and guidelines to the condition assessment of post-tensioned concrete structures need to be conceived and validated on virtual models that reproduce their behavior, for the structural preservation and rehabilitation, this requiring numerous and detailed information about the structure under analysis. The investigations conducted on Morandi's pavilion have been integrated in a virtual numerical model of the structure in order to obtain a digital twin of this complex spatial system.

The numerical model, resulted from the experimental corroboration with updating techniques, has been conceived to face two main challenges: evaluate the residual service life of a structure that was constructed decades ago, and assess the structural safety and reliability of this building with respect to current safety standards, including the new seismic regulations. An important aspect for determining the model parameters of Morandi's pavilion is the effect of structural

joints. The presence of joints introduces complexity in the modal response and high sensitivity of the stiffness parameters, affecting the design of the experimental setups. Consequently, a simplified model has been considered to aid in the modal identification process.

Finally, in order to investigate the uncertainty on the sensitivity to possible damage scenarios and environmental factors due to the complexity of the structure's dynamic behavior, a sensitivity analysis of changing environmental conditions has been carried out. In fact, sensitivity to damage scenarios and environmental factors on structures represent a relevant aspect in SHM. This analysis allowed to show the effects of the variation of the elastic modulus of the structure's components on the modal frequencies. Consequently, useful information for an upcoming permanent monitoring have been determined, considering different temperature sensitivity scenario.

Part of the work described in this chapter has been previously published in the papers:

- Scussolini, Linda; Coletta, Giorgia, Oliva, Valerio; Miraglia, Gaetano; Lenticchia, Erica; Ceravolo, Rosario. "Sensitivity analysis of the environmental effect on the dynamics of concrete historical architectures with structural joints." European Workshop on Structural Health Monitoring (2022).
- Ceravolo, Rosario; Lenticchia, Erica; Miraglia, Gaetano; Oliva, Valerio; Scussolini, Linda. "Modal identification of structures with interacting diaphragms." Applied Sciences, 12(8), 4030, (2022).
- Ceravolo, Rosario; Lenticchia, Erica; Miraglia, Gaetano; Oliva, Valerio; "Use of experimentally corroborated models in the condition assessment of early post-tensioned systems." (Under Peer Review as of November 2021).
- Oliva, Valerio; Lenticchia, Erica; Ceravolo, Rosario. "Aspetti costruttivi e strutturali del Padiglione ipogeo di Riccardo Morandi a Torino." In: Colloqui.AT.e, Torino, 25-28 settembre 2019, p. 349-357, (2019).

6.1 Review of available documentation and building's history and identify the structural conception

Archival research for the pavilion produced a comprehensive database of historical documents in terms of original drawings, notes of structural design, construction reports, as well as a limited number of reports concerning occasional surveys and inspection campaigns through the life of the structure.

Pavilion V was built in 1959 by Riccardo Morandi, commissioned by Società Torino Esposizioni, almost entirely owned by the FIAT motor company, to expand the existing exhibition spaces dedicated to hosting the Automobile Shows, also in view of the celebrations of 100 years from the unity of Italy, in 1961 (Bruno, 2013). The project became an opportunity for Morandi to take advantage of the long years of experimentation on pre-stressed reinforced concrete. The scheme adopted by Morandi for Pavilion V is the so-called balanced beam, widely used by the designer between the 1950s and 1960s in bridges and overpasses (Levi & Chiorino, 2004). The pavilion consists of a single wide space, 69 m in width and 151 m in length, located 8 m below ground level (Figure 30).

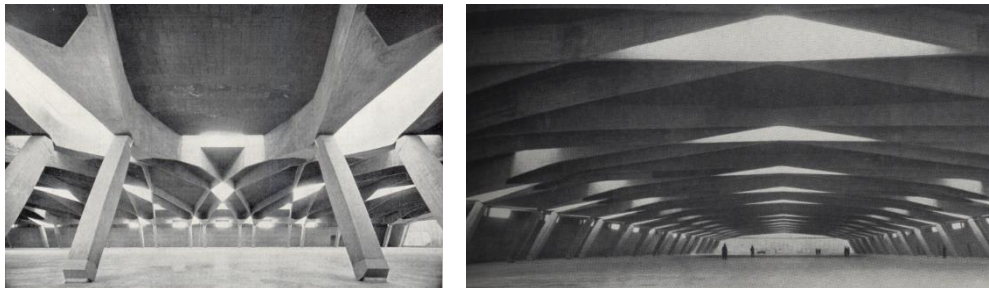


Figure 30: Turin Exhibition Center, underground Pavilion by Riccardo Morandi: general views

The structural scheme is composed of post-tensioned beams on two inclined supports, with two cantilevering side spans subsequently anchored by post-tensioning tendons at their ends, exerting a balancing effect on the bending moments in the main span. Unlike the usual bridge scheme, in Pavilion V, the main post-tensioned ribs are not parallel beams but are diagonally directed and multiply reciprocally interconnected to obtain a spatial structure offering high overall rigidity and lateral stability and to contrast the instability of the very thin webs (16 cm) of the main ribs. Furthermore, the post-tensioned ties at the ends of the lateral spans of the ribs are not inclined tendons anchored on the foundations of the main

inclined supports, as in the bridges by Morandi, but are short prestressed concrete prismatic elements (shorter strut–beams, located above the retaining walls), whose tension forces are balanced by the lateral retaining walls and by the load of the soil acting on their foundations.

Morandi used the balanced beam scheme with subtended tie rods to reduce the bending moment at mid-span. This scheme produced important economic savings for the amount of material used. In fact, both the height of the ribs and the number of cables needed were reduced, compared to the beam with simply supported scheme. The balanced beam scheme has lateral cantilevers, which provide a first reduction of bending moment in the span. Furthermore, the scheme with subtended tie rods (shorter strut beams) acquires greater efficacy accentuating the cantilever effect, thanks to the application of a concentrated force at the endpoint of the cantilevers and to the use of inclined inwards longer strut beams (capable of naturally providing an additional axial compression component to the rib).

The load applied at the endpoints by tensioning the shorter strut beams balances the maximum and minimum bending moments so as to reach the most efficient configuration. Figure 31 shows the bending moment diagrams for different static schemes of the beam qualitatively, considering a uniformly distributed load.

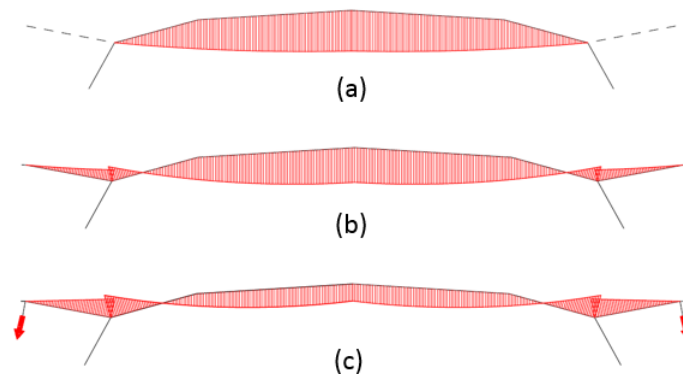


Figure 31: Qualitative comparison of the bending moment between simply supported beam (a), balanced beam with lateral cantilevers (b), and balanced beam with subtended tie elements (c)

A wide range of formal solutions and dimensional ratios between the resistant sections of various parts of the structure can be obtained considering the different inclinations attributable to the longer strut beams and the induction of pre-stressing force both in the ribs and in the shorter strut beams.

Various structures were conceived and built by Morandi with balanced beam scheme: the bridge over the Cerami in Enna (1953-1954), the overpass of the Via Olimpica in Rome (1958-1959), the bridge over the Vella in Sulmona (1960-1962) and finally the underground pavilion for the Turin Exhibition Center (1958-1959), which is the focus of this PhD thesis. In the case of the bridge over the Cerami, the first to be built with this methodology, it can be observed that the minimum vertical encumbrance of the beams was obtained by subjecting the terminal tie rods to a pretension capable of induce a useful moment in the span to compensate the moment of the beam considered in a simply supported scheme Figure 32. The tie rods are made of high strength steel, inside fibre cement sheaths Figure 33.



Figure 32: Bridge over the Cerami, Enna, 1953-1954: general view (Boaga, 1984)

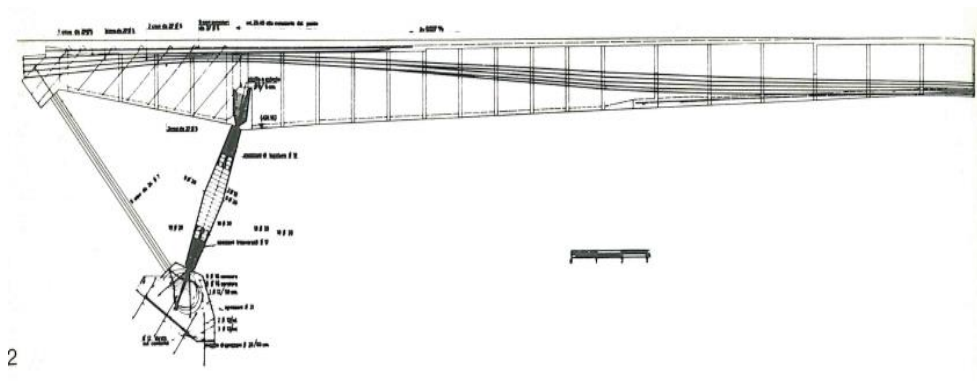


Figure 33: Bridge over the Cerami, Enna, 1953-1954: longitudinal half section (Boaga, 1984)

Subsequent works, such as the Via Olimpica overpass in Rome, represent the culmination of the most advanced solutions with balanced beam with which Morandi express the whole theory of prestress technique (Figure 34 and Figure 35).



Figure 34: Via Olimpica overpass, Rome, 1958-1959: bottom view (Boaga, 1984)

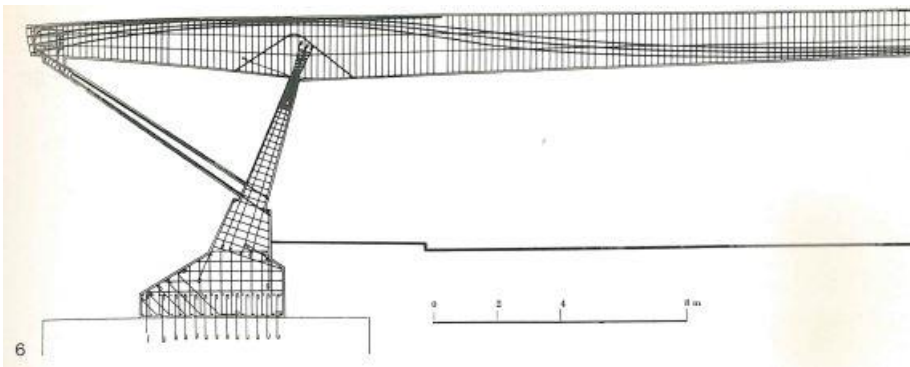


Figure 35: Via Olimpica overpass, Rome, 1958-1959: longitudinal half section (Boaga, 1984)

In the case of Pavilion V, these shorter strut beams follow the inclination of the internal longer ones (Figure 36 and Figure 37). The elements were conceived with the aim of transforming the static scheme from determined to undetermined.

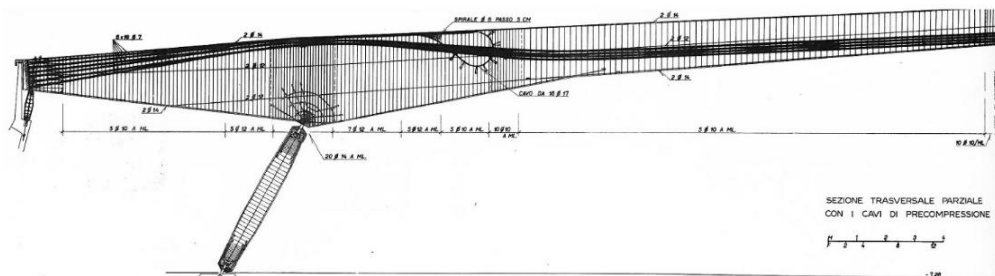


Figure 36: Post-tensioning cables of the Pavilion V balanced beam (half section) from a drawing in Morandi's documents (Morandi, 1959)

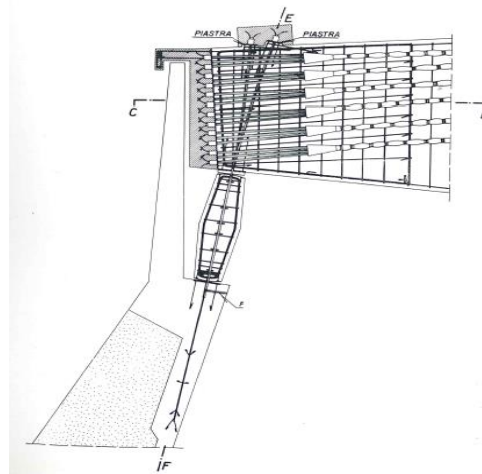


Figure 37: Construction detail of the shorter strut beam connection with rib and retaining wall (Boaga, 1984)

The internal inclined strut beams represent the other support for the entire structure. These elements have a hexagonal shape, tapering from the center to the two ends to perform the hinge constraint at the extremity points. At the top of these elements, the steel plates provide the connection with the ribs. The steel plates allow the rotation with respect to the vertical plan, ideally creating an element capable of supporting actions only along its axis but unable to absorb bending moments (Figure 38).

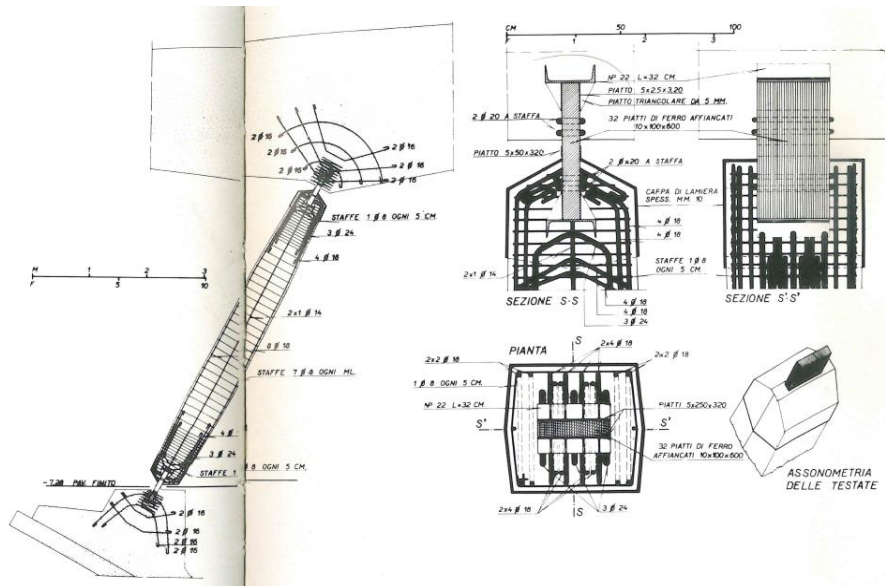


Figure 38: Construction details of the inclined longer strut beams and the connection elements with the ribs (Boaga, 1984)

From the analysis of the original documentation consisting of executive drawings and the calculation report, it was possible to identify the static scheme used by Morandi, as shown in Figure 39.

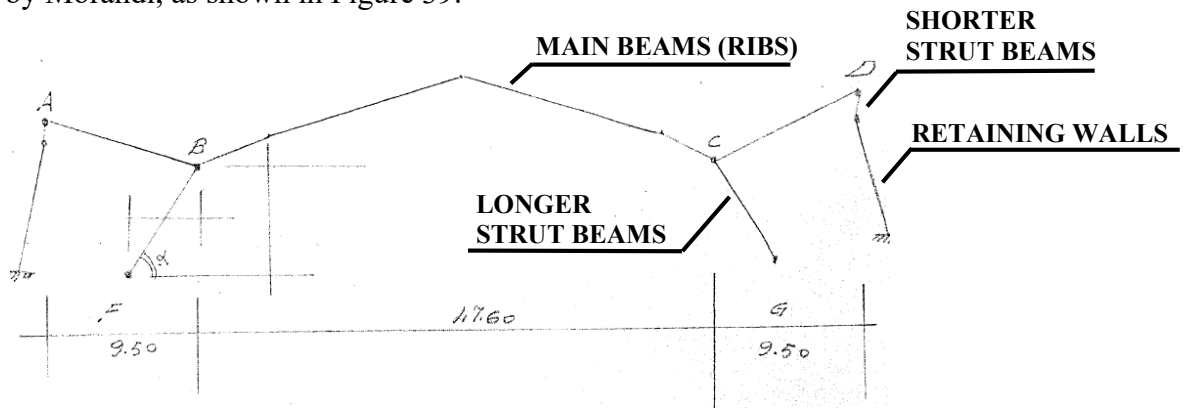


Figure 39: The static scheme of the Pavilion V balanced beam from a sketch inside Morandi's calculation report (Morandi, 1959)

The entire structure is composed of three blocks linked by two expansion joints, crossing the roof and the external walls. The division of the underground structure into three blocks is observable in Figure 40 and Figure 41. On each side of the structure there are 14 pairs of longer strut beams, having a distance of 11 m between two different pairs and 3.20 m between the two struts of the same pairs. Each pair supports two crossed ribs (Figure 42). The thin ribs would be singularly unstable, but their intertwining makes the structure mostly rigid and robust. One of the intersections is in correspondence with the inclined strut, creating a dovetail geometry, as shown in Figure 43.

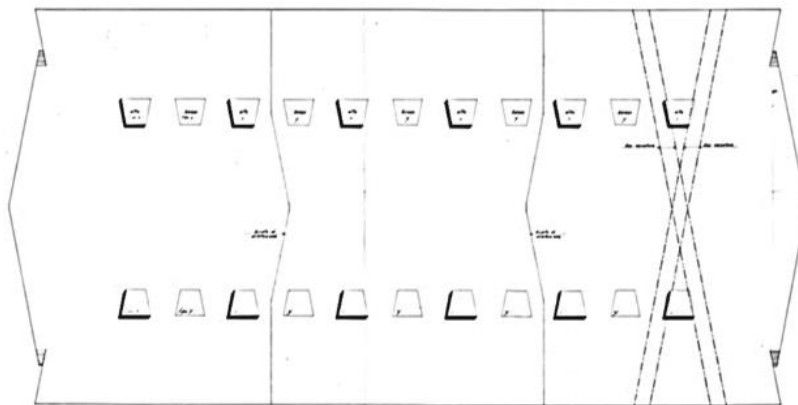


Figure 40: Scheme of the plan of Morandi's Pavilion V showing the division into three blocks linked by joints

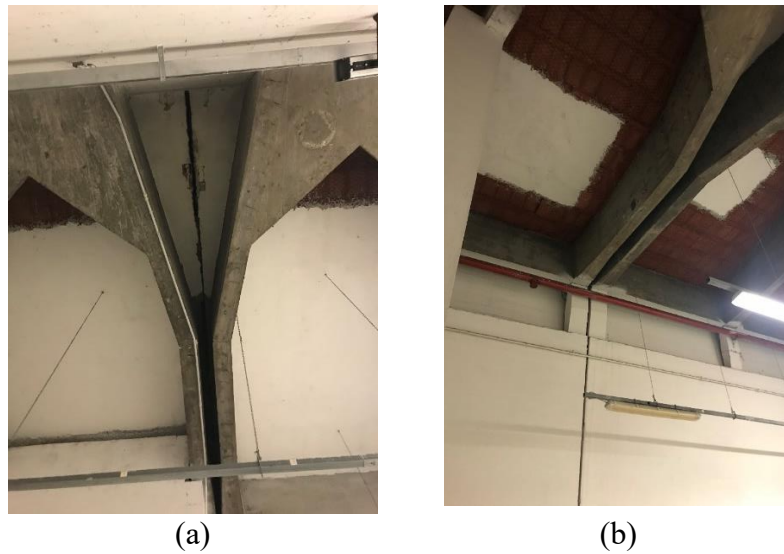


Figure 41: Details of the expansion joint: (a) between the roof and the ribs; (b) between the shorter strut beams and the retaining walls

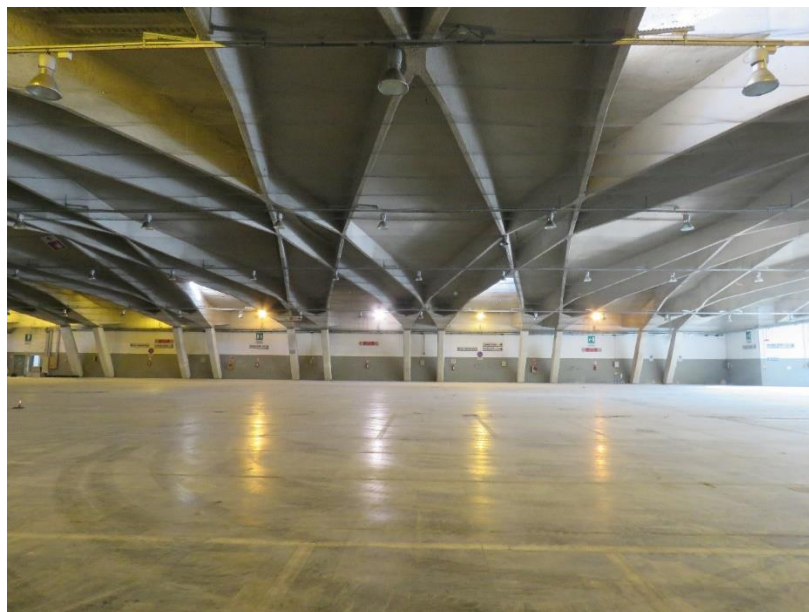


Figure 42: Turin Exhibition Center, underground Pavilion by Riccardo Morandi: internal view with ribs arrangement

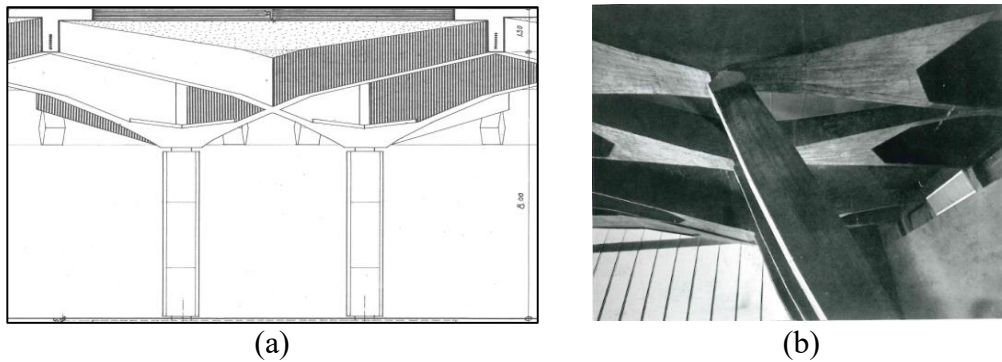


Figure 43: Intersection of the thin ribs creating a dovetail geometry: (a) general section (Bonadè Bottino & Morandi, 1959); (b) detail of the restraints of the shorter strut beams (Boaga & Boni, 1962)

The pairs of prestressed reinforced concrete ribs rest on the pairs of inner inclined strut beams and are anchored to the perimeter walls supporting the ground by means of the shorter strut beams. The perimeter walls (with their dead load and that of the earth) are able to provide a load with a static effect similar to that of the tie rods, not used in this structure. These walls oppose the thrust of the earth with an inclination of 15° toward the inside of the pavilion, creating a harmonious relationship with the inclined connecting strut beams. They have a thickness of 20 cm and a foundation with a continuous rectangular base, having a section of 350x55 cm, extended along the entire development of the perimeter walls. The foundation is also connected by means of a slab to the foundation below the longer strut beam (Figure 44). The stiffening system of these walls consists of ribs embedded in the ground, arranged every 3.4 m, 25 cm thick, and having a base of about 2 m and a height of 4.93 m.

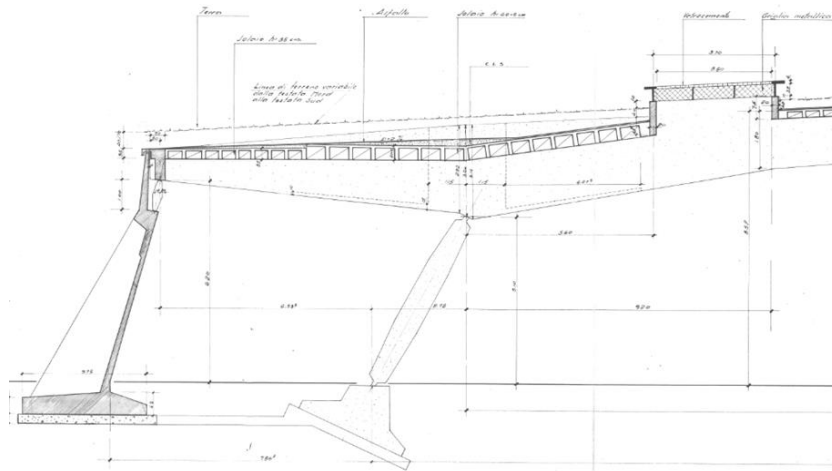


Figure 44: Section B-B from the original drawings in Morandi's documents (Bonadè Bottino & Morandi, 1959).

The horizontal hollow block slabs between the ribs have a thickness between 25 and 45 cm. These floors have the main direction according to the longitudinal axis of the building and have the prestressed ribs as supports. In the point of maximum distance between the pair of ribs, there are spans of 7.5 m, while between the ribs of the same pair the spans are constant and equal to 3 m. Figure 45 shows the roof plan of the pavilion from the original drawings in Morandi's documents. Figure 46 and Figure 47, in turn, report the reinforcement and the section of the generic rib, respectively, from the original drawings. The ribs have variable thickness along their development, in the transverse direction of the structure.

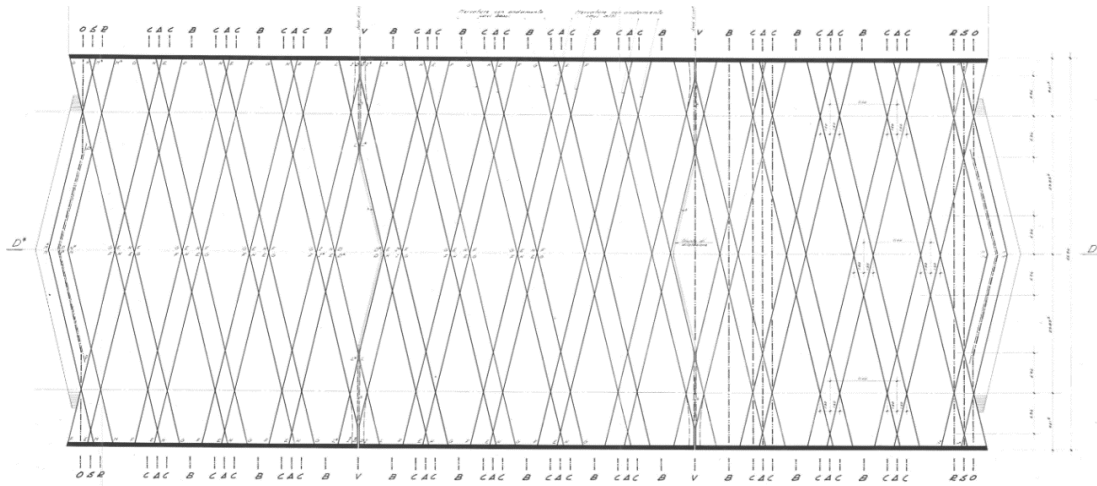


Figure 45: Roof plan from the original drawings in Morandi's documents (Bonadè Bottino & Morandi, 1959)

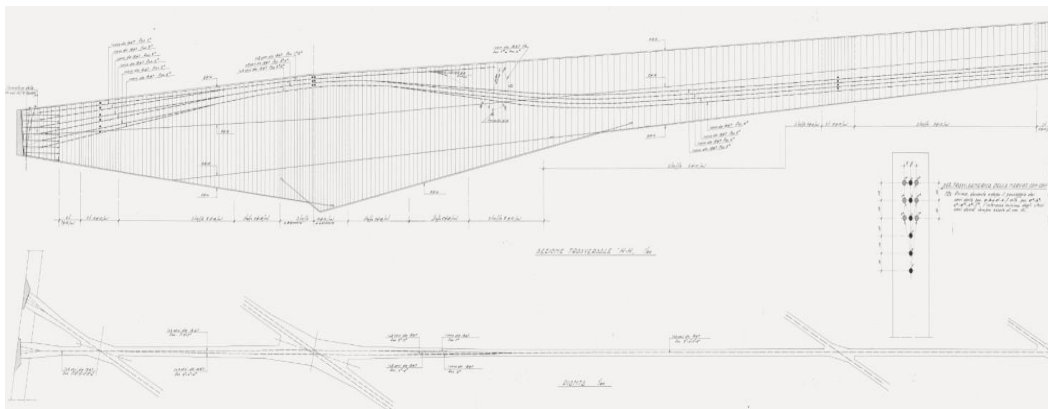


Figure 46: Generic cross section of the ribs with cables from the original drawings in Morandi's documents (Bonadè Bottino & Morandi, 1959)

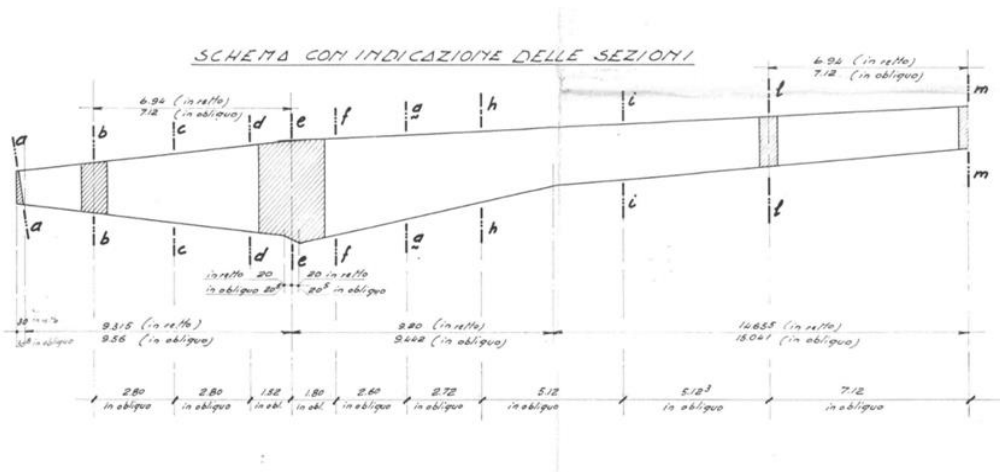


Figure 47: Scheme with the sections of the generic rib from the original drawings in Morandi's documents (Bonadè Bottino & Morandi, 1959)

A service area behind the perimeter wall dedicated to the toilets and technical rooms of the systems is introduced and designed from the side of the pavilion nearest to the city. Access to services is guaranteed through openings in the perimeter walls for a height of 3.38 m, which is useful to avoid damaging the prestressing cables of the shorter strut beams (Figure 48). This additional area covers a surface of 410 m² according to the dimension 56.7 x 7.2 m (Figure 49). The walls are in reinforced concrete while the floor is made of a 45 cm thick hollow block slab to withstand the soil load acting on it.

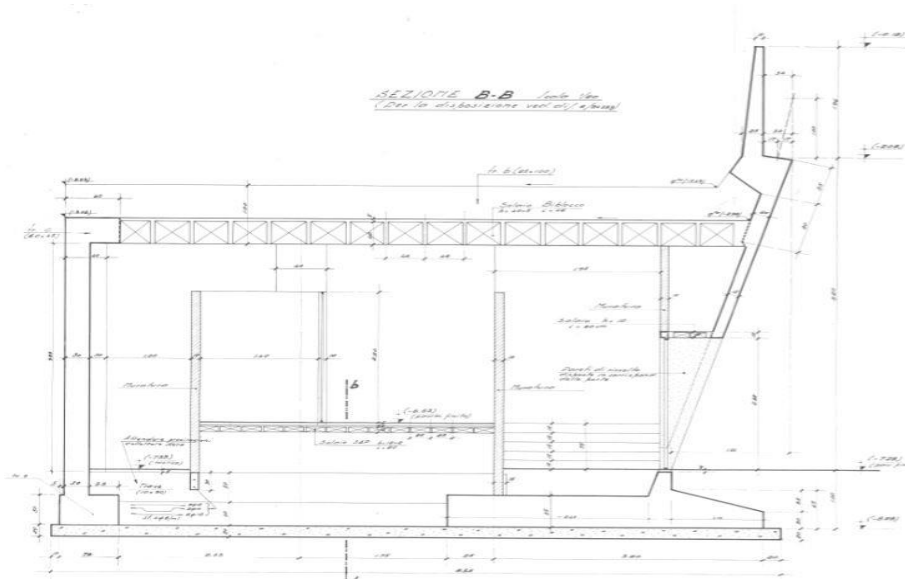


Figure 48: Service area, section B-B from the original drawings in Morandi's documents (Bonadè Bottino & Morandi, 1959)

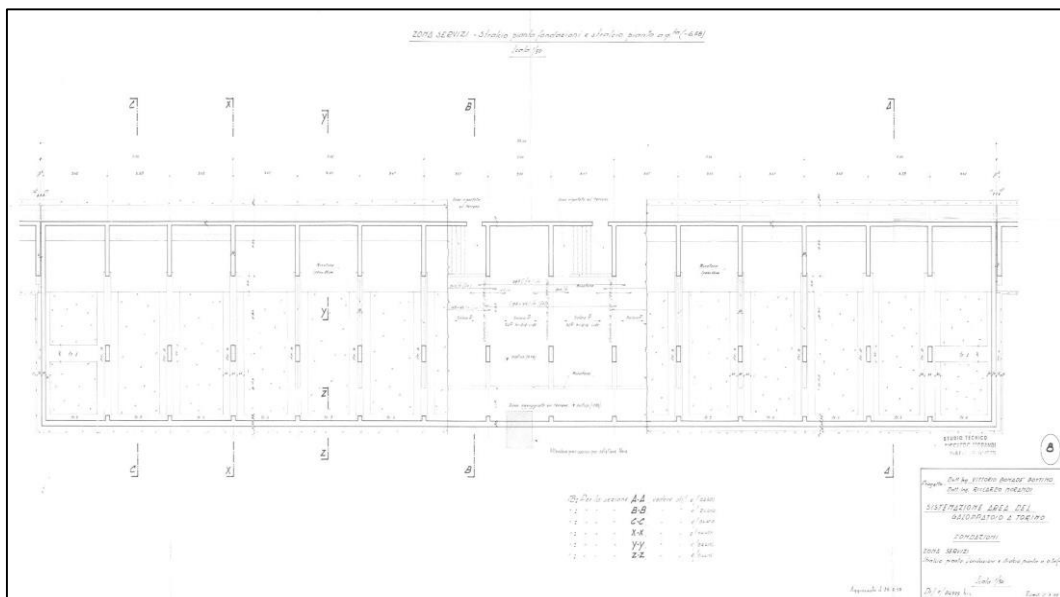


Figure 49: Service area, extract of the foundations plan at -6.68 m from the original drawings in Morandi's documents (Bonadè Bottino & Morandi, 1959)

Figure 50 and Figure 51 report the disposition of the reinforcement of retaining wall and service area walls, respectively.

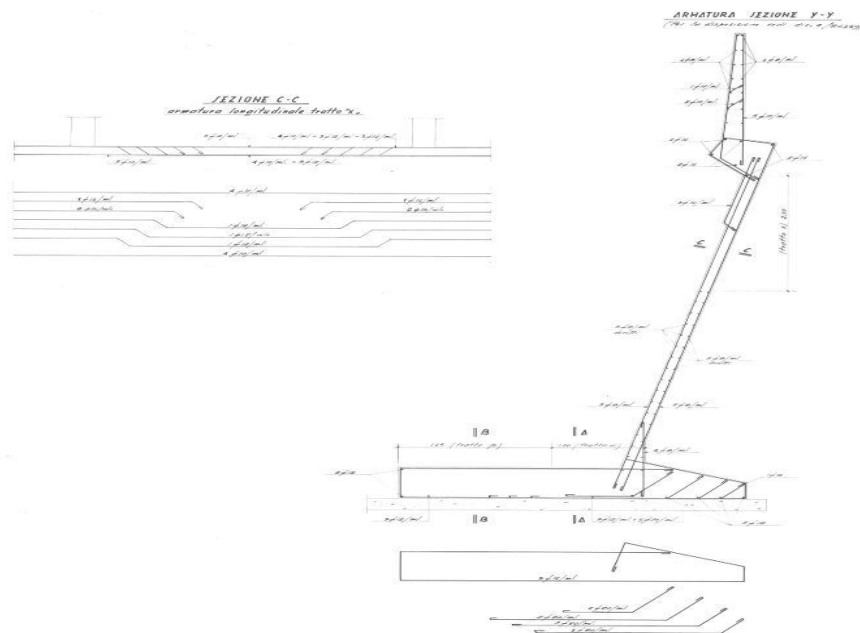


Figure 50: Disposition of the reinforcement of retaining wall from the original drawings in Morandi's documents (Bonadè Bottino & Morandi, 1959)

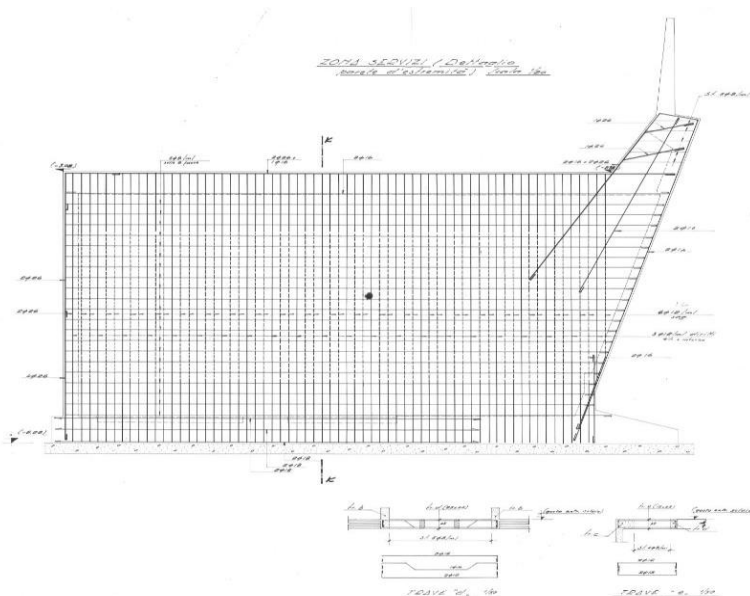


Figure 51: Disposition of the reinforcement of service area walls from the original drawings in Morandi's documents (Bonadè Bottino & Morandi, 1959)

The external ribs of the pavilion constitute the terminal portions of the rhomboidal mesh of the structure and they could have suffered torsional deformations. In order to avoid this problem, Morandi enclosed the external pair of ribs between two reinforced concrete floors capable of generating a closed stiffening box system (Figure 52). Figure 53, Figure 54, Figure 55 and Figure 56 report some extracts and construction details of the external ribs from the original drawings in Morandi's documents.



Figure 52: View of the closed stiffening box system between for the external pair of ribs (Boaga, 1984)

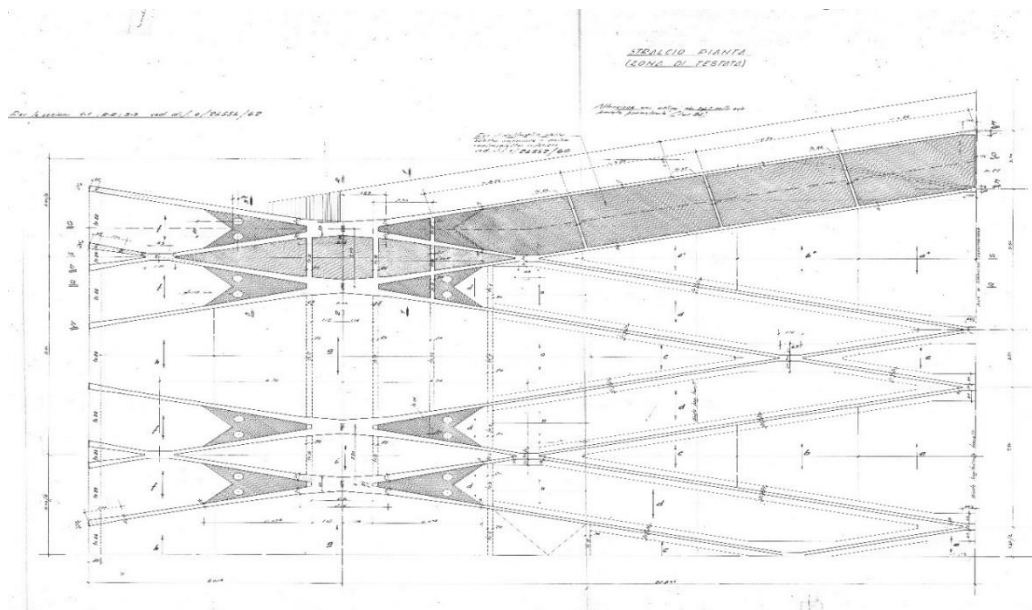


Figure 53: External ribs, extract floor plan from the original drawings in Morandi's documents (Bonadè Bottino & Morandi, 1959)

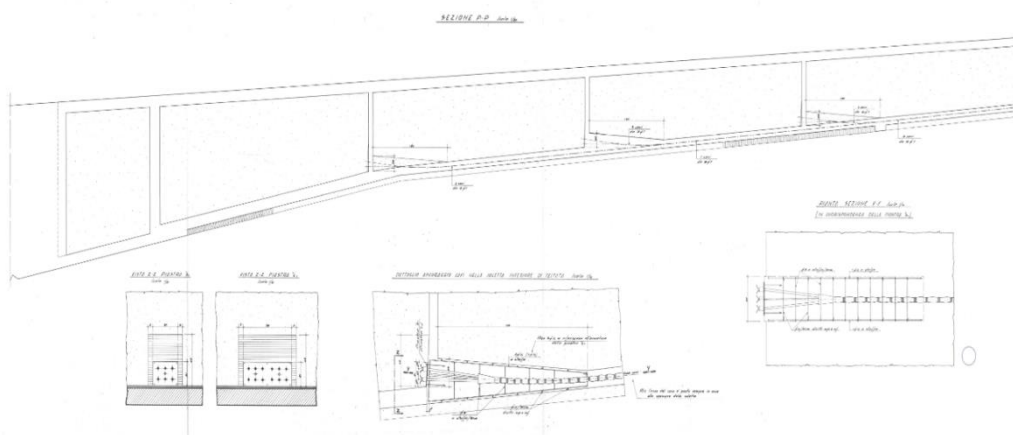


Figure 54: External ribs, section P-P with cables and details from the original drawings in Morandi's documents (Bonadè Bottino & Morandi, 1959)

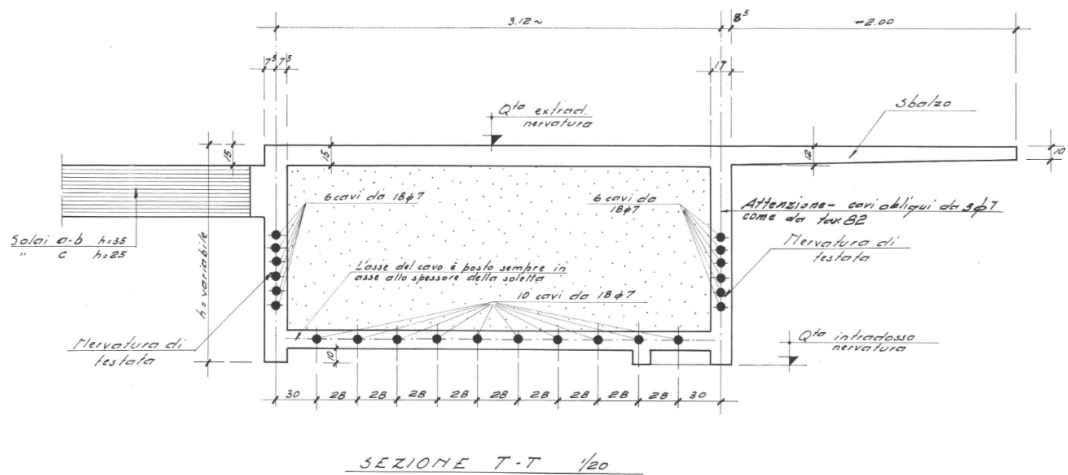


Figure 55: External ribs detail, section T-T from the original drawings in Morandi's documents (Bonadè Bottino & Morandi, 1959)

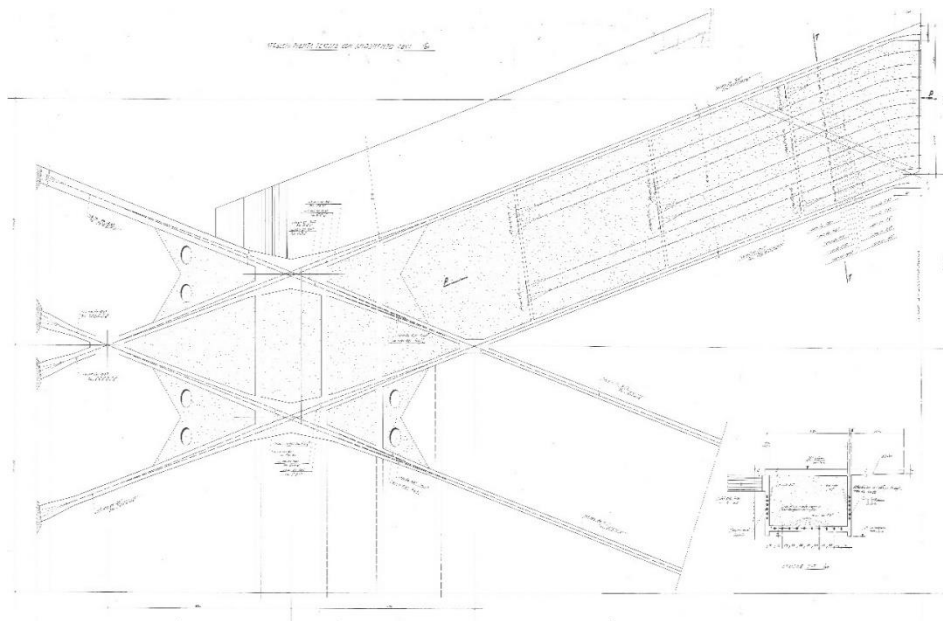


Figure 56: External ribs, extract floor plan with cables arrangement from the original drawings in Morandi's documents (Bonadè Bottino & Morandi, 1959)

As regard the lighting system, this was initially constitute by 22 trapezoidal skylights arranged halfway between the inner supports and the midspan of the ribs. An appropriate division into two different types was also envisaged: a higher type which provided for lateral ventilation grids and lower type just above the green line of the coverage area (Figure 40). The lighting system turned out to be one of the most debated topics, especially when in the 90's the pavilion changed its use,

becoming an underground parking and no longer requiring a high light contribution. Following the waterproofing of the roof with the elimination of the embankment and the introduction of a synthetic green turf in 2005, the skylights were reduced, keeping only the most emerging ones and closing the rest with corrugated sheets.

Another focal point in the construction of pavilion V was the introduction of the two closing windows along the short sides of the building. They consist of large vertical transparent surfaces supported by aluminum frames (Figure 57).

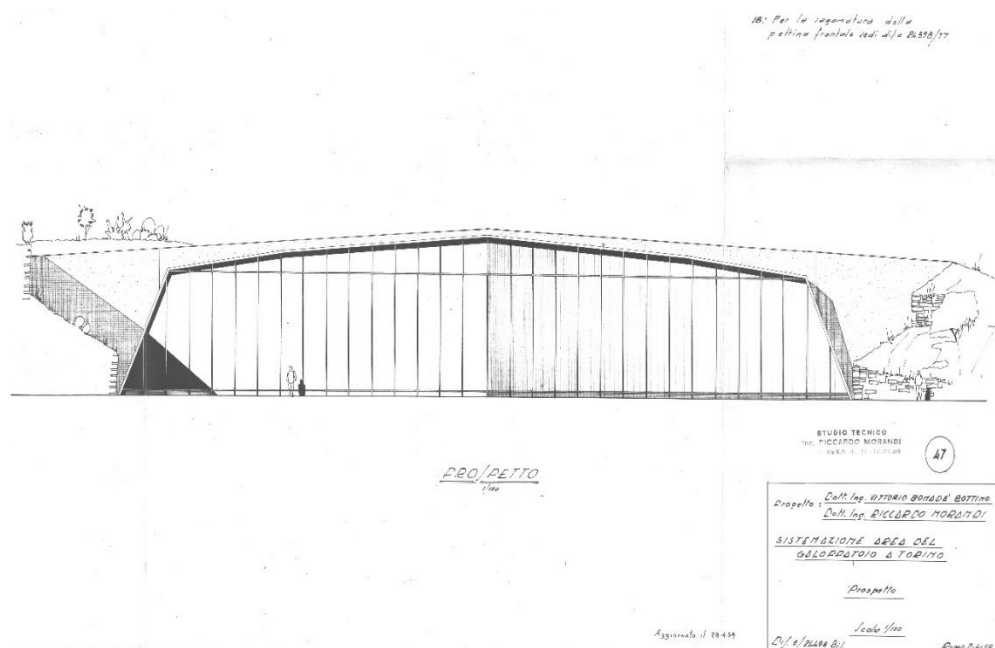


Figure 57: Elevation of Morandi's Pavilion V with a view of the façade along the short side of the structure (Bonadè Bottino & Morandi, 1959)

In the 90's, when the pavilion was converted from an exhibition hall to an underground parking, non-structural inner walls made of cellular concrete were inserted as fire walls. The presence of the fire walls relegates the shorter strut beams to the inside of the side galleries, hiding the visual entirety of the static scheme of the pavilion (Figure 58).



Figure 58: Internal view of the pavilion after the insertion of the fire walls

In the calculation report, the geometric characteristics of different segments of the rib, the weights of the various segments, the permanent loads, the weight of the filling soil acting on the extrados of the roof, and finally, the imposed crowd load on the roof (equal to 4 kN/m^2) were defined.

For the permanent loads Morandi assumed a static scheme in which the constraints in A and D (Figure 39) were not present because the shorter strut beams were not connected to the ribs in the initial stage of the construction process. Subsequently, he introduced the action of the shorter strut beams placed in A and D in order to reduce the positive bending moment at mid-span. Finally, with the delayed constraints in A and D present on the ribs, he introduced the crowd loads on the roof. The structural calculations were performed in different sections of the rib. The internal loads acting in the middle-span section are produced by the bending moment, the pre-stressing of the longitudinal cables and the self-compression deriving from the obliquity of the longer strut beams. The section is entirely compressed, both for permanent and crowd loads. Among the various configurations, Morandi also considered the behavior for the structure subjected to thermal expansion, which generates a variation in the bending moments. At worst, an increase of the moment due to thermal effects was estimated in the order of 1%. Another effect concerns the obliquity of the frames since an inclination angle of 13° with respect to the transverse axis affects the span of the rib. As a whole, the deviation in the bending moments was summarized by the simple ratio of the spans (1.025), which Morandi included in the approximation of the calculation.

In Morandi's documentation, the maximum permissible stresses are reported for the materials used in the Pavilion. For the foundation, concrete with cubic strength at 28 days of 15 MPa was used, 35 MPa for the retaining walls and 45 MPa for the shorter, longer strut beams and ribs. Regular Aq 50 reinforcement bars were used in the structure, with yield strength no less than 270 MPa. Regular reinforcing bars in Italy have nowadays a nominal yield strength of 450 MPa (B450C steel (Ministero delle Infrastrutture e dei Trasporti, 2018)), thus about 66% greater than that one used by Morandi at that time. Finally, special steel was employed for pre-stressing cables with a diameter of 7 mm and rupture stress of 1750 MPa.

The construction phases aimed at the realization of Pavilion V of Turin Exhibition Center lasted only six months; in fact, they began in April '59 and ended in October of the same year. The supervision of the works was entrusted to engineer Ravelli, while the contract for the construction was entrusted to the Roman company "fratelli Giovannetti", which had already collaborated with Morandi. The construction phases were developed in a precise and accurate manner and under the supervision of Morandi. In the first instance, Morandi used the existing ground as a support for the formworks for the construction of the floor and the various rhomboidal mesh ribs (Figure 59) and then, in a subsequent phase, excavated the embankment under the roof (Figure 60). The ribs were made through the assembly of prefabricated segments characterized by holes for the passage of cables. The floors were casted starting from the two ends to continue to the center.



Figure 59: View of the construction site of Pavilion V of Turin Exhibition Center, 1959



Figure 60: View of the construction site of Pavilion V of Turin Exhibition Center, 1959

As shown in Figure 36, with a symmetrical half section from the original drawing, in each balanced beam, four long cables have been positioned longitudinally that cross the entire rib and two short cables for each of the two lateral cantilevers. Moreover, vertical cables have been placed into the shorter strut beams to apply a concentrated downward load at the edges. The process of tensioning these elements was based on a series of successive operations: once the construction was completed and after the hardening of all the resistant parts, and with the shorter strut beams free from the ribs, the following steps were carried out: i) tensioning of the four long cables at 600 MPa; compensation for an equal intensity from the opposite extremity; filling with soil above the roof; ii) tensioning of the short longitudinal cables at 1150 MPa; dismantling of formwork outside the longer strut beams; iii) tensioning of the vertical cables at 289 MPa; iv) tensioning from one end to 1150 MPa of the longitudinal cables (second tensioning); compensation for an equal intensity of the opposite edge; total dismantling of the formworks; locking of the connection of short strut beams with plates; v) tensioning of the vertical cables at 315 MPa; recalibration and grouting of injection grout inside the sheaths (Morandi, 1959).

The study of this complex sequence of tensioning phases and the understanding of the cable layouts, previously described, are useful for a correct interpretation of both the structural behavior and numerical analysis. However, it must always be

considered that the structures often do not fully match what was considered during the design phase or is contained in the drawings since changes were frequently encountered during the construction phase.

An archive research for certificates concerning "Laboratory Tests" of the Pavilion V, starting from those of April 1959, up to October 1959 ones, was carried out at the official lab of the Politecnico di Torino, hypothesizing which structural elements these certificated belonged to. The archives selected for the research have been:

- Archive 586: Certificates from 6201 to 6400
- Archive 589: Certificates from 6801 to 7000
- Archive 591: Certificates from 7201 to 7400
- Archive 593: Certificates from 7601 to 7800
- Archive 594: Certificates from 7801 to 8000
- Archive 595: Certificates from 8001 to 8200
- Archive 596: Certificates from 8201 to 8400

Thanks to the material specifications and to the construction site photographs has been possible to associate each laboratory certificate found with the structural element of the Pavilion V to which it belonged, referring also to the dosage of cement and the date of packaging. The first certificate found was the n°6304, dating back to May '59. It was assumed that this certificate could belong to the longer strut beams (Figure 61). In temporal succession were found the certificates n°6891-7456-7649 dating back to June / July '59, attribute to the retaining walls (Figure 62). Finally, certificates n°7853-8015-8267 were found, dating back to July / August '59. It is assumed that these certificates may belong to ribs and shorter strut beams (Figure 63).



Figure 61: Photography of Pavilion V construction site: longer strut beams



Figure 62: Photography of Pavilion V construction site: retaining walls

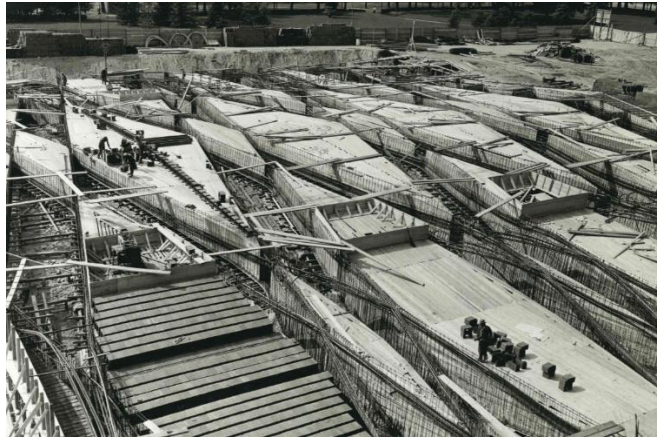


Figure 63: Photography of Pavilion V construction site: retaining walls

6.2 Preliminary investigation

As for diagnostic investigations, in addition to traditional physical-chemical tests on materials, the original program included tests on concrete, geometric characteristics in terms, e.g., of position and diameters of reinforcing bars, layout, and characteristics of post-tensioning cables, and concrete cover, possible grouting defects, adverse effects in terms of the progression of carbonation front, steel corrosion, and other chemical attacks, etc. Moreover, advanced techniques to ascertain the characteristics, e.g., of the concrete mix at the nanoscale, can be helpful to better understand the progression of adverse effects, as well as the provision of physical-chemical remedial actions. The principle of combined techniques for more reliable ascertainment is highly recommended (Levi & Chiorino, 2004). Among the usual diagnostic objectives of reinforced and prestressed concrete structures, the inspections and diagnostic investigations must account for the specific problems of Morandi's pavilion. In fact, the main challenge is represented by the need to accurately diagnose the conditions concerning the corrosion of the post-tensioning cables in the main ribs, in consideration of the very thin thickness (16 cm) of their webs and of the possible grouting defects, typical of early prestressing technologies.

Pavilion V was subjected to a broad range test campaign by Politecnico di Torino (MASTRLAB DISEG, 2019) (Laboratorio di Dinamica e Sismica, 2019). The test campaign was executed in 2019 (Figure 64 and Figure 65) to assess the structural safety conditions of the structure. Both destructive and non-destructive tests were performed (e.g., see Figure 66) to evaluate the health state of the various structural elements (MASTRLAB DISEG, 2019). In detail, inspections on the

structures were carried out to determine the concrete cover, layout and characteristics of post-tensioning cables, possible grouting defects, steel corrosion and other chemical attacks, and geometric characteristics in terms of position and diameters of reinforcing bars (pacometric investigations). Moreover, a direct check was carried out for each element type through a scarification.

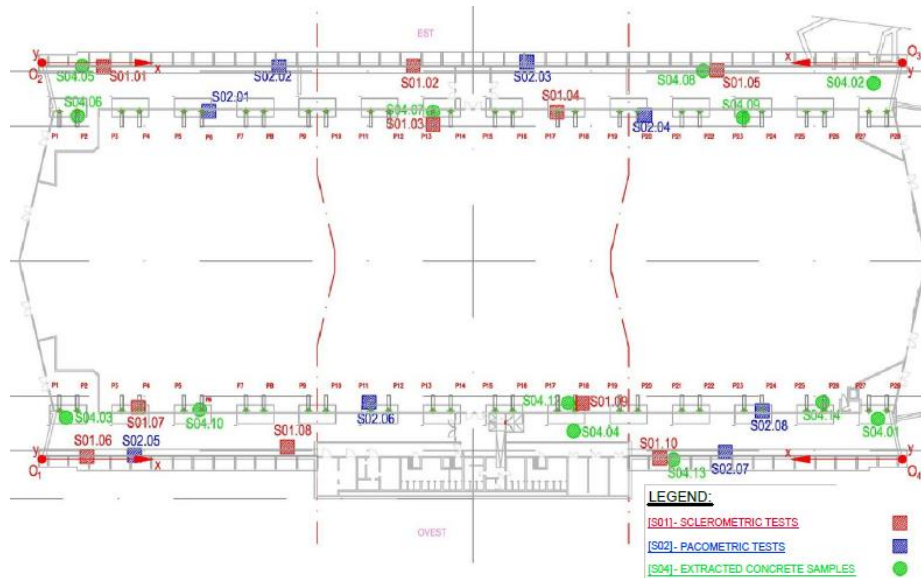


Figure 64: Pavillion V: Test positions at the underground floor (MASTRLAB DISEG, 2019)

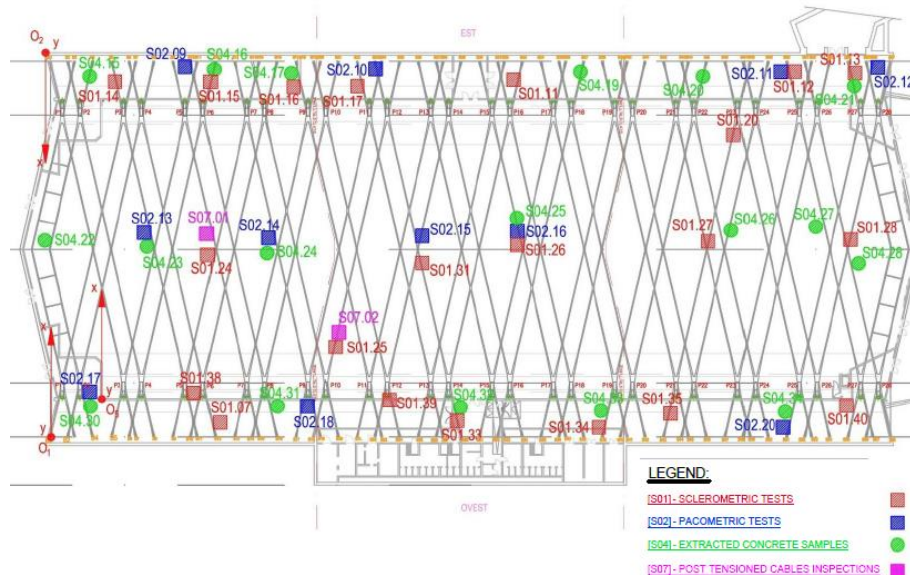


Figure 65: Pavillion V: Test positions at the roof level (MASTRLAB DISEG, 2019)

Finally, mechanical tests have been executed to evaluate the compressive strength of the different elements of the structure: samples were extracted from foundations, retaining walls, ribs, and longer strut beams (see Figure 66 left). Each sample was analyzed with phenolphthalein to determine the progression of the carbonation front (Figure 66 center) and then subjected to a compression test. The specimens were extracted and tested according to UNI EN 12504-1:2009 (Testing on concrete in structures – Part 1: Cored specimens – Taking, examining and testing in compression) and UNI EN 12390-3:2009 (Testing hardened concrete – Part 3: Compressive strength of test specimens). The total number of specimens extracted and tested was 32, divided as follows: 5 from the foundations; 3 from the retaining walls; 6 from the longer strut beams; 18 from the ribs. The depth and the diameters of the cores was between $(97.57 \div 218.34)$ mm and $(93.73 \div 104.40)$ mm, respectively. The ratios depth/diameter was between $0.98 \div 2.11$ (MASTRLAB DISEG, 2019). Table 2 summarizes the depth, diameters, ratios depth/diameter, compressive strengths, and carbonation depths of the cores.

These results show that the structure is made of concrete with reasonably high compressive strength. Different strength values can be ascribed to distinct causes. The higher values in the retaining walls could be due to humidity conditions that could have influenced the hardening of concrete. Furthermore, the carbonation levels of most samples are relatively low. The investigations have also verified the position of the reinforcement through cover meter and rebar detector tests, as well as the state of the post-tensioning system through the scarification of some ribs and shorter strut beams. These latest investigations have proved useful in diagnosing the important state of corrosion of cables and grouting defects.

Table 2: Results of concrete compression tests: average depth h , average diameter d , ratio h/d , ultimate load F , compressive strength f_c and average carbonation depth c (MASTRLAB DISEG, 2019)

Specimens	h (mm)	d (mm)	h/d (-)	F (kN)	f_c (MPa)	c (mm)
S04-01 (Foundations)	107.32	104.35	1.03	278.1	32.5	0
S04-02-A (Foundations)	116.36	104.23	1.12	253.2	29.7	0
S04-02-B (Foundations)	110.82	104.25	1.06	170.6	20.0	0
S04-03 (Foundations)	213.28	104.26	2.05	273.7	32.1	0
S04-04 (Foundations)	218.34	104.35	2.09	493.2	57.7	0
S04-05 (Retaining walls)	215.53	104.40	2.06	398.7	46.6	10
S04-08 (Retaining walls)	110.03	104.32	1.05	538.9	63.0	10
S04-13 (Retaining walls)	109.54	104.33	1.05	523.3	61.2	10
S04-06 (Longer strut beams)	194.82	93.80	2.08	407.9	59.0	3
S04-07 (Longer strut beams)	198.17	93.80	2.11	248.6	36.0	20
S04-09 (Longer strut beams)	194.54	93.90	2.07	363.3	52.5	4
S04-10 (Longer strut beams)	194.57	93.75	2.08	459.9	66.6	5
S04-12 (Longer strut beams)	194.94	93.73	2.08	341.0	49.4	5
S04-14 (Longer strut beams)	105.84	93.76	1.13	290.0	42.0	15
S04-15 (Ribs)	115.37	104.38	1.11	328.0	38.3	45/-
S04-16 (Ribs)	113.77	104.40	1.09	217.3	25.4	70/70
S04-17 (Ribs)	102.08	104.40	0.98	529.6	61.9	20/25
S04-19 (Ribs)	98.67	93.93	1.05	351.2	50.7	27/-
S04-20 (Ribs)	101.00	93.86	1.08	277.6	40.1	30/-
S04-21 (Ribs)	184.86	93.91	1.97	259.3	37.4	25/20
S04-22 (Ribs)	101.69	93.91	1.08	223.8	32.3	40/40
S04-23 (Ribs)	99.42	93.91	1.06	329.0	47.5	30/20
S04-24 (Ribs)	103.99	93.84	1.11	237.1	34.3	40/40
S04-25 (Ribs)	102.52	93.86	1.09	293.3	42.4	35/35
S04-26 (Ribs)	100.98	93.83	1.08	260.6	37.7	35/30
S04-27 (Ribs)	104.50	93.87	1.11	212.7	30.7	45/40
S04-28 (Ribs)	97.57	93.90	1.04	317.0	45.8	45/40
S04-30 (Ribs)	195.49	93.95	2.08	277.0	40.0	35/30
S04-31 (Ribs)	193.17	93.92	2.06	259.2	37.4	35/25
S04-32 (Ribs)	98.22	93.95	1.05	334.4	48.2	-/20
S04-33 (Ribs)	99.67	93.93	1.06	277.7	40.1	30/-
S04-34 (Ribs)	98.42	93.87	1.05	330.0	47.7	20/-

The testing campaign also included static tests on two different ribs, to assess the bearing capacity of the structure under the characteristic combination of actions (see Figure 66 right). The load tests have been carried out using 7 hydraulic jacks with a maximum capacity of 100 kN, connected in parallel to an hand pump equipped with a pressure sensor and a load cell. Each jack has been connected to the structure by means of a steel chain, passed through a hole made in the rib (maximum diameter of 80mm and position determined following both pacometric and endoscopic inspection aimed at avoid interference with cables and reinforcements), and contrasted by fully loaded three-axle trucks (approximately 300kN). Displacement potentiometric transducers (novotechnik, model TR0050) have been used for the measurement of the displacements.



Figure 66: Pavilion V: Extraction of a concrete sample from a longer strut beam (left); carbonation tests on the samples of the ribs (center); view of the static tests with trucks connected to the ribs through jacks (right) (MASTRLAB DISEG, 2019)

The normalized vertical displacements progressively measured during the test on a rib are reported in Figure 67. At the end of each loading phase, the displacement measures stabilization has been checked before proceeding with the next increase or decrease. The forces measured by the load cell (reported in Figure 8) are to be considered as applied equally at each loading points. The displacements measurement points have been located adjacent to the loading points and also in correspondence of adjacent ribs to evaluate the transversal collaboration (MASTRLAB DISEG, 2019).

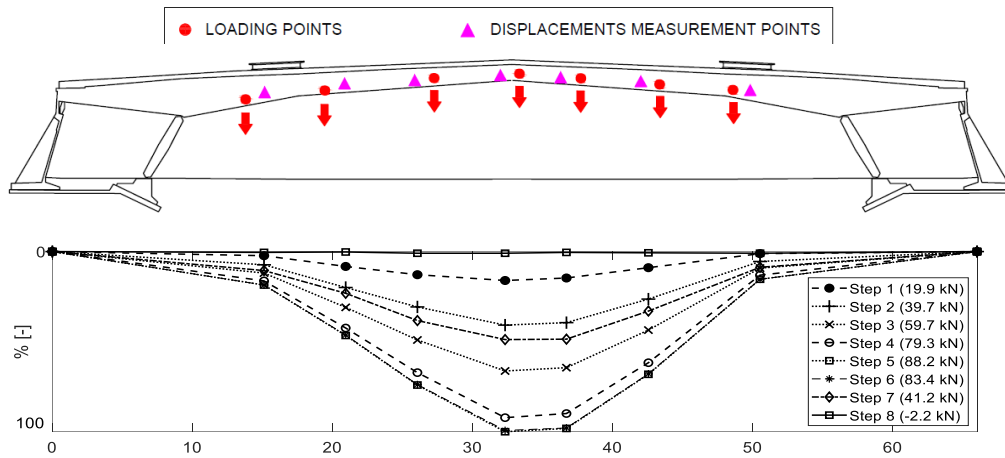


Figure 67: Pavilion V: normalized vertical displacements measured during the static test on a rib (MASTRLAB DISEG, 2019)

The maximum displacement measured during the static test on a rib was 4.36 mm. This result showed a high stiffness of the structure under the imposed loads, despite a span of approximately 48 m between the inner supports. Moreover, the small displacements have proven a significant transversal collaboration of the ribs due to the numerous intersections between these elements, confirmed by the displacement measurement on the adjacent rib (equal to 3.20 mm in Step 5).

6.3 Creation of the preliminary model

The activities related to the condition assessment typically begin with creating a geometric model based on information obtained from the existing documentation, as well as from additional data collected in tests and surveys. Figure 68 (left) reports the geometric model of the pavilion with detailed geometric information, which allowed for appropriate understanding of the structural characteristics of the pavilion and the recognition of possible design and construction principles. The structure is divided into three main bodies by means of two expansion joints, which cross the roof and the external walls, and whose behavior was uncertain. For a correct reproduction of the internal forces in the pavilion, the elastic FE model has been created as much as possible following the actual dimensions and thickness of the real structure. The resulting mechanical model (Figure 68 right) was corroborated with the data acquired in the experimental tests.

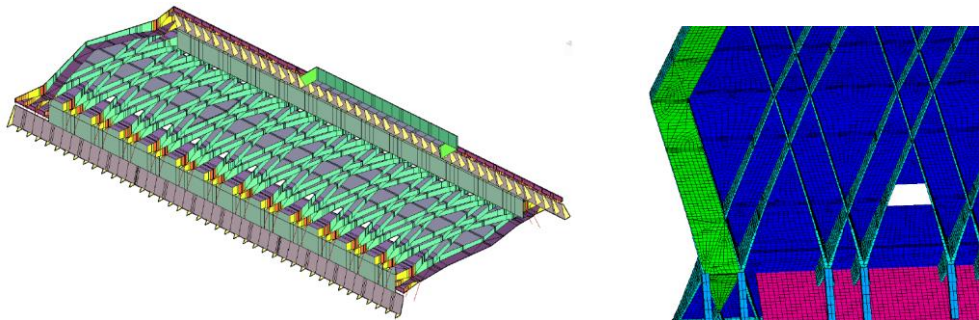


Figure 68: Pavilion V: geometric model (left) and detail of the FE model at the ribs (right)

The FE model was mostly made of shell and beam elements to represent the macro-elements composing the structure. In particular, the shorter and the longer strut beams were modelled with Timoshenko beams (Link188 Element), while for the roof, the ribs, and the retaining walls, Mindlin-Reissner shell elements (Shell281 Element) were used (ANSYS.Inc, 2013). The materials, defined as linear elastic isotropic, were characterized by inserting specific mechanical properties for the macro-elements. Densities were defined equal to 2500 kg/m^3 , except for the expansions joints which have zero mass and walls in cellular concrete which density is 400 kg/m^3 ; Poisson's ratios were defined equal to 0.2; while the values of elastic moduli are discussed in paragraph "6.12 Corroboration of the FE model".

6.4 Structural assessment

The structural reassessment should be conducted first recurring to the original calculation schemes, which are often available for 20th century architecture, and then with the FE model, accounting for the outcomes of the experimental tests, with particular attention to the critical elements of the building.

For the assumed case study of Pavilion V, the structural assessment of the post-tensioned rib has been carried out according to EC2 (CEN, EUROCODE 2, 2004) at different stages: a) design stage, in accordance with the values reported by Morandi; b) design stage, based on the compression strength of samples taken during construction, following the values reported in the test certificates issued in 1959 by the official lab of the Politecnico di Torino; c) after 60 years, in accordance with the strength values reported in the test certificates issued in 2019 by the same lab.

The plots in Figure 69 refer to the samples tested in 2019, and correspond to the prior and posterior probability density functions for compression strength, f_c ,

obtained from Bayesian updating formulations (Joint Committee on Structural Safety, 2001), (Ditlevsen & Madsen, 1996). In particular, the density functions of both probability and cumulative (posterior PDF and CDF) have been calibrated on 18 samples extracted from the ribs and then tested.

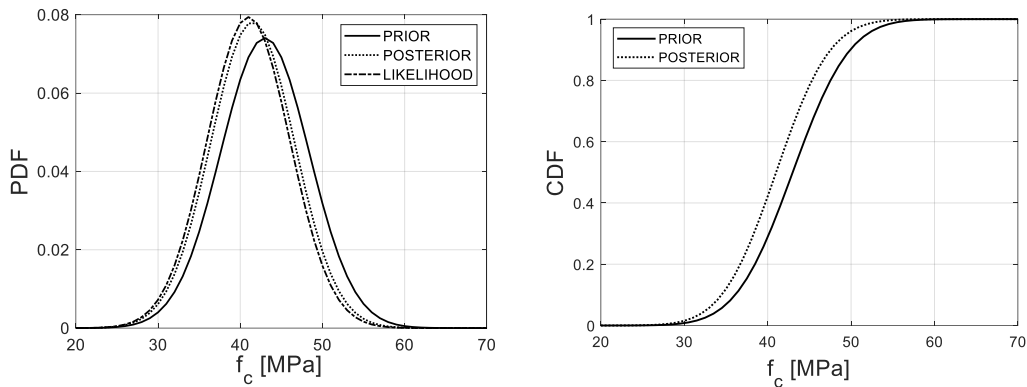


Figure 69: Concrete compression strength in a post-tensioned rib of Pavilion V as a results of 2019 campaign: prior and posterior probability density function (PDF) (left) and cumulative density function (CDF) (right)

Figure 69 shows the Bayesian updating of the average concrete compression strength of the ribs, as a result of 2019 campaign, from 43.00 MPa to 41.51 MPa. As reported in the paragraph “6.5 Preliminary structural analysis”, this decrease on material strength (approximately 3÷4%) leads to a reduction of the ultimate load multiplier on the rib from 1.55 to 1.40 (approximately 10%), considering the cables in good health state.

6.5 Preliminary structural analysis

Morandi’s results are reported in Figure 70, where the bending moment diagrams of the rib refer to permanent loads (b), post-tensioning of the shorter strut beams (c), and imposed crowd loads (d), respectively. According to the original calculations, the diagrams take into account the vertical offset between the rib axis and the hinge of the longer strut beam, which amounts to 1.47 m (Figure 70 a).

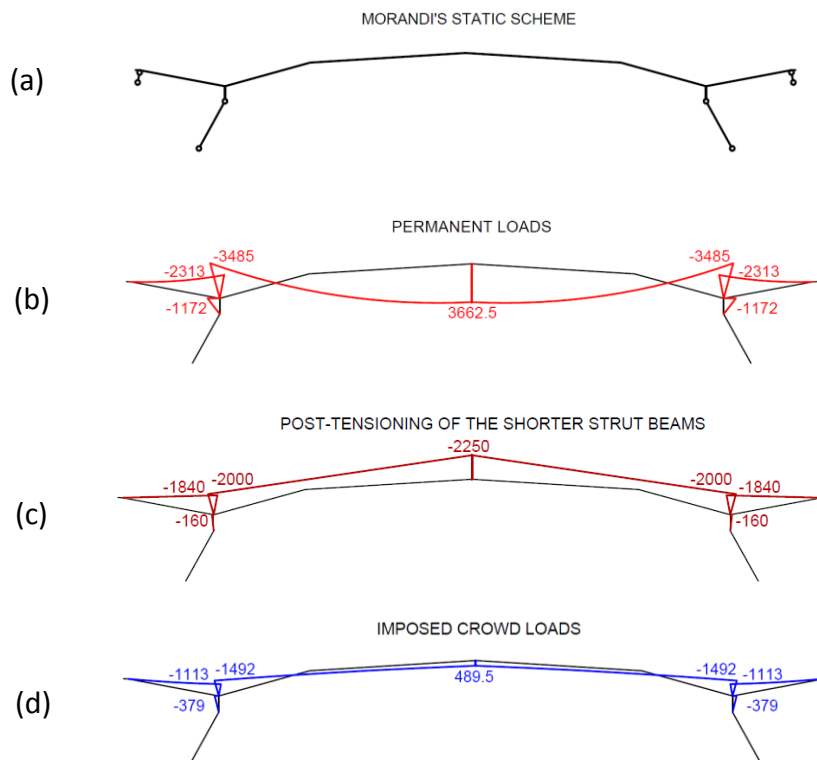


Figure 70: Scheme with vertical offset from Morandi's calculation report (a) and bending moment (kNm) acting on a rib as resulting from Morandi's scheme; (b) due to the permanent loads; (c) due to post-tensioning effect of the shorter strut beams; (d) due to the imposed crowd loads (Morandi, 1959)

In full consistency with these schemes, Table 3 contains a comparison between the ultimate load multipliers (for bending moment verification at midspan and at the supports) calculated with the design values of concrete strength and those resulting from the posterior values for the ribs. In particular, ultimate load multipliers $\alpha = q_{Rd}/q_d$ were defined as the ratio between the ultimate crowd load on the roof with respect to a specific verification, q_{Rd} , and the imposed load, q_d . Accordingly, these multipliers were calculated: i) at the design stage with the regulation in force at the time (Gazzetta Ufficiale del Regno d'Italia, 1939) using nominal values of actions and strengths (*RD39*), ii) at the design stage with the current standards (*EC*), iii) at a reassessment stage with the compression strengths evaluated on samples taken during construction (with the current standards) (*REASS,1959*), and iv) at a reassessment stage with the posterior values resulting from the tests conducted in 2019 (with the current standards) (*REASS,2019*). It is worth highlighting that Morandi assumed a crowd load on the roof, q_d , equal to 4 kN/m² (imposed load in Figure 70 d).

Table 3: Comparison between ultimate load multipliers (with respect to bending moment verification at midspan and at the supports) calculated: at the design stage (*RD39*); at the design stage with the current standards (*EC*); at the reassessment stage during construction (*REASS 1959*); at the reassessment stage in 2019 (*REASS 2019*). μ and σ represent the mean and standard deviation assumed for the concrete compression strength

	<i>RD39</i>	<i>EC</i>	<i>REASS 1959</i>	<i>REASS 2019</i>
μ_{fcm} (MPa)	-	43.00	42.17	41.51
σ_{fcm} (MPa)	-	5.38	5.08	5.10
α_{midspan} (-)	1.68	1.55	1.47	1.40
α_{supports} (-)	4.04	4.77	4.74	4.71

From Table 3 it can be noted that at the supports the load multipliers are greater than at midspan. Moreover, the previous results show that, as regards concrete, the updated load multipliers approximately remain in line with Morandi's original project. However, the structural assessment in such structures depends above all on the condition of the tendons, which in the post-tensioned ribs plays a fundamental role.

6.6 Investigations on the post-tensioned reinforced concrete system

As described in paragraph "3.4 Diagnosis of post-tensioned concrete structures", partial rupture or corrosion of pre-stressing tendons are difficult to directly locate. Therefore, local checks on the post-tensioned system of some sample balanced beams have been executed. In fact, despite the impossibility of making an exhaustive program of endoscopies and local assays, the inspections on the tendons of two ribs have revealed: i) presence of corrosion or full-blown rupture of some wires in the tendons, ii) poor grouting; iii) positioning errors. The poor grouting allowed to carry out an endoscopy inspection inside the duct (Figure 71).



Figure 71: Visual inspection of post-tensioning tendons in the ribs (left), and endoscopy inspection inside a duct of the rib (right) (MASTRLAB DISEG, 2019)

In particular, hardened gray grout was found along the lower portion of the ducts, while poor segregated grout was found at the upper portion of the tendon, probably due to the gravity separation process. Moreover, presumably because segregation involved gravimetric causes, the poor grout forms have been most pronounced in the higher visual inspection. The grout filling of the ducts was not complete and regions where grout was segregated exhibited air voids along the top of the duct, where endoscopy inspections were conducted. Grout contamination by Cl^- , which facilitates corrosion when in exceeding concentrations, have not been investigated. However, regions of different grout quality and presence of strand corrosion products were visually assessed. In fact, although not easily quantifiable, corrosion products at some of the strand surfaces were visible. Indeed, air voids and segregation defects are the major issues for post-tensioned structures and accelerate corrosion, potentially affecting the durability of the elements.

6.7 Preliminary sensitivity analysis

The inspections on the tendons of two ribs have revealed some broken wires in the tendons, together with poor grouting and positioning error. These defects accelerate corrosion, potentially affecting the durability of the elements. According to (Limongelli, et al., 2016), the sensitive parameters should be assessed in real-time, and for particular loading conditions, to evaluate the possible trends induced by pre-stress steel losses or corrosion. Consequently, as in this case it is not possible to perform endoscopies in an exhaustive way for the entire building, the condition assessment has been conducted in terms of sensitivity analysis with respect to the percent reduction of the post-tensioning steel area, as well as to the errors in positioning the cables.

The sensitivity analysis concerned the parameters A_r (area of the pre-stressing tendons) and d_p (effective depth of the cross-section) of the resistant section, which constitute the main terms for the calculation of ultimate bending moment capacity at midspan. In particular, these analyses were performed considering the bending moment verification at midspan and at the supports, with reference to the ribs under direct investigation, i.e. S07.01 (Figure 65). The structural scheme of this rib (Figure 70 a) can be assumed to be that typical of Morandi, except for the external ribs that are also affected by torsion. Since it was not possible to investigate all cables, it has been assumed at this stage that wire corrosion (and error in positioning) increases uniformly and spreads across all ribs of the structure. This assumption is tantamount to focusing on the assessment of the single rib, neglecting the possible redistribution effect due to the redundancy of the entire system. Accordingly, the plots in Figure 72 report the ultimate load multipliers (for bending moment verification at midspan and at the supports) as a function of the assumed corrosion in the wires of the ribs and the positioning error (in percent of effective depth) referring to the cables centroid, respectively. At midspan, referring to Morandi's documents, the centroid was at 105.5 cm with respect to the extrados of the rib (with an overall depth of 130 cm). Thus, in the Figure 72 b, 10% error means an error of approximately 10.5 cm, which corresponds to the position of the centroid at 95 cm with respect to the extrados. At the supports, referring to Morandi's documents, the centroid was at 272.5 cm with respect to the intrados of the rib (with an overall depth of 292 cm). Thus, in the Figure 72 d, 10% error means an error of approximately 27 cm, which corresponds to the position of the centroid at 245.5 cm with respect to the intrados. The ultimate load multipliers for the balanced beam has been calculated for the fundamental combination (CEN, EUROCODE 2, 2004).

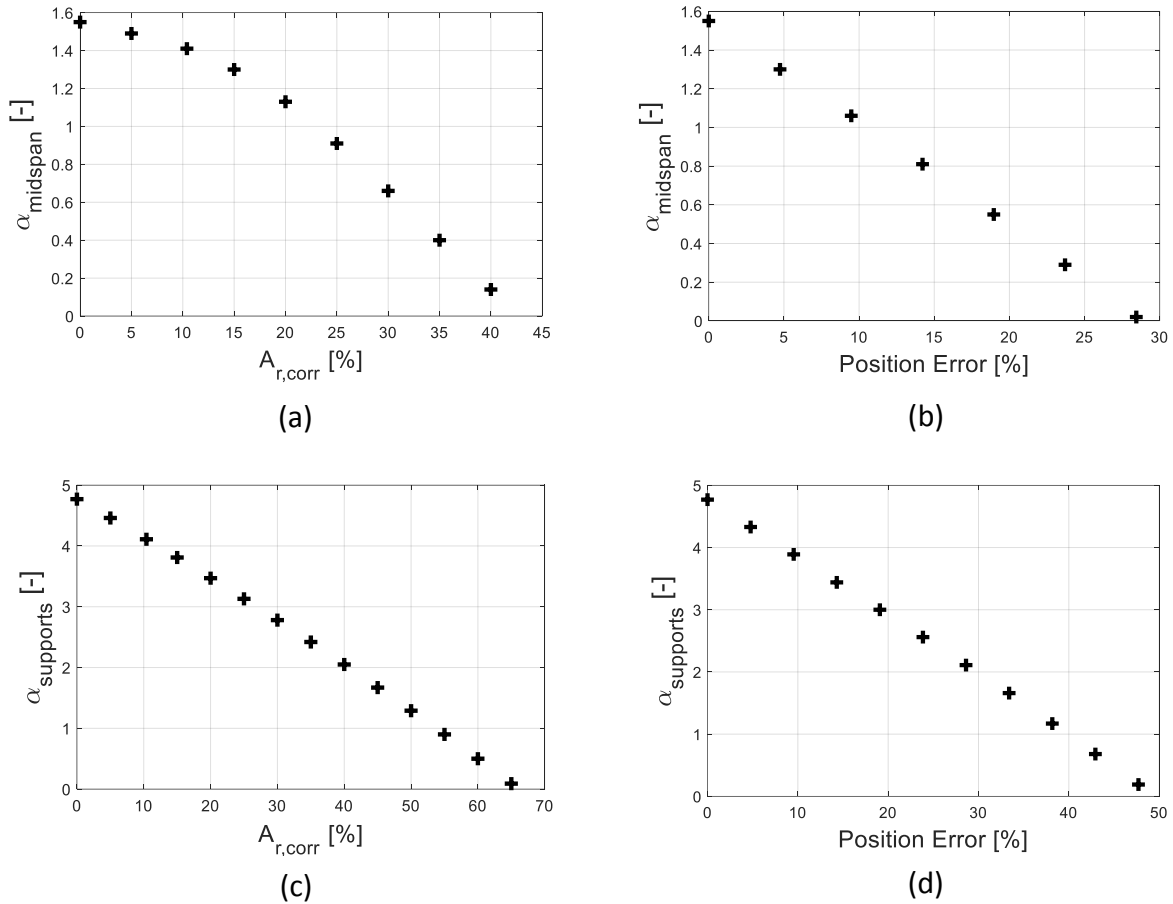


Figure 72: Sensitivity analysis conducted on the rib element: the ultimate load multiplier (for bending moment verification) on Morandi's scheme as a function of corroded post-tensioning steel area in the rib at midspan (a), at the supports (c) and of the positioning error (in percent of the effective depth) in the vertical direction of tendons respect to the extrados of the rib at midspan (b), respect to the intrados of the rib at the supports (d)

Additionally, a sensitivity analysis has been conducted for the condition assessment concerning also the reduction of post-tensioning steel area of the shorter strut beam elements. The corrosion in these elements causes an increase of bending moment in the middle of the rib and a reduction (in terms of absolute value) of bending moment at the supports. Figure 73 reports the ultimate load multipliers (with respect to bending moment verification at midspan) as a function of the assumed corrosion in the wires both of the ribs and the shorter strut beams.

The results expressed in Figure 72 and Figure 73 show the sensitivity of the load multipliers for the balanced beam scheme concerning the analysed parameters,

without considering the possible redistribution effect between the interconnected ribs.

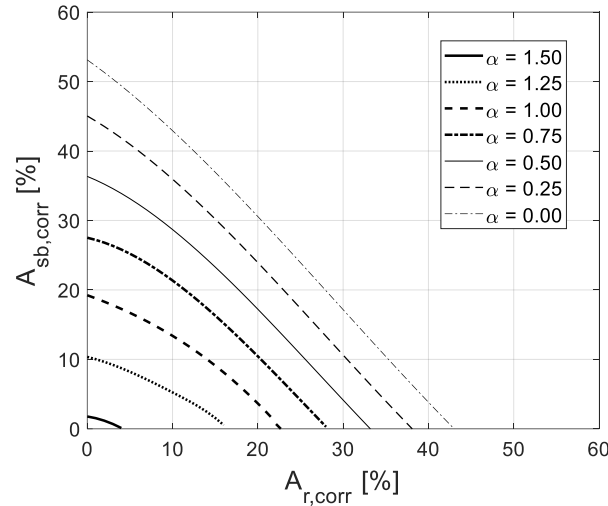


Figure 73: Sensitivity analysis conducted at midspan of the rib element: the ultimate load multiplier (for bending moment verification) on Morandi's scheme as a function of both corroded post-tensioning steel area in the rib ($A_{r,corr}$) and corroded post-tensioning steel area in the shorter strut beams ($A_{sb,corr}$)

6.8 Preliminary seismic analysis

The baseline model was used for a preliminary seismic assessment according to Italian National Standard (Ministero delle Infrastrutture e dei Trasporti, 2018). A standard Lanczos eigensolver was applied for mode calculation (ANSYS.Inc, 2013). A standard multimodal analysis with elastic response spectra was executed to evaluate the main criticalities and vulnerabilities of the Pavilion. The seismic actions were applied along the two horizontal and vertical directions, taking into account the accidental eccentricity of the masses. Then the effects, in terms of internal forces, were combined with those produced by other actions. All the partial safety factors in the verifications were considered according to Italian Standard. For the seismic action a return period $T_R=949$ years and a probability of exceedance $P_R=10\%$ were considered (strategic structure use).

In the seismic assessment, a confidence factor FC equal to 1.2, corresponding to a level of knowledge LK2 was considered for concrete; and a confidence factor FC equal to 1.35 corresponding to a level of knowledge LK1 was considered for steel. These levels of knowledge were acquired on the basis of investigations,

findings and tests on material according to NTC2018 (Ministero delle Infrastrutture e dei Trasporti, 2018) and the ministerial circular (Ministero delle Infrastrutture e dei Trasporti, 2019).

As a result of the seismic assessment, both shorter and longer strut beams of the pavilion were recognized as critical elements. The assessment on the selected elements provided the following results along the longitudinal axis: i) verifications of the longer strut beams not satisfied with respect to axial and bending forces (Figure 74 left); ii) insufficient shear reinforcement in the shorter strut beams (Figure 74 right). However, it is essential to highlight that at the time of the conception of Pavilion V the buildings in Italy were designed and built with no, or very limited, seismic provisions due to the lack of technical standards. So these results were expected.

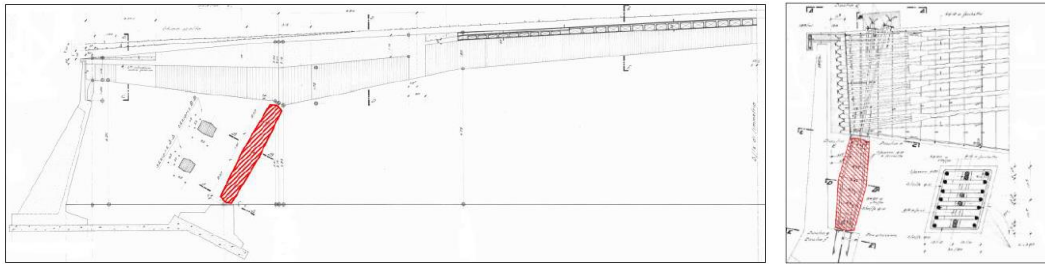


Figure 74: Critical elements of the Pavilion V: longer strut beams (left) and shorter strut beams (right)

In this preliminary assessment, the main uncertainty inherent in the model concerns the effectiveness of the joints, simulated by shell elements with a fictitious thickness. As it was difficult to predict their contribution to the structural behavior of the pavilion, an elastic modulus was assigned to the joints as a first attempt to ensure overall behavior. However, on the basis of the results coming from the following vibration tests, the behavior of the joints proves to be considerably different from that assumed in the preliminary analysis, as the three bodies of the buildings tend to vibrate with distinct frequencies. Starting from these observations, the deformability of the joints was subject to specific investigations.

6.9 Design detailed investigation strategy

Ambient vibration tests were performed to identify the modal characteristics, reconstruct the global dynamic behavior of the pavilion, and highlight possible criticalities in the seismic response (Laboratorio di Dinamica e Sismica, 2019) (Ceravolo, Coletta, Lenticchia, Minervini, & Quattrone, 2020).

The structural complexity of Pavilion V directly affects its dynamic behavior and the design of a successful design of the dynamic tests setup. First, a non-negligible source of complexity is due to the great rigidity of the system and, secondly, to the uncertainties related to behavior of the joints, as well as its interaction with soil and non-structural inner walls in cellular concrete. In these conditions, the proper design of the dynamic tests plays a key role in the characterization process. The dynamic tests were conducted in February 2019. A preliminary FE model of the pavilion, reported in (Ceravolo & Lenticchia, 2019), provided valuable data to design acquisition setups in order to maximize the content of extractable information and the spatial visualization of the modes.

The study aimed to reconstruct the dynamic behavior of the pavilion both on a global and a local level, especially on some structural elements, in order to highlight the possible criticalities of the structure. The acquisition system was composed of 20 monoaxial piezoelectric accelerometers (PCB Piezotronics, model 3701G3FA3G, sensitivity 1 V/g, Frequency Range 0 to 100 Hz, Resonant Frequency ≥ 400 Hz, Overload Limit ± 3000 g pk, Temperature Range -40 to $+185$ °F), positioned on the ribs, struts and rods. Overall, two setups were designed, paying close attention to favouring the modal decoupling. The first configuration was designed to obtain information in the horizontal (x-y) plane, while the second one mainly focuses on the vertical direction (Figure 75 and Figure 76) (Ceravolo, Coletta, Lenticchia, Minervini, & Quattrone, 2020).

The red arrows in Figure 75 and in Figure 76 represent the horizontal channels of the accelerometers. The latter were indicated adding an “x” symbol inside the circle when a vertical channel is also considered. Whereas, the blue circles indicate accelerometers with only a vertical channel.

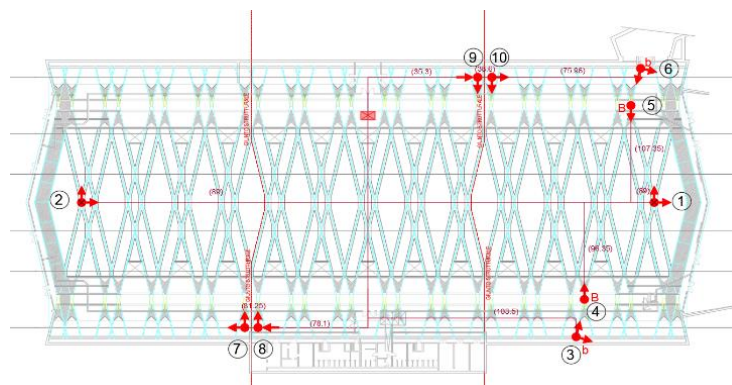


Figure 75: Accelerometers configurations for setup 1 (Ceravolo, Coletta, Lenticchia, Minervini, & Quattrone, 2020)

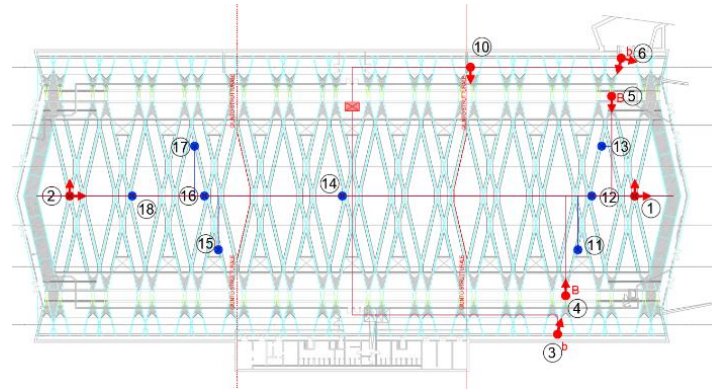


Figure 76: Accelerometers configurations for setup 2 (Ceravolo, Coletta, Lenticchia, Minervini, & Quattrone, 2020)

The dynamic tests were conducted on the 18 and 19 February 2019. The signals measured correspond to the structure response to environmental noise excitation, produced by external stochastic forces such as wind and vehicular traffic. The acquisitions lasted between 18 and 98 minutes. The signals, in terms of accelerations, were acquired adopting a sampling frequency of 128 Hz and 256 Hz for setup 1 and setup 2, respectively, whilst the main modes were confined in the first 20 Hz.

6.10 Analysis and processing of the dynamic tests

The modal parameters were estimated from a data processing procedure that includes an output only system identification algorithm of the Stochastic Subspace Identification (SSI) family. In particular, the third algorithm considered by the unifying theorem of Van Overschee and De Moor, known as “Canonical Variate Analysis” (CVA), was implemented (Van Overschee & De Moor, 2012) (Ceravolo & Abbiati, 2013). The procedure starts with data cleaning and pre-processing, including de-trending, decimation, and filtering. Since both SSI-data identification performance and processing times generally increases with signal length, a compromise between performance and computation duration needs to be found. In this case, signal segments of 5 min length are extracted from longer records and introduced as identification algorithm input. More specifically, having defined for each signal the time interval with the higher RMS (Root Mean Square) values, the final temporal interval was chosen so that the RMS values would be higher for the maximum number of channels.

For a given data set, the results of SSI-CVA depend on the structure of the Hankel matrix and on the system order of the algorithm. Appropriate system orders

are be chosen to contain computational time. The over-modelling associated to high order values introduces spurious poles, which reproduce the noise content of experimental data. For this reason, the algorithm is integrated with a procedure for automatic analysis of stabilization diagrams and automatic clustering analysis. Hard validation and stability criteria are applied to the results of the identification to remove spurious poles. Some spurious poles are removed using a hard criterion based on the expected value of the damping ratio. In particular, poles characterized by a damping ratio outside the range 0-10% are not physically realistic for the Pavilion and therefore are discarded. The remaining poles are then analysed through the stabilization diagram. The consistency of the poles is defined in terms of distances in frequency, damping, and modal shape between the closest poles identified for two consecutive system orders. The distance between two poles in terms of absolute frequency, damping ratio and modal shape and their maximum value to consider the poles authentic are reported in the following:

$$d(f_{i,n}, f_{j,n+\Delta n}) = |f_{i,n} - f_{j,n+\Delta n}| \leq 0.025 \text{ Hz} \quad (12)$$

$$d(\xi_{i,n}, \xi_{j,n+\Delta n}) = \frac{|\xi_{i,n} - \xi_{j,n+\Delta n}|}{\max(|\xi_{i,n}|, |\xi_{j,n+\Delta n}|)} \leq 50\% \quad (13)$$

$$MAC(\Phi_{i,n}, \Phi_{j,n+\Delta n}) = \frac{|\Phi_{i,n} * \Phi_{j,n+\Delta n}|^2}{|\Phi_{i,n}|^2 |\Phi_{j,n+\Delta n}|^2} \geq 0.95 \quad (14)$$

Where $f_{i,n}$, $\xi_{i,n}$, and $\Phi_{i,n}$ represent the frequency, the damping ratio and the modal shape identified for a system order n ; and $f_{j,n+\Delta n}$, $\xi_{j,n+\Delta n}$, and $\Phi_{j,n+\Delta n}$ represent the frequency, the damping ratio and the modal shape of the closest poles obtained for a consecutive higher system order.

A cluster analysis has been used to group the possible physical modes into homogeneous sets representing the same physical mode. Among the different types of clustering analysis, the agglomerative hierarchical clustering has been implemented in the code (Pecorelli, Ceravolo, & Epicoco, 2018).

The algorithm output gives estimates of the main frequencies, damping, and modal shape. A great density of modes, for frequencies between 2 and 8 Hz, underlines the presence of several vertical plate modes due to the bending of the roof slab. A further acquisition related to the setup 1 was found useful to identify the first torsional mode of the structure at 3.59 Hz. Therefore, it is highlighted how several acquisitions were necessary to identify the main horizontal modes. Setup 2

was of great help in identifying the main vertical modes of the pavilion, as it is characterized mainly by accelerometers with a z-direction. Some of the results obtained for the South block with setup 2 (vertical mode) are evidenced in Figure 77 in terms of stability diagram (left) and clustering diagram (right), respectively, while Figure 78 reports similar diagrams for the same block identified with setup 1 (horizontal modes). Figure 79, in turn, illustrates the mode shapes associated to the three main horizontal modes, limited to the South block, as resulting from the same identification sessions.

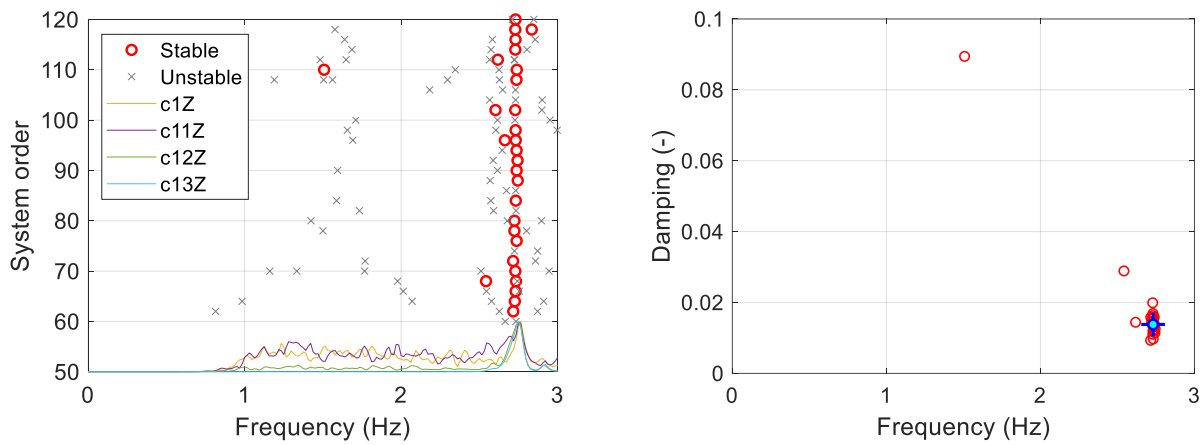


Figure 77: Identified vertical mode of the South block with setup 2: stability diagram with power spectrum density (PSD) curves of the considered signals (left) and clustering diagram (right)

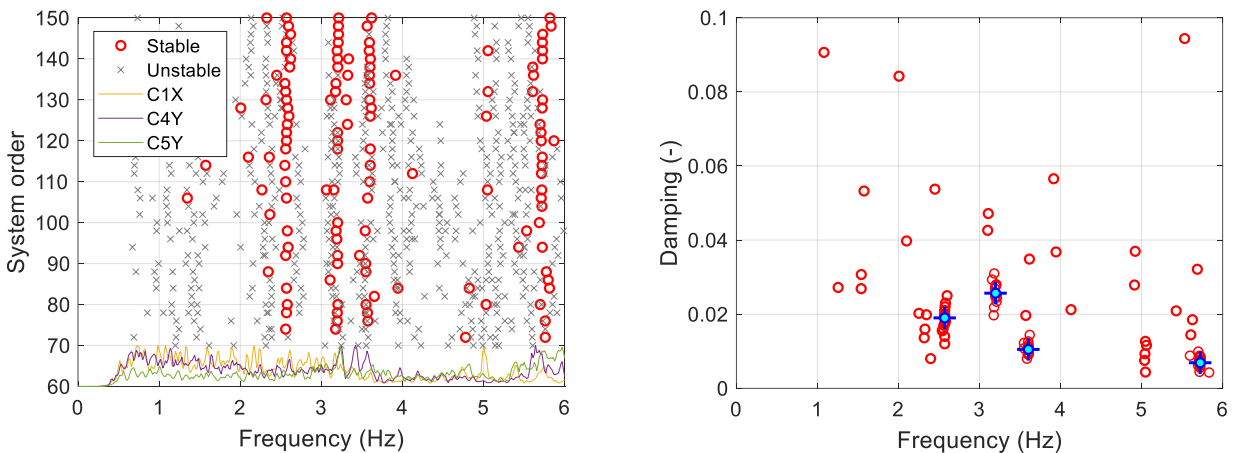


Figure 78: Identified horizontal mode of the South block with setup 1: stability diagram with power spectrum density (PSD) curves of the considered signals (left) and clustering diagram (right)

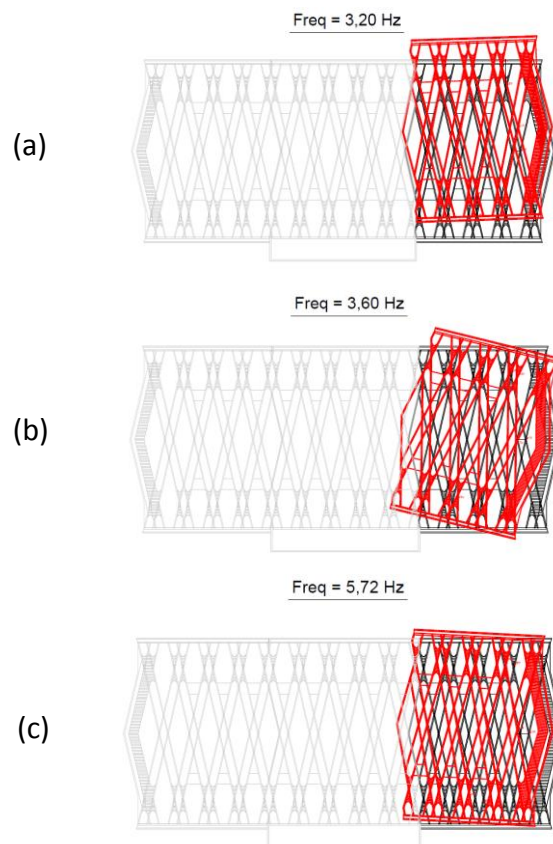


Figure 79: Identified mainly horizontal modes of the South block: (a) $f=3.20$ Hz: translational mode in transverse direction; (b) $f=3.60$ Hz: torsional mode; (c) $f=5.62$ Hz: translational mode in longitudinal direction

Table 4 reports the comparison between the identified frequencies of the three block, whose values highlight a sort of symmetry in terms of modal behavior. Table 5, in turn, shows the same comparison in terms of equivalent viscous damping. The first two modes can be considered as a mixed horizontal-vertical mode and a vertical mode. The modes from three to five result to be mainly horizontal modes.

The most evident finding, resulting from the ambient vibration-based tests, is the substantial effectiveness of the two joints, as demonstrated by the appearance of distinct modes for each of the three blocks. The deformability at the shorter strut beams tends to govern the horizontal behavior of the building, especially in the transverse direction. Instead, the longitudinal behavior seems to be also affected by non-structural wall elements that stiffen the structure. The effectiveness of structural joints will be the object of further investigations in the stage of model corroboration.

Table 4: Comparison between the frequencies (f_{EXP}) identified for the three blocks of the pavilion

		North Block	Central Block	South Block
Mode	Description	f_{EXP} (Hz)	f_{EXP} (Hz)	f_{EXP} (Hz)
1	horizontal (with roof bending) mode	2.57	2.57	2.57
2	mainly vertical mode	2.68	2.73	2.73
3	mainly translational-transverse	3.28	3.36	3.20
4	mainly torsional	3.59	3.41	3.60
5	mainly translational-longitudinal	5.72	5.67	5.72

Table 5: Comparison between the damping (ζ_{EXP}) identified for the three blocks of the pavilion

		North Block	Central Block	South Block
Mode	Description	ζ_{EXP} (%)	ζ_{EXP} (%)	ζ_{EXP} (%)
1	horizontal (with roof bending) mode	2.11	2.11	1.90
2	mainly vertical mode	0.98	2.36	1.38
3	mainly translational-transverse	2.14	1.35	2.57
4	mainly torsional	1.43	0.64	1.05
5	mainly translational-longitudinal	0.80	4.18	0.70

6.11 Parametric study for modal identification of structures with interacting diaphragms

Since great difficulties can arise when dealing with system identification of structure composed of many connected bodies, a parametric analysis has been carried out for the Pavilion V to confirm the results obtained in paragraph “6.10 Analysis and processing of the dynamic tests”. The main criticalities concern the sensitivity of the identification process to the mutual constraints of the diaphragms and the choice of the model used in the identification process. A possible approach consists on the improvement of analytical models using test data (Berman & Nagy, 1983), recurring to surrogate models to increase the computational efficiency of the

whole process (Sobester, Forrester, & Keane, 2008). In fact, these tools allow to overcome the problem of the high number of modes resulting from the identification and also to identify and differentiate local modes from global ones.

Initially, the dynamic equation for rigid diaphragms, assumed for simplicity to have only three degrees of freedom, interacting at linear elastic joints is developed. The degree of freedom of the diaphragms are two in-plane translations, along x and y directions, and the rotation around the z direction. The dynamic equilibrium of the *i*-th diaphragm in free undamped vibration conditions, and with a connection only to the ground, is:

$$\begin{bmatrix} m_i & 0 & m_i^{xy} \\ 0 & m_i & m_i^{yy} \\ m_i^{xy} & m_i^{yy} & J_{0,i} \end{bmatrix} \begin{Bmatrix} \ddot{u}_i \\ \ddot{v}_i \\ \ddot{\gamma}_i \end{Bmatrix} + \begin{bmatrix} \bar{k}_i^x & 0 & \bar{k}_i^{xy} \\ 0 & \bar{k}_i^y & \bar{k}_i^{yy} \\ \bar{k}_i^{xy} & \bar{k}_i^{yy} & \bar{k}_i^y \end{bmatrix} \begin{Bmatrix} u_i \\ v_i \\ \gamma_i \end{Bmatrix} = \begin{Bmatrix} 0 \\ 0 \\ 0 \end{Bmatrix} \quad (15)$$

where can be defined m_i as the mass, $J_{0,i}$ as the polar moment of inertia and m_i^{xy} and m_i^{yy} as static moments, \bar{k}_i^x and \bar{k}_i^y as, respectively, the translational stiffnesses in the x-direction and in the y-direction, \bar{k}_i^y as the torsional stiffness, \bar{k}_i^{xy} and \bar{k}_i^{yy} mixed stiffness terms that regulate the coupling between the translational and rotational degree of freedom, and u_i , v_i and γ_i as the displacements in the x-direction, in the y-direction, and the rotation, respectively.

Now, considering that the generic *i*-th diaphragm is part of a system of n interacting diaphragms, the interaction is assumed to be chain-like (only between adjacent diaphragms) and it is described by means of linear springs. In analogy with Equation 15, it is possible to define the mass matrices of the system M_{xx} and M_{yy} , the matrix of polar moments of inertia $M_{\gamma\gamma}$ and the matrices of the static moments M_{xy} and M_{yy} , as well as the stiffness matrices along the three directions K_{xx} , K_{yy} and $K_{\gamma\gamma}$, and the mixed terms stiffness matrices K_{xy} and K_{yy} , so that the equilibrium equation in compact form writes in terms of $3n \times 3n$ matrices:

$$\begin{bmatrix} M_{xx} & 0 & M_{xy} \\ 0 & M_{yy} & M_{y\gamma} \\ M_{xy} & M_{y\gamma} & M_{\gamma\gamma} \end{bmatrix} \begin{Bmatrix} \ddot{u} \\ \ddot{v} \\ \ddot{\gamma} \end{Bmatrix} + \begin{bmatrix} K_{xx} & 0 & K_{xy} \\ 0 & K_{yy} & K_{y\gamma} \\ K_{xy} & K_{y\gamma} & K_{\gamma\gamma} \end{bmatrix} \begin{Bmatrix} u \\ v \\ \gamma \end{Bmatrix} = \begin{Bmatrix} 0 \\ 0 \\ 0 \end{Bmatrix} \quad (16)$$

Defining the translation stiffness of the spring connecting the i -th diaphragm with two adjacent diaphragms in the x direction as k_i^x and k_{i+1}^x , the stiffness matrix along the x-direction K_{xx} results:

$$K_{xx} = \begin{bmatrix} k_1^x + k_2^x + \bar{k}_1^x & -k_2^x & \dots & \dots & 0 \\ \dots & \dots & \dots & \dots & \dots \\ \dots & -k_i^x & k_i^x + k_{i+1}^x + \bar{k}_i^x & -k_{i+1}^x & \dots \\ \dots & \dots & \dots & \dots & \dots \\ 0 & \dots & \dots & -k_n^x & k_n^x + \bar{k}_n^x \end{bmatrix} \quad (17)$$

The stiffness matrix along the y direction, K_{yy} , and rotation γ , $K_{y\gamma}$, can be formulated similarly to Equation 17.

Figure 80 shows the interaction between the i -th diaphragm and the adjacent ones by means of linear springs.

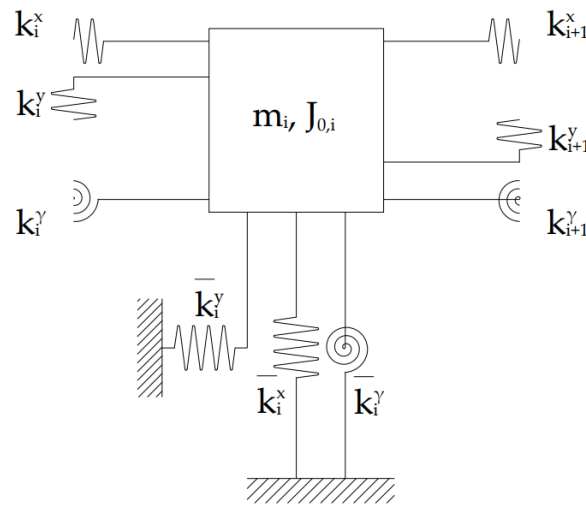


Figure 80: Lumped mass model of the interacting i -th diaphragm

In analogy with the Pavilion V, the numerical benchmark with the lumped mass model of three adjacent interacting diaphragms represented in Figure 81 has been considered. The system, presenting a diaphragmatic behavior with a chain-like interaction, is composed of three masses m_1 , m_2 and m_3 , and their respective polar moments of inertia $J_{0,1}$, $J_{0,2}$ and $J_{0,3}$.

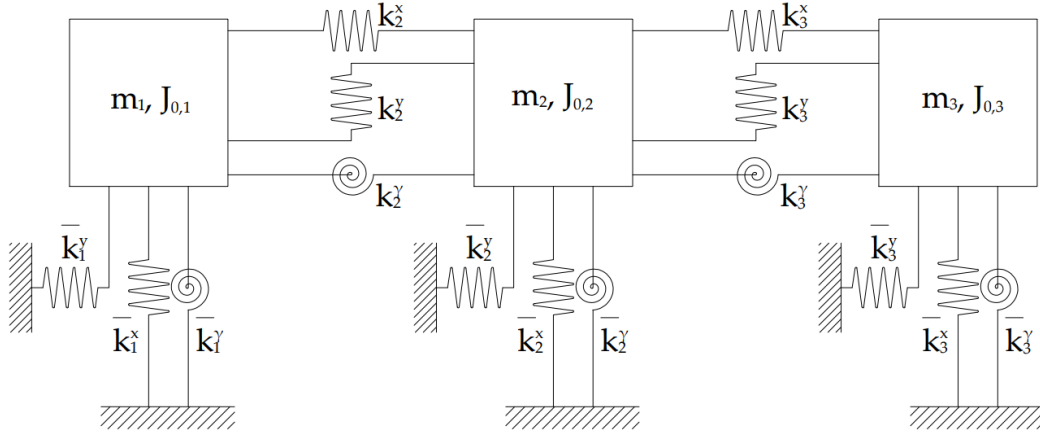


Figure 81: Lumped mass model of three adjacent interactive diaphragms

The values of the translational stiffnesses along the x-direction, \bar{k}_1^x , \bar{k}_2^x and \bar{k}_3^x , the translational stiffnesses along the y-direction, \bar{k}_1^y , \bar{k}_2^y and \bar{k}_3^y , the torsional stiffnesses \bar{k}_1^y , \bar{k}_2^y and \bar{k}_3^y around γ , were chosen to represent typical values of square concrete diaphragms of 50 m on each side. The mixed terms of stiffnesses \bar{k}_1^{xy} , \bar{k}_2^{xy} , \bar{k}_3^{xy} and \bar{k}_1^{yy} , \bar{k}_2^{yy} , \bar{k}_3^{yy} , and the static moments S_1^x , S_2^x , S_3^x and S_1^y , S_2^y , S_3^y have been calculated accordingly. The numerical values of masses, polar moments of inertia, static moments, and stiffnesses are reported in Table 6.

The stiffnesses describing the interaction k_2^x , k_2^y , k_2^y , and k_3^x , k_3^y , k_3^y are set as a fraction (factor varying between 0 and 2), defined as k_{var} , of the values shown in Table 6, which corresponds to the continuity of the spring. The eigenvalue problem of this system has been solved in order to extract the modal parameters (natural frequencies and mode shapes). In order to study the relative variation of the modal frequencies of this system parametric simulations with respect to k_{var} were conducted, considering a simultaneous uniform variation of k_2^x , k_2^y , k_2^y , and k_3^x , k_3^y , k_3^y . To this aim, the modal frequencies of the system, generally called f_r (with r varying from 1 to 9), were normalized with respect to the fundamental frequency. The variation of the 9 modes and of the 9 natural frequencies of the system with respect to k_{var} are represented in Figure 82, Figure 83 and Figure 84. The

representation is divided into groups of 3 modes each in order to have a better visualization: Figure 82 represents the modes from 1 to 3, Figure 83 from 4 to 6, and Figure 84 from 7 to 9. It is worth noting that the y-axis scales between the three figures (Figure 82, Figure 83 and Figure 84) are different.

Table 6: Numerical values of parameters

Parameter	Numerical Value	Unit
$m_1 = m_2 = m_3$	4.2×10^6	kg
$J_{0,1}$	1.0×10^{10}	N·m ²
$J_{0,2}$	3.2×10^{10}	N·m ²
$J_{0,3}$	7.5×10^{10}	N·m ²
m_1^{yy}	1.1×10^8	kg·m
m_2^{yy}	3.2×10^8	kg·m
m_3^{yy}	5.4×10^8	kg·m
$m_1^{xy} = m_2^{xy} = m_3^{xy}$	-1.5×10^8	kg·m
$\bar{k}_1^x = \bar{k}_2^x = \bar{k}_3^x$	8.7×10^8	N/m
$\bar{k}_1^y = \bar{k}_2^y = \bar{k}_3^y$	3.4×10^8	N/m
\bar{k}_1^y	2.2×10^{12}	N/m
\bar{k}_2^y	3.9×10^{12}	N/m
\bar{k}_3^y	7.4×10^{12}	N/m
$\bar{k}_1^{xy} = \bar{k}_2^{xy} = \bar{k}_3^{xy}$	-3.0×10^{10}	N·m/m
\bar{k}_1^{yy}	8.6×10^9	N·m/m
\bar{k}_2^{yy}	2.6×10^{10}	N·m/m
\bar{k}_3^{yy}	4.3×10^{10}	N·m/m
$k_2^x = k_3^x$	8.7×10^8	N/m
$k_2^y = k_3^y$	3.4×10^8	N/m
$k_2^y = k_3^y$	2.2×10^{12}	N/m

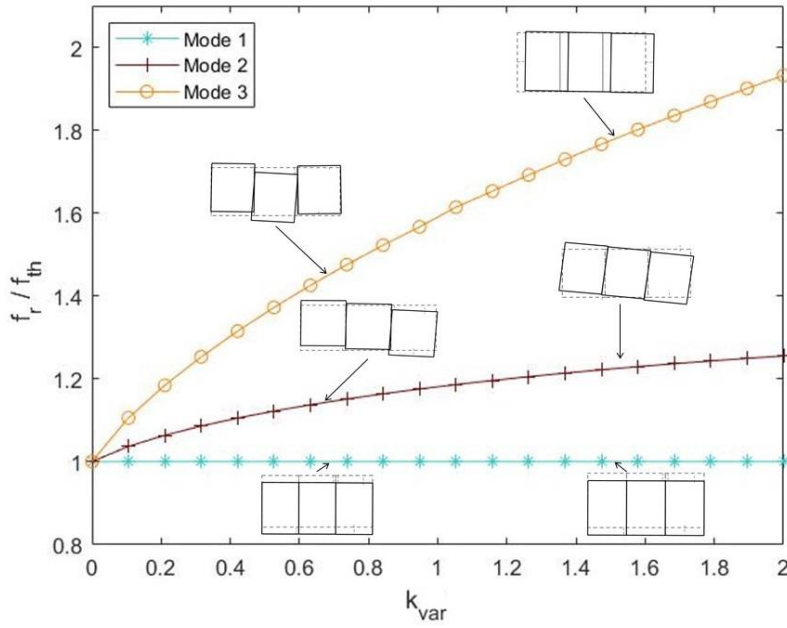


Figure 82: Variation of the modes and of the natural frequencies of the system from 1 to 3 as a function of k_{var}

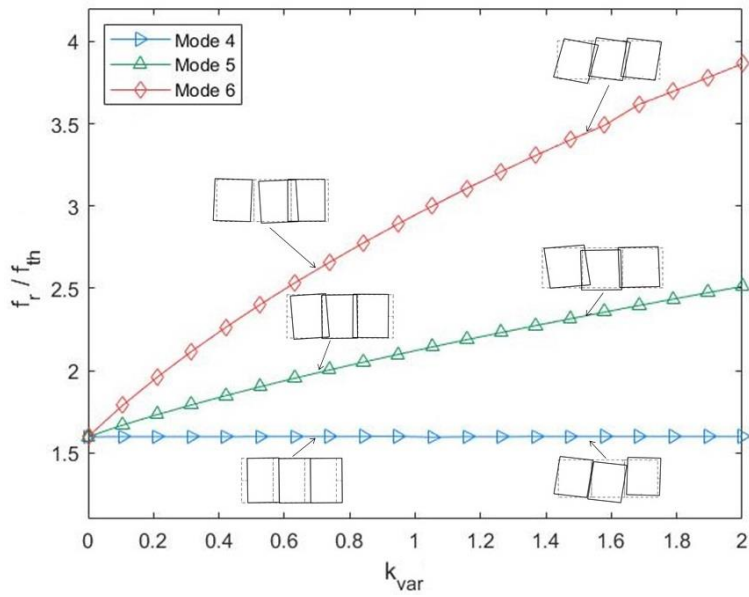


Figure 83: Variation of the modes and of the natural frequencies of the system from 4 to 6 as a function of k_{var}

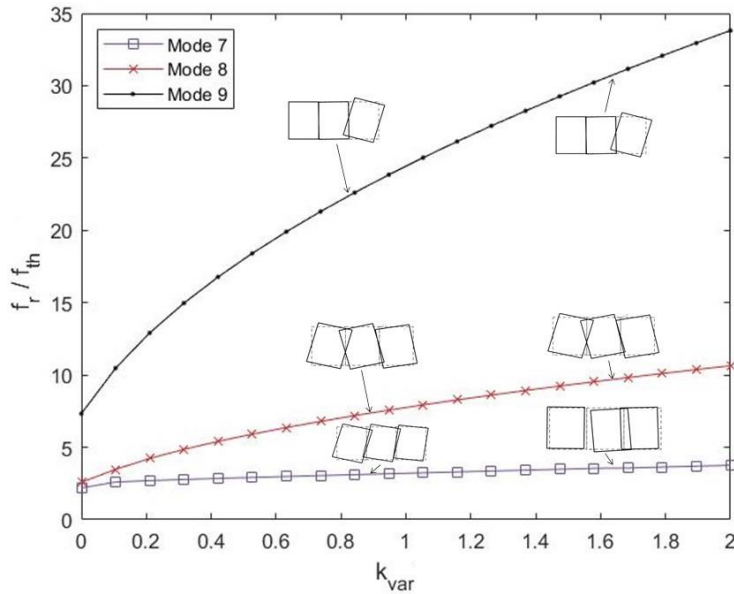


Figure 84: Variation of the modes and of the natural frequencies of the system from 7 to 9 as a function of k_{var}

In general, in the case of the natural frequencies an increasing linear trend can be observed. Figure 82 shows that the curve corresponding to the first natural frequency f_1 is almost flat, while a clear variation of f_r can be observed for the curves corresponding to the second and the third ones (f_2 and f_3). A similar trend can be observed for the other two groups reported in Figure 83 and Figure 84. Therefore, it can be said that increasing values of the stiffness characterizing the interaction clearly affect the higher modal frequencies of each group more. Comparing the three figures, it is noticeable that in the case of the groups of frequencies f_1, f_2, f_3 and f_4, f_5, f_6 , for values of k_{var} equal to 0, the numerical value of the frequencies is almost the same. The same behavior is not found for the group of frequencies f_7, f_8 and f_9 , where the numerical value of f_9 is almost double the numerical values of f_7 and f_8 .

Concerning the mode shapes, when k_{var} is equal to 0 the diaphragms are uncoupled and show the same three modes. The first mode corresponds to a translational mode along the transversal direction of the system, while the second mode corresponds to a rotational one. While the first mode does not change as a function of k_{var} , in the case of the second mode, the stiffening effect of the springs characterizing the interaction can be clearly observed: indeed, if the presence of the interaction is clearly visible for values of k_{var} equal to 0.8, in the case of higher

values of k_{var} the three masses tend to rotate as one single mass, showing therefore a monolithic behavior (see Figure 82).

Since the frequency curves present a crossing, the modes undergo the so-called re-ordering phenomenon, consisting of a change of order of the modes of the system. In this numerical benchmark, the re-ordering can be observed in two cases, as reported in Figure 85.

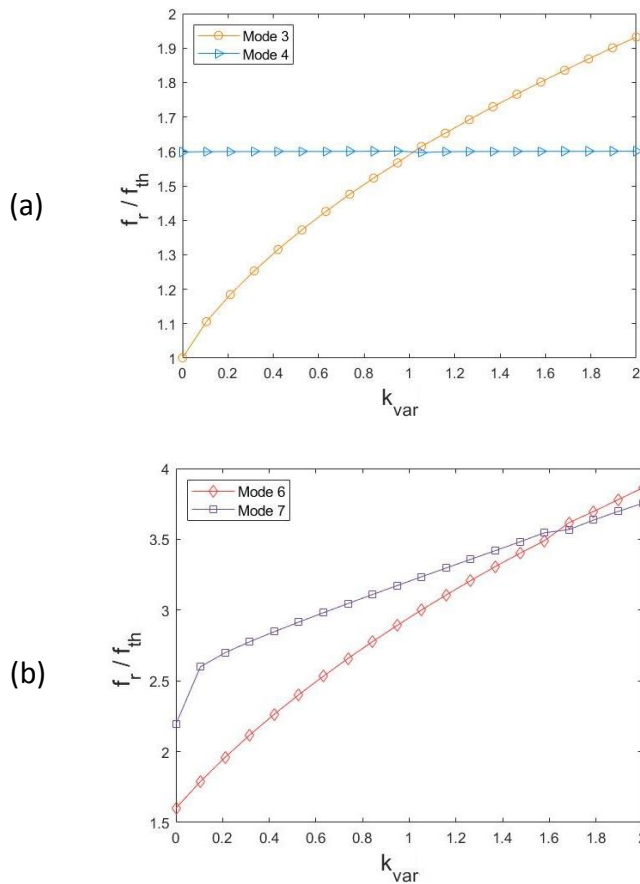


Figure 85: Re-ordering of modes: (a) modes 3 and 4; (b) modes 6 and 7

A first re-ordering of modes can be observed in correspondence with the third and fourth natural frequencies f_3 and f_4 of the system for increasing values of k_{var} (Figure 85a): indeed, in the case of the third one, a translational mode along the longitudinal direction is observed for high values of k_{var} , instead of a mixed torsional-bending one, observed at low values of k_{var} . A similar situation can be observed in Figure 85b for the sixth and seventh mode. It can be said that for very high values of k_{var} (when the three masses behave as one single mass) the first

three modes result to be the global modes of the system, corresponding to the translations in the directions x and y and to the rotation. On the other hand, the modes from 4 to 9 can be defined as local modes of the system. The application of the reported dynamic equation on a numerical benchmark has highlighted the influence of the interaction between adjacent diaphragms on the dynamic behavior of this system.

After having numerically analyzed how the interaction between adjacent diaphragms plays a key role in the comprehension of the dynamic behavior of a system, the dynamic model previously described has been exploited in the modal parameters identification of the Morandi's Pavilion V. Figure 86 reports the measured acceleration responses and their Power Spectral Density (PSD) estimated for setup 1. The signal length is about 64 min and the identification sessions were performed on both the entire signal and 8 sessions of 8 min each.

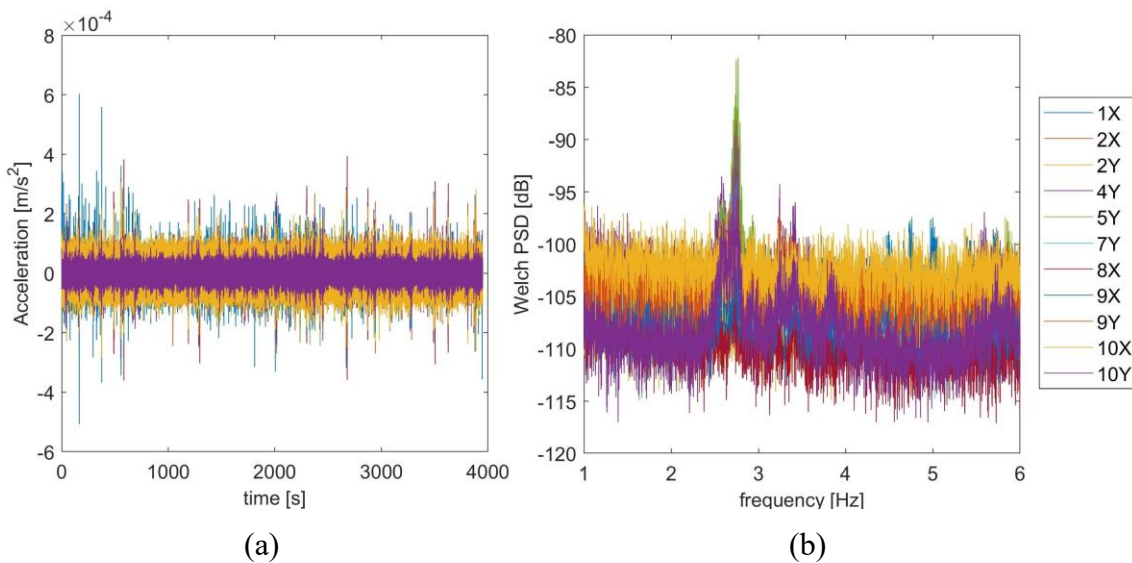


Figure 86: Measured acceleration responses for setup 1: (a) time-domain; (b) frequency-domain

The most recurrent experimental mode was seen to be the one at 2.57 Hz. By way of example, the stabilization and clustering diagrams of the identification of a sub-signal are reported in Figure 87.

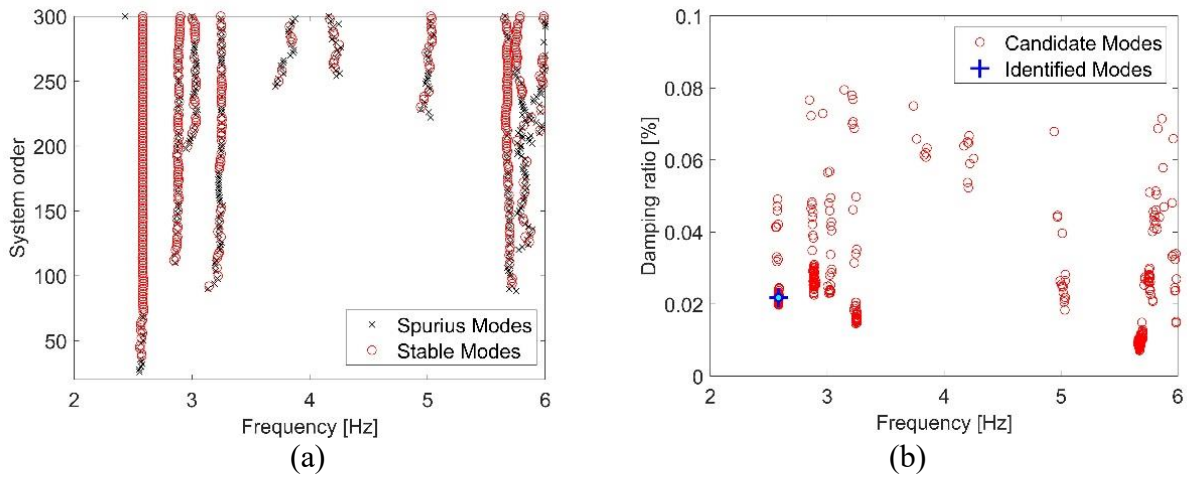


Figure 87: Stabilization (a) and clustering (b) diagram of the identification performed on the sixth sub-signal of setup 1 of the entire Pavilion V, with evidence of the mode at 2.57 Hz

The main identified modes are reported in Table 7 in terms of natural frequency and damping ratio. From Figure 12, it can be observed that several clusters are likely to indicate authentic modes. For instance, additional modes are detectable at 3.24 Hz and 5.67 Hz. However, it is worth pointing out that the results presented in this work descend from the assumption that the three blocks belong to the same dynamic system, and a safe attribution, in the presence of a limited number of sensors, will require an accurate mechanical FE model to be calibrated. Due to the redundancy of the measured degrees of freedom with respect to the ones of the diaphragmatic model, the representation of the modal shapes would require an optimization problem to be solved.

Table 7: Identified modes of the entire pavilion

Mode	Description	f_{EXP} (Hz)	ζ_{EXP} (%)
1	horizontal (with roof bending) mode	2.57	2.11
2	mainly vertical mode	2.73	0.91

The reason that led to use the simplified analytical model for the identification of Morandi's pavilion is the presence of non-structural materials, including waterproofing layers, connected the roofing system. Moreover, while the expansion joints between the bodies measure about 0.04 m, to create continuity on the walking

surface, the bodies are connected by a thin concrete screed, approximately 0.05 m thick.

Since the model admits only diaphragmatic degrees of freedom, to compare the experimental results with the model prediction, the horizontal components of the first horizontal mode (identified at 2.57 Hz) have been estimated with the least squares method, also to reduce spillover effects. If Θ_{id} denotes the identified eigenvector matrix, the equivalent diaphragmatic body mode components of the eigenvectors can be estimated with a linear transformation matrix \mathbf{D} as $\Theta_{D,id} = \mathbf{D} \Theta_{id}$, where $\Theta_{D,id}$ contains the diaphragmatic components, i.e., the two horizontal translations and the rotation about the vertical axis of each block, and \mathbf{D} is the linear transformation matrix. In accordance with the theoretical model, Figure 88 reports the representation to the horizontal components of the examined mode (undeformed configuration in dashed lines, with sensor positions).

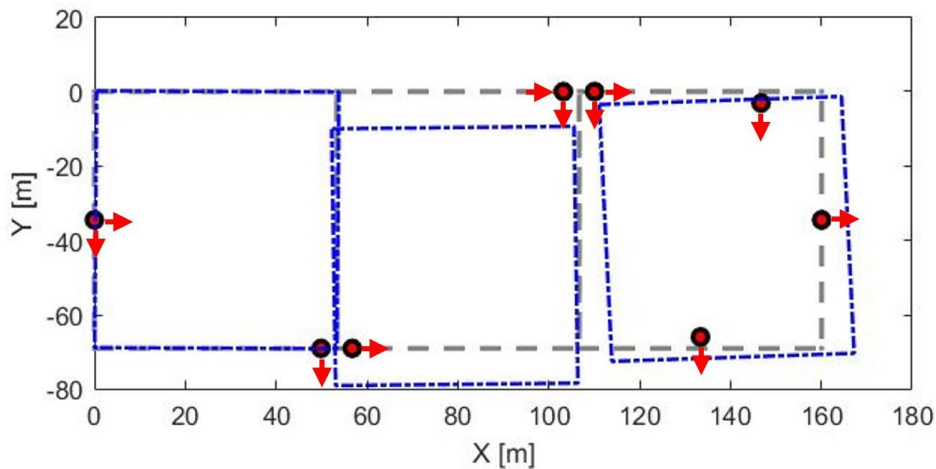


Figure 88: Horizontal component of the mode shape identified at 2.57 Hz

From a preliminary analysis of the Figure 88, the mode shape at 2.57 Hz is not appreciably affected by mutual interaction of the blocks, and this is indicative of the full effectiveness of the joints. Therefore, the three blocks are likely to behave as fairly separated dynamic systems. This observation can be extended also to joints with relatively low nominal stiffnesses (see Figure 82, Figure 83 and Figure 84). On the other hand, this uncoupled behavior is reflected in Figure 88.

Finally, it was decided to carry out a numerical study on the nominal values of the model stiffnesses of the joints, in order to shed light on their effectiveness. The

range of variation of the multiplier of the three stiffness components of each joint has been set between 0 and 1. In particular, two multipliers have been defined: $k_{var,left}$ and $k_{var,right}$. For each combination of the two multipliers was then calculated the Modal Assurance Criterion (MAC) (Allemang, 2003) between the identified mode shape and the predicted ones. Having defined m as the double of the number of modes, the objective function $J(k_{var,left}, k_{var,right})$ is (Mercede, Doz, de Brito, Macdonald, & Friswell, 2007) (Moller & Friberg, 1998):

$$J(k_{var,left}, k_{var,right}) = \sum_{j=1}^{m/2} \alpha_w \left| \frac{f_j^{id} - f_j}{f_j^{id}} \right| + \beta_w \left| \frac{1 - \sqrt{MAC_j}}{1} \right| \quad (18)$$

where, for each j -th combination of the two multipliers, α_w and β_w are the weights of the residuals in frequency and mode shapes, respectively, f_j^{id} is the j -th identified natural frequency, f_j is the j -th predicted natural frequency, and MAC_j is the j -th MAC between the identified mode shape and the j -th predicted mode shape. Figure 89 shows the resulting objective function plot considering only the first vibration mode.

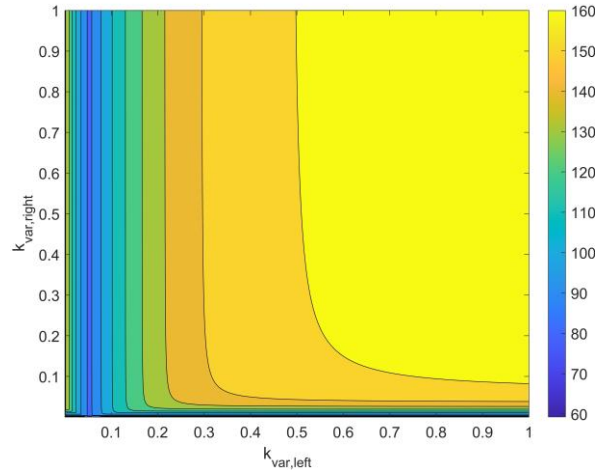


Figure 89: Objective function for a variation of $k_{var,left}$ and $k_{var,right}$ in the range between 0 and 1

As can be observed from Figure 89 the objective function tends to dramatically decrease for very low values of $k_{var,left}$ and $k_{var,right}$, corresponding to total effectiveness of all the joints. A further investigation has been conducted for the values of $k_{var,left}$ and $k_{var,right}$ varying between 0 and 1×10^{-3} . The results reported

in Figure 90 show that the absolute minimum happens when the joints are total effective.

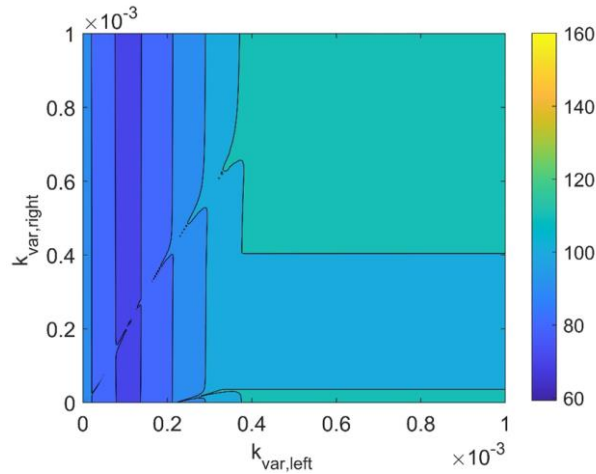


Figure 90: Objective function for a variation of $k_{var,left}$ and $k_{var,right}$ in the range between 0 and 1×10^{-3}

The described analyses also highlighted a high sensitivity to the joint stiffnesses for values of $k_{var,left}$ and $k_{var,right}$ close to zero.

6.12 Corroboration of the FE model

The results of the experimental tests can be used to corroborate the baseline FE model, which relies essentially on original drawings as verified in surveys. In the case of Pavilion V, the Young's moduli in the FE model were initially assumed to be equal to those obtained from mechanical tests, in particular for the elements detailed in Table 8 (ribs, retaining walls and longer strut beams). A more comprehensive calibration of the model, based on identified modes, was then performed by recurring to standard local sensitivity model updating techniques (for details, see (Ceravolo, Pistone, Zanotti Fragonara, Massetto, & Abbiati, 2016)) on a simplified model (described in paragraph “

6.11 Parametric study for modal identification of structures with interacting diaphragms”). To this aim, the joints were simulated by a homogeneous material whose elastic properties have been the subject of a parametric study, which showed that the error between the model and the experimental results fell to zero for values of the stiffness of joints close to zero, indicating an effectiveness of these (Ceravolo, Lenticchia, Miraglia, Oliva, & Scussolini, 2022). Thus, the stiffness of the joints was assumed zero, and the blocks are weakly connected through the inner walls.

Table 8: Values of the elastic moduli as resulting from the mechanical tests

Element	Elastic moduli from mechanical characterization tests (GPa)
Ribs	33.0
Retaining walls	37.0
Longer strut beams	32.0

In the described example the deflections measured during static tests also contributed to updating the roof model. In fact, the inertial and elastic properties of the roof were adjusted in the FE model to fit vertical displacements in Figure 67 and, at the same time, the main vertical modes. In particular, an increment of the density from 2500 kg/m^3 to 3500 kg/m^3 has been applied for the shell elements of the roof (with thickness variable between 25 cm and 45 cm) to simulate the permanent load acting on it as an overlaying distributed mass. Whereas, the Young's modulus has been increase from 25 GPa to 39.9 GPa to simulate the equivalent stiffness of the roof, considering the layers positioned over the concrete slab: the concrete screed and the cement stabilized soil. Instead, for the shorter strut beams, the Young's modulus was initially imposed by literature, then, given the aging conditions in common with the ribs, the value was modified in accordance to the experimental value obtained for those elements, i.e., 33 GPa.

A typical Young's modulus, i.e., 3 GPa, has been assumed, according to *SIA266* regulations, for the non-structural inner walls made of cellular concrete. These elements were inserted in the 90s as fire walls in order to convert the structure from an exhibition hall to an underground parking. Since the high uncertainty of this parameter (that range approximately from 0.9 to 4 GPa in accordance to *SIA266*, based on the type of blocks), and given the lack of information on this material, the value was calibrated recurring to automatic FE model updating techniques (Ceravolo, De Lucia, Miraglia, & Pecorelli, 2020) by fitting the first identified mode in terms of mode shape and natural frequency (see Table 4).

Table 9 reports the values of the parameters for which no data were available from mechanical tests (roof, shorter strut beams and non-structural walls). Table 10, in turn, reports the natural frequencies predicted by the updated FE model (which can be compared with the experimental values reported in Table 4), while Figure 91 reports the main modes of the updated FE model, which reproduce the effectiveness of the joints. Even the vertical mode seems to be influenced by the

flexibility of the roof in proximity of the joints area. This highlights a problem similar to that faced by Morandi during construction, when following a confrontation with Franco Levi and Piero Marro of the Italian advisory body for pre-stressed constructions based at Politecnico di Torino, he introduced box beams to stiffen the edges (see Fig. 5, right side). In fact, due to the planar inclination of the post-tensioned elements (offering rigidity where multiple interconnections are present), the external ribs and the ribs close to the joints suffer torsional deformations. If the torsional stiffness was increased in the external elements thanks to the introduction of box beams, the same cannot be said for the ribs close to the joints, which show their flexibility in the FE model also due to the effectiveness of the joints (mainly vertical modes in Figure 91).

Table 9: Values of the elastic moduli before and after the updating based on the results of the dynamic tests

Element	Elastic moduli of the initial FE model (GPa)	Elastic moduli updated (GPa)
Roof	25.0	39.9
Shorter strut beams	30.0	33.0
Non-structural walls	3.0	2.12

Table 10: Predicted natural frequencies (f_{FEM}) by the updated FE model. Experimental values are reported in Table 4

		North Block	Central Block	South Block
Mode	Description	f_{FEM} (Hz)	f_{FEM} (Hz)	f_{FEM} (Hz)
1	horizontal (with roof bending) mode	2.59	2.79	2.57
2	mainly vertical mode	2.31	2.75	2.32
3	mainly translational-transverse	-	-	-
4	mainly torsional	-	-	-
5	mainly translational-longitudinal	5.00	5.00	5.00

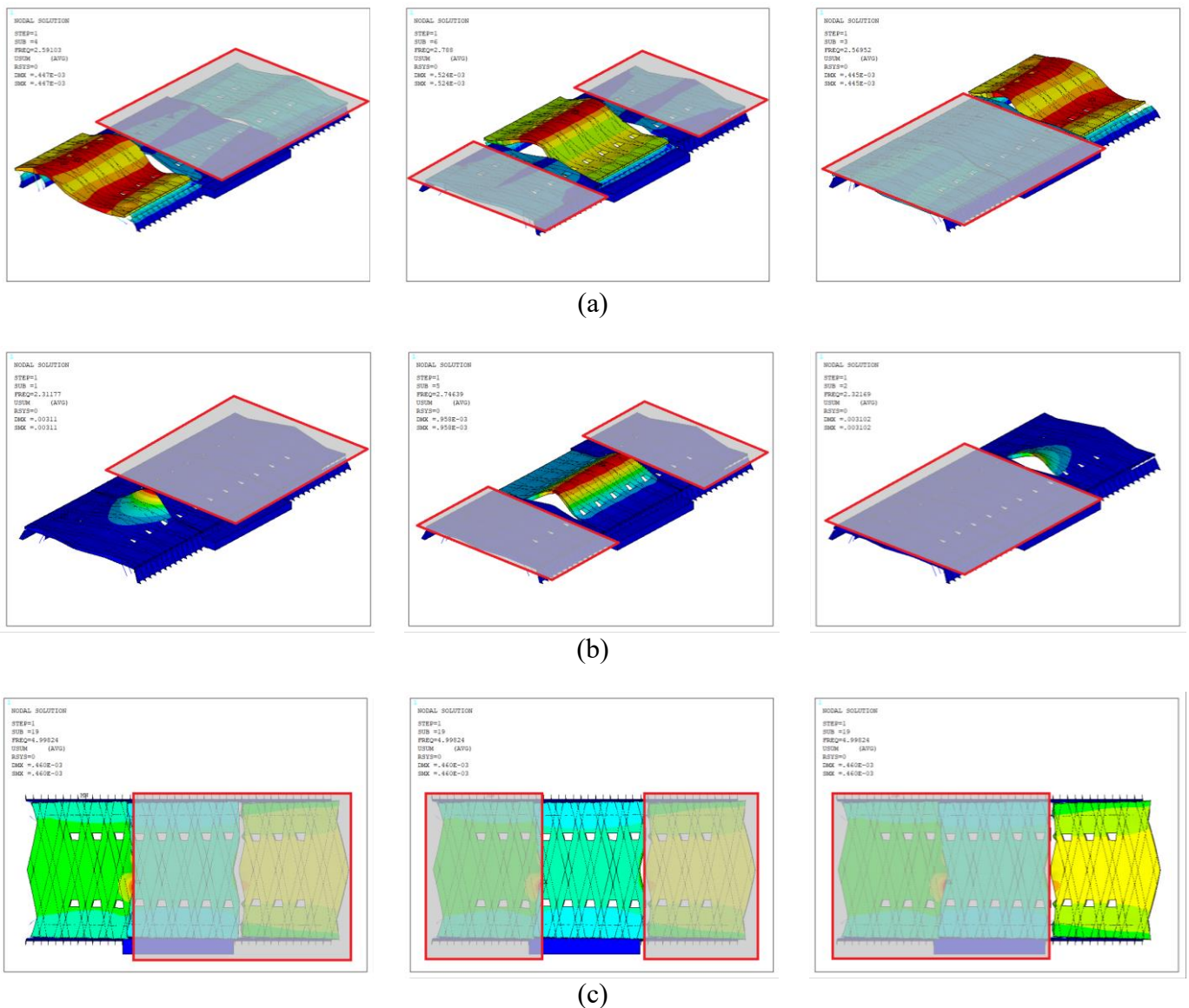


Figure 91: Modes of the updated FE model: (a) horizontal (with roof bending) modes; (b) mainly vertical modes; (c) mainly translational modes in longitudinal direction

Thanks to the calibration process, the model simulates as close as possible the actual behavior of the real structure. In particular, the MAC between the experimental and predicted mode by the calibrated FE model is equal to 0.86 (first mode), with a residual normalized error in frequency of 0.08%. The presence of effective joints in the roof could constitute a factor of vulnerability due to the possible pounding between the three distinct bodies. Pounding could be aggravated by the lack of edge beams at some sections of the joints. Most importantly, any retrofitting interventions must consider that seismic action is mainly entrusted to

the shorter strut beams, which were not conceived to withstand important horizontal shear actions.

6.13 Structural reassessment based on the corroborated model

A comparison between the load multipliers resulting from Morandi's structural analysis and the updated FE model has then been executed. The same steps developed so far, based on the simplified calculation schemes used by Morandi, have been repeated using the updated model after the test campaign conducted in 2019. Figure 92, in particular, shows the bending moment diagrams due to permanent (a) and imposed (b) loads on a rib resulting from the updated FE model.

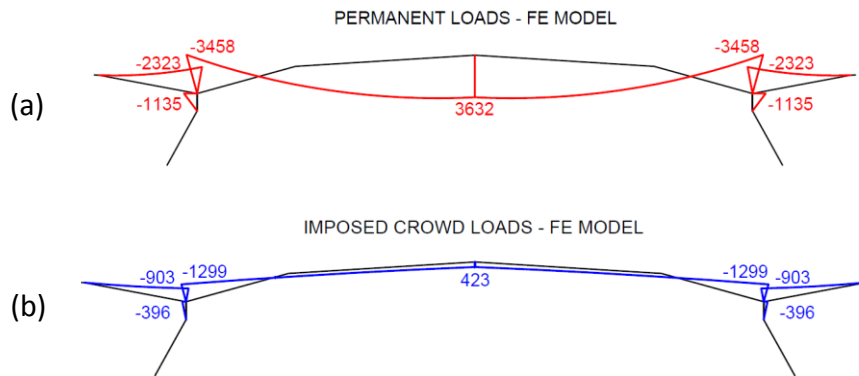


Figure 92: Bending moment diagrams (kNm) on a rib resulting from the updated FE model: due to the permanent loads (a); due to the imposed crowd loads (b)

The comparison between Figure 70 and Figure 92 shows that the bending moments evaluated with the updated FE model are lower than the values obtained from simplified Morandi's schemes. In particular, at midspan the reduction in bending moments due to the permanent and crowd loads are approximately 1% and 13%, respectively. At the support, the same quantities are lower of approximately 0% and 18%. Furthermore, as for Morandi's results, the bending moments due to the crowd loads remain much lower than those due to the permanent loads (about 12% at midspan and 39% at the support).

As a consequence of the above, at the reassessment stage the sensitivity curves will undergo updating, based on the corroborated model. At the end of the process, after the test campaign conducted in 2019, the condition assessment results are shown in Figure 93, in terms of ultimate load multipliers α (with respect to bending

moment verification at midspan) as a function of the corroded steel areas. The comparison between Figure 73 and Figure 93 shows that the load multipliers evaluated with the FE model are slightly higher than the values obtained from simplified Morandi's schemes. In particular, the reduction in bending moments mentioned above leads to an increase in ultimate load multipliers of approximately 17%. In fact, the capacity increases from 1.40 (calculated with the updated concrete strength) to 1.65, considering the cables in good health state. Therefore, considering also the Bayesian updating of the concrete strength, the corroborated model allows "a posteriori" condition assessment for the ribs. Clearly, for the purposes of possible reuse, the progression of the corrosive phenomenon must be taken into account for the safety margin level evaluation and the possible reuse of post-tensioned systems.

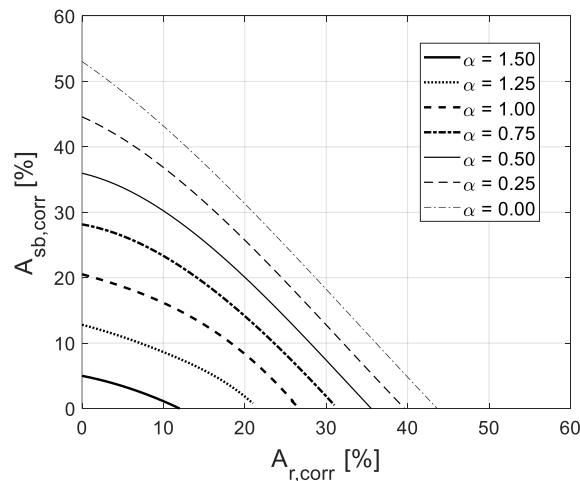


Figure 93: Sensitivity analysis conducted at midspan of the rib element with the calibrated FE model: the ultimate load multiplier (for bending moment verification) as a function of both corroded post-tensioning steel area in the rib ($A_{r,corr}$) and corroded post-tensioning steel area in the shorter strut beams ($A_{sb,corr}$)

In a subsequent condition reassessment stage, a portion of the structure made by the typological section (in transverse direction of the building) and a module by 11 m of depth (in longitudinal direction) has been analyzed. This portion of the building constitutes a system containing 4 interconnected ribs, 4 longer strut beams and 8 (4 pairs) shorter strut beams. On this system, which also corresponds to that used by Morandi for the loads analysis and the calculation of stresses in the structure, sensitivity analysis have been carried out considering the redistribution effect of the imposed crowd loads between the ribs. These analysis focused on the capacity of the main ribs, assuming that the other elements did not encounter capacity problems due to the redistributions effects of the crowd loads. Figure 94

(a) reports the ultimate load multipliers of the rib system as a function of the assumed corrosion in the wires at midspan of the different ribs, $A_{r,corr,midspan}$, assuming absence of corrosion at the supports of the ribs. Figure 94 (b), in turn, reports the ultimate load multipliers of the rib system as a function of the assumed corrosion in the wires at the supports of the different ribs, $A_{r,corr,support}$, assuming absence of corrosion at midspan. In this second case, the load multipliers of the rib system cannot in any case exceed the maximum value of 1.65 allowed by the bending moment capacity at midspan even in absence of corroded wires. In the case of combined corrosion condition at midspan ($A_{r,corr,midspan}$) and at the supports ($A_{r,corr,support}$) the ultimate load multiplier of the rib system is the minimum between the two single conditions.

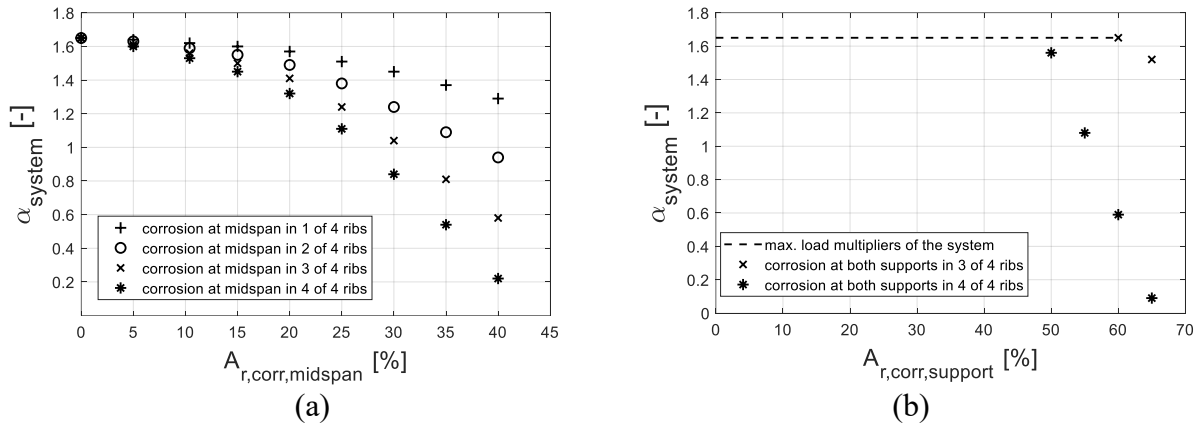


Figure 94: Sensitivity analysis conducted on the considered system composed of 4 ribs: ultimate load multipliers (for bending moment verification) with the updated FE model as a function of corroded post-tensioning steel area in the different ribs at midspan (a) and at the support (b)

Figure 95 reports the sensitivity analysis conducted for the condition assessment of the rib system concerning also the reduction of post-tensioning steel area of different shorter strut beams (sb). In this analysis the corrosion in the wires at midspan, $A_{r,corr,midspan}$, is assumed to progress uniformly and spread across all the examined ribs, while for shorter strut beams two symmetric different cases of progressive corrosion have been considered. In particular, it can be noticed that the redistribution of the crowd loads between the ribs allows an increase of ultimate load multipliers from the condition in which the corrosion interests all pairs of shorter strut beams (Figure 95 a) to the condition in which the corrosion interests two pairs of shorter strut beams of the system (Figure 95 b).

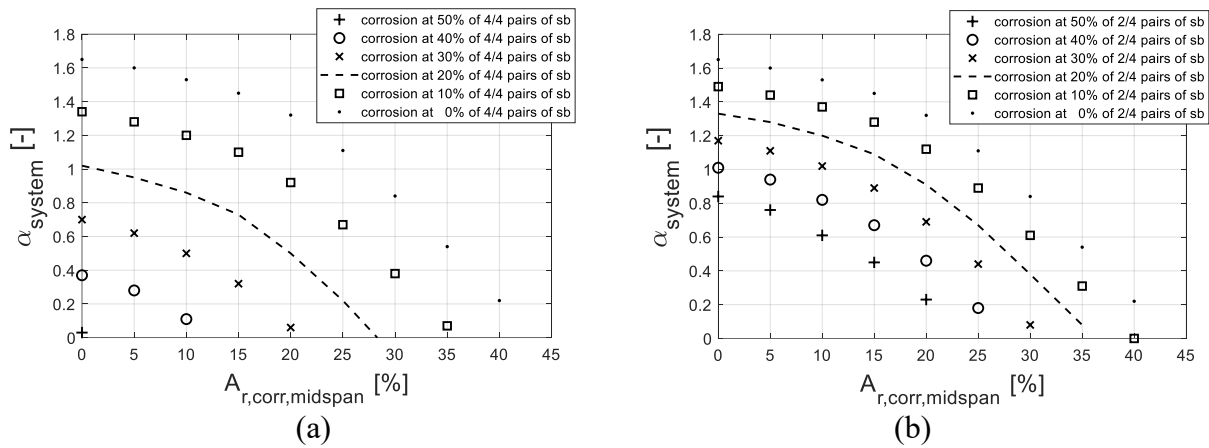


Figure 95: Sensitivity analysis conducted on the considered system composed of 4 ribs: ultimate load multipliers (for bending moment verification at midspan) with the updated FE model as a function of both corroded post-tensioning steel area in the ribs ($A_{r,\text{corr},\text{midspan}}$) and corroded post-tensioning steel area in the different pairs of shorter strut beams (sb)

The results reported in Figure 93, Figure 94 and Figure 95 represent a tool, based on a corroborated model, which allows to understand how the safety margin level decreases in a single rib, and in the considered portion of the structure, with the progression of the strands corrosion. In particular, once $A_{r,\text{corr}}$ and $A_{sb,\text{corr}}$ are probabilistically estimated, it is possible to evaluate (or update) the capacity of the post-tensioned elements, from the sensitivity curves. Decrease in residual prestressing force can also be taken into account.

6.14 Probabilistic estimation of the safety margin level of the post-tensioned systems

According to standards of proven validity, a specific investigation campaign on post-tensioned system is required to define a probabilistic estimation of the parameters influencing the safety margin level. The majority of these standards agree on the steps to follow during the inspection process: i) review the as-built plans, post-tensioned drawing, specifications and construction procedures; ii) visual inspection to evaluate the overall condition of the structural system and identify possible defects and signs of deterioration; iii) void identification with non-destructive techniques; iv) obtain grout samples v) visually assess the grout condition and signs of tendon defects with direct investigations; vi) residual prestressing evaluations (detensioning techniques or X-Ray diffraction method) and residual strength evaluations (hardness tests). The inspection process is shown in Figure 96.

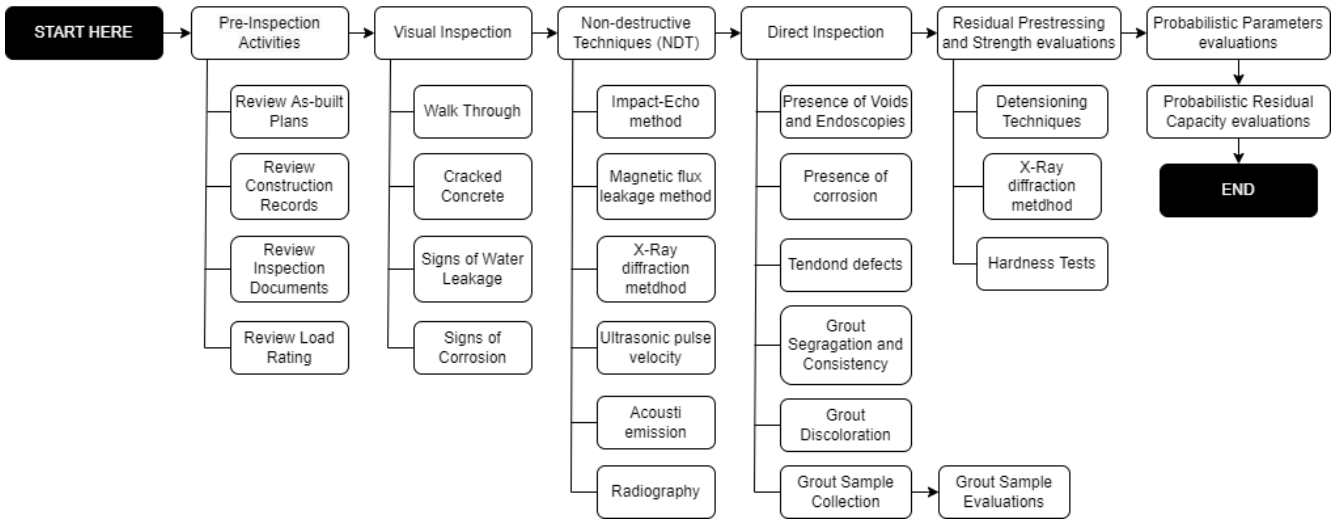


Figure 96: Flowchart for inspection process of post-tensioned systems

The recommended minimum number of inspected tendons depends on element risk and the possibility of creating distress for the structure through intrusive inspection. In particular, the considerations about the tendons regard: the number for each tendon type, the risk category, the probability of defect indicator, the consequence of failure indicator, and the structural distress caused by sampling tendons (Theryo, Hartt, & Paczkowsk, 2013).

The definition of the parameters to probabilistically assess the safety margin level, also using the corroborated model and the sensitivity curves, is the conclusion step of this process.

6.15 Sensitivity analysis of the environmental effect on the modal parameters

The confounding effect of Environmental and Operational Variations (EOVs) represents a critical aspect in the vibration-based SHM of structures. The changes in the external environment factors, especially the temperature, in most cases significantly affect the structural response (Salawu, 1997). As showed by (Peeters & De Roeck, 2001), percentage variation of natural frequencies of 10% could be reach under changing environmental conditions. This variation could be greater than that caused by structural damage. Therefore, in the damage identification the temperature variations effects should be carefully evaluated and considered, in order to avoid mistakes. In particular, the temperature variations could be easily

confused with the presence of damage or, even worse, it could compensate for a variation due to real damage, making it unnoticeable.

For this reason a numerical analysis with respect to different scenarios of temperature variation has been carried out on Morandi's pavilion, exploiting the FE model to predict dynamic response of the structure under changing environmental conditions and for different values of the Young's modulus of the joints. The results of this analysis will be useful in the case of permanent monitoring of the pavilion.

On the base of the results of a previous study (Xia, Hao, Zanardo, & Deeks, 2006), the methodology used to determine the correlation between the Young's modulus of the reinforced concrete and the temperature was defined. In this previous study a reinforced concrete slab was built, placed outdoors and exposed to weather conditions. During this period of exposition to changing conditions, which lasted nearly two years, the slab was periodically subjected to vibration tests. In particular, in the monitoring period its vibration properties (namely frequencies, modal shapes, and damping) were measured together with temperature and humidity during each measurement.

For small temperature variations such as environmental ones, a linear variation of Young's modulus, E , is assumed as follows:

$$\frac{\delta E}{E} = \vartheta_E \delta T \quad (19)$$

In the previous equation δ is an increment in the corresponding parameter and ϑ_E represents the temperature coefficient of Young's modulus. In this model any gradient between the different areas is neglecting and a uniform variation of the temperature is assumed.

Rewriting the last equation in a more explicit form and as a function of the measurements relating to specific observation, which derive from the modulus and temperature values obtained from the experimental tests at a temperature of 10 °C, it results:

$$E(T) = E_{10^\circ C} [1 + \vartheta_E (T - 10)] \quad (20)$$

For the coefficient of elastic modulus of concrete in the ambient temperature range, ϑ_E , a value of $-4.5 \times 10^{-3}/^\circ C$ has been obtained according to (Xia, Hao, Zanardo, & Deeks, 2006) and (Zhou & Huang, 2013), thanks to a procedure of curve fitting of experimental data starting from Baldwin and North's report

(Baldwin & North, 1973). This relationship has been exploited to calculate the elastic modulus values of the various macro-elements as the temperature varies.

In this study, a variation of temperature values (T) from -1 to 30 ° C have been considered, on the base of the minimum and maximum daily environmental temperature values recorded by the weather station nearest to the pavilion in 2021 in Turin. The sensitivity analysis performed regards the changes of the expansion joints stiffness, as the ambient temperature varies. In particular, since the actual mechanical properties of the expansion joints are not fully defined, various cases with different values of the Young's modulus (E_j) have been considered, spacing from a case of complete effectiveness to a case of complete ineffectiveness, which corresponds to a monolithic structural behavior.

The FE model used for this study reproduces the structural condition prior to the modification of the non-structural loads acting on the roof, consisting in the implementation of several layers of waterproofing instead of a fairly thick layer soil. Moreover, as reported in Table 11, some values of the elastic moduli were not the same as those obtained at the end of the updating process. Table 12 reports the natural frequencies obtained from the FE model with these elastic moduli.

Table 11: Values of the elastic moduli of the FE model in the sensitivity analysis

Element	Elastic moduli (Pa)
Ribs	33.0×10^9
Retaining walls	37.0×10^9
Longer strut beams	32.0×10^9
Roof	39.9×10^9
Shorter strut beams	20.0×10^9
Non-structural walls	3.0×10^9
Expansion joints	0.01×10^9

Table 12: Natural frequencies of the FE model used for the sensitivity analysis

Mode	Description	f (Hz)
1	horizontal (with roof bending) mode	2.35
2	mainly vertical mode	2.72
3	mainly translational-transverse (Y)	3.13
4	mainly rotational	3.25
5	mainly translational-longitudinal (X)	5.97

According to the reference system reported in Figure 97, the sensitivity analysis has been performed with the FE model only on the last three modes of Table 12: the translational mode in Y direction, the rotational one and the translational one in X direction. These modes, in fact, are particularly affected by the effectiveness of the joints as they are mainly horizontal.

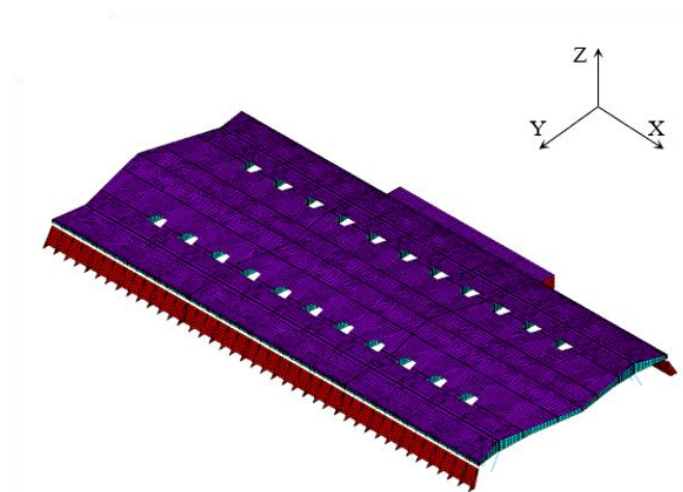


Figure 97: FEM of Morandi's Pavilion V

Figure 98 shows the results obtained changing the Young's moduli of all the macro-elements as a function of T and considering various magnitude order of E_j . In particular, it is possible to observe a monotonous decreasing trend for all the cases and modes as the temperature increases (Figure 98). The stiffening effect of the joints can be observed for higher values of E_j from the general increase of the natural frequencies values. In fact, until a value of E_j equal to $1e^6$, which is a ten

thousandth of the magnitude order of the macro-blocks moduli, no significant slope variation can be noticed. In particular, in the case of rotational mode can be noticed a significant sensitivity to the stiffening effect of the joints. This is due to the disjointed behavior of the blocks for very low values of E_j , where each block vibrates almost independently from the others, at very close frequencies. For sufficiently high values of E_j , i.e. E_j equal to $1e^{10}$, a monolithic behavior occurs and the frequency corresponding to the rotational mode increases until it overcomes the frequency trend of the translational mode in the longitudinal direction.

For low values of E_j (ineffective joints) the geometry of the structure, which is more elongated in x direction, has a greater impact on the modal frequencies than the increase in deformability of the material caused by the temperature. This can be observed in the trend of the frequency-temperature curve of the rotational mode, which is substantially flat, while the curve of translational mode in x direction decreases as the temperature increases. Moreover, the re-ordering of the modes highlights that the stiffening of the joints has a greater effect on rotational mode, than on the translation ones (especially in the transverse direction). In fact, the frequency corresponding to the rotational mode significantly grows, almost doubling its absolute value. For greater clarity, the calculation of the maximum Modal Assurance Criterion (MAC) among the extracted numerical modal shapes has been used in order to follow the evolution of the frequency when the variation of the stiffness of the joints changes.

Since for values of E_j until $1e^6$ the behavior results to be quite stable and not affected by the stiffening of joints, while a variation of the pattern is observed when going from $1e^6$ to $1e^7$, a further analysis has been performed within this specific range to investigate the latter hypothesis. As can be expected, when varying E_j from $3e^6$ to $6e^6$, two different intermediate situations occur (Figure 99), confirming the sensitivity of the mechanical parameters of the joints within this range.

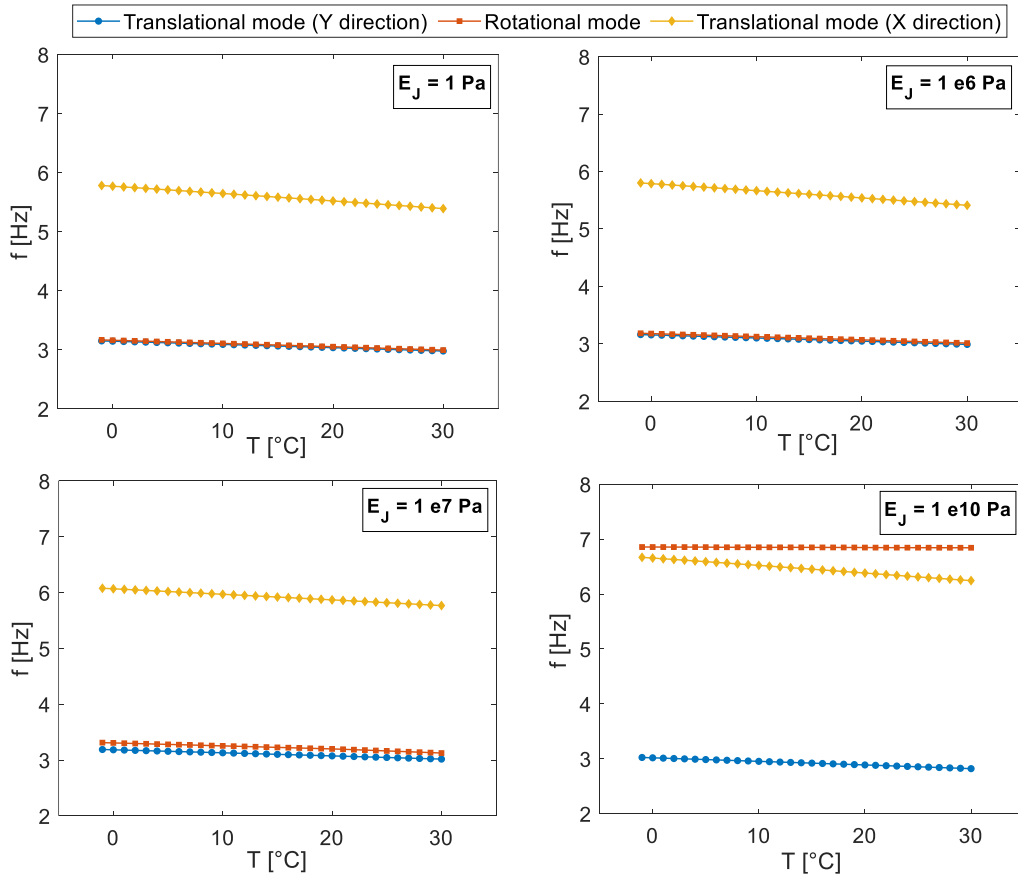


Figure 98: Temperature-frequencies relationships for different scenarios of effectiveness of joints

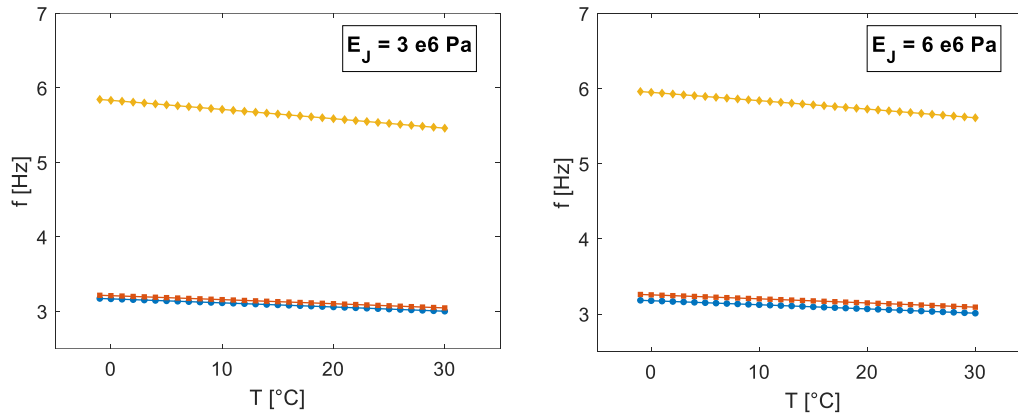


Figure 99: Temperature-frequencies relationships for an intermediate range between two significant magnitude orders

This study represents a numerical base for a potential future permanent monitoring of the building, reporting different scenarios that could correspond to the real behavior, considering the uncertainties about temperature and joints effects.

Chapter 7

Methodological approaches to the condition assessment of reinforced concrete heritage structures

In this Chapter, the proposed methodological approaches for the condition assessment of reinforced concrete architectural heritage, in full consistency with international documents and guidelines and with the current building regulations, are summarized. The proposed approaches, firstly described and then summarized in general flowcharts, are based on experimentally corroborated models that allow to carry out the static and seismic condition assessments of the structure.

The following methodologies are defined for both reinforced concrete heritage structures, according to the cases studies reported in Chapter 4, and early post-tensioned systems, according to the main case study application of this research (widely described in Chapter 6).

7.1 Reinforced concrete heritage structures

In this paragraph a methodology for the condition assessment and diagnosis of concrete heritage structures is presented. To this aim, experimentally corroborated models are proposed for both the structural and seismic assessments. This multidisciplinary activity demands that a team who has appropriate technical

knowledge and experience is engaged in all the project phases. Therefore, the collaboration of architects and structural engineers is needed.

Based on the interdisciplinary principle, Macdonald & Arato Gonçalves (Macdonald & Arato Gonçalves, 2020) developed a 5-phase possible methodology to illustrate the entire concrete conservation process, combining best practices in concrete repair and conservation processes (Figure 100).

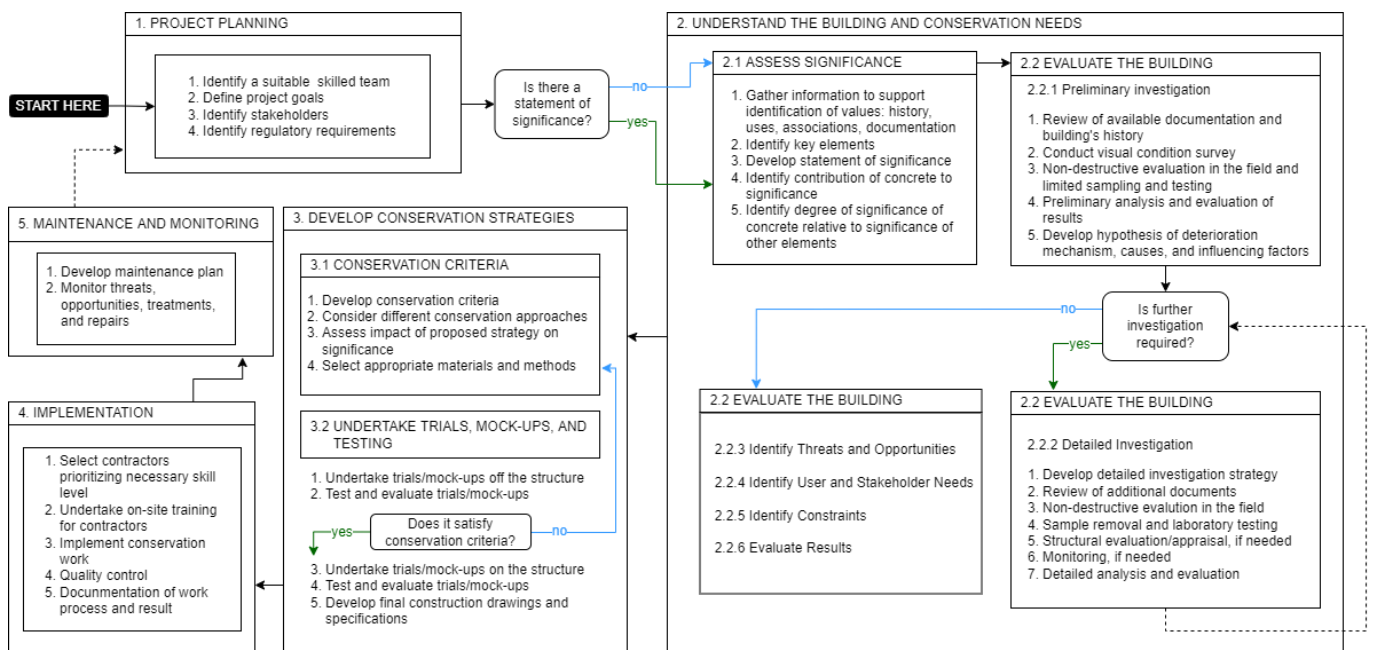


Figure 100: Flowchart illustrating the entire concrete conservation process, combining best practices in concrete repair and conservation processes (Macdonald & Arato Gonçalves, 2020)

This methodology has been developed according to the international documents and guidelines on conservation and protection of modern heritage structures. The approach used to conserve culturally significant concrete shares the same basic methodology with the general repair of concrete. However, historic structures demands additional care to ensure that any work performed retains their cultural significance. Therefore, the impact on significance of any repair work must be carefully considered. As the conservation of concrete draws on knowledge from both the concrete repair and conservation fields, this logical approach proposes basic principles based on current best practices from both of these area (repair standards and international conservation principles), to guide concrete conservation practice and improve outcomes for concrete heritage around the world.

The principles outlined by Macdonald & Arato Gonçalves are intended to provide a logical approach to concrete conservation, guiding practitioners through the typical conservation methodology, from investigation to the development of conservation strategies to implementation and maintenance. It follows the widely accepted step-by-step conservation process of a heritage site, based on the Burra Charter Process (ICOMOS, Australia, 2013) , summarized in the following (Macdonald & Arato Gonçalves, 2020):

Stage 1: Understand the Place

- Gather documentary and physical evidence
- Identify attributes of the site

Stage 2: Assess Significance

- Define the heritage values
- Assess integrity and authenticity
- Compare similar sites
- Develop a statement of significance
- Identify relative levels of significance of attributes

Stage 3: Identify Factors and Issues

- Assess physical condition
- Identify external requirements (regulations/building codes)
- Identify conservation obligations
- Identify vulnerabilities and risks
- Establish owners' and users' needs
- Recognize constraints and opportunities for future use and development
- Identify and engage stakeholders

Stage 4: Develop Policies or Actions to Conserve and Sustain Significance

- Develop overarching policies on use, maintenance and repair, infrastructure treatment of fabric, and implementation
- Devise detailed policies on attributes and their qualities (function, form, fabric, location, and intangible values)
- Develop specific conservation actions

Stage 5: Implement Policies or Actions

- Develop implementation plan including priorities, resources, and timing

- Progressively implement policies/work
- Document implementation

Stage 6: Monitor, Maintain and Review

- Monitor progress
- Review the policies/work

In full consistency with (Macdonald & Arato Gonçalves, 2020) and other international documents and guidelines, a methodological approach that focuses specifically in the condition assessment of concrete structures is summarized in the following. This methodology, describing the aspects of the condition assessment, is to be considered in combination with the process that follows the conservation principles shown in Figure 100.

As reported in Figure 101, the process starts with the project planning phase, which emphasizes the most crucial general areas for the condition assessment of concrete heritage structures. In addition, the understanding of the project goals, which should be refined and agreed early on with the team, should be used to guide the process from its inception. In this phase is also necessary to identify the current codes, safety and accessibility relevant standards.

The second phase of the presented methodology is characterized by preliminary investigations, which consist in reviewing the available documentation, the building's history, including past uses and maintenance executed. After an in-depth analysis of the original documentation and a comparison with the results of the visual inspections and in situ surveys, a crucial point is represented by the identification of the building structural conception. At this stage, preliminary investigation can be used to identify some key structure characteristics. Subsequently, the preliminary structural assessment of the post-tensioned system can be carried out at the design stage with both the standards in force at the construction time and the current standards. For this purpose, as well as to perform a preliminary seismic assessment, a preliminary FE model is usually necessary.

The detailed investigation, based on the results of the preliminary one, is another fundamental step in this methodology for identifying mechanical and/or modal parameters, determining the state of health of the structure, and predicting the response to imposed or seismic actions. In particular, to assess the condition of concrete structures, the proposed experimental activities include both destructive and non-destructive tests such as checks on reinforcement, concrete cover,

mechanical test on concrete and steel, and ambient vibration tests. This strategy should consider some alternative approaches to reduce the engineering context of interest on identifying the variable parameters when not all structural elements can be investigated.

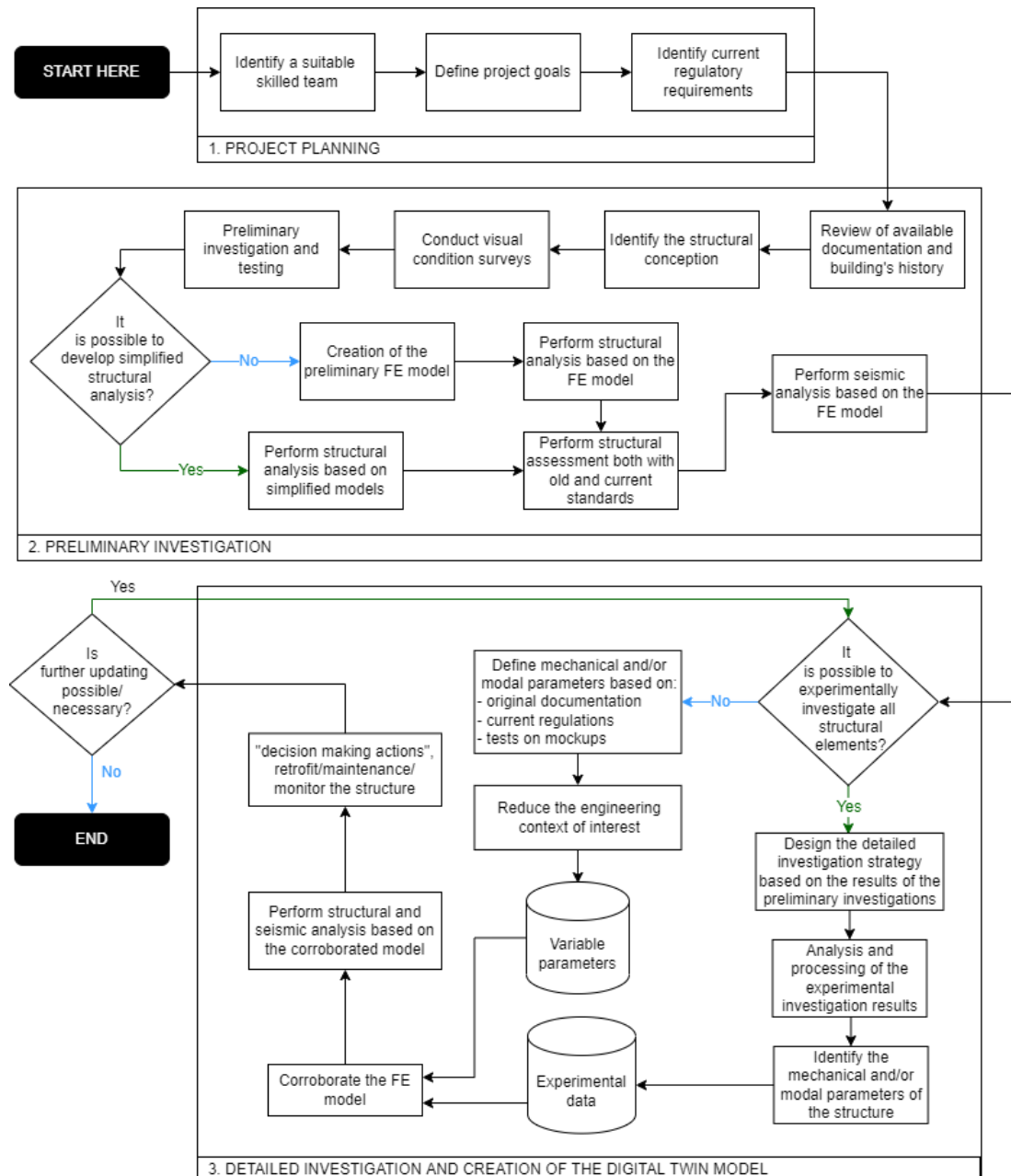


Figure 101: Flowchart illustrating the methodology for the condition assessment of concrete structures

The FE model is finally corroborated with the data acquired and processed from the experimental tests, obtaining a sort of digital twin of the structure where experimental data are released as a part of an updating and condition assessment process. A digital twin has not a unique definition, however it can be defined as a digital replication of a living as well as nonliving physical entity that enable data to be transmitted seamlessly between the physical and the virtual world (El Saddik, 2018). The digital twin is helpful for design, verification, monitoring and life-cycle assessment, in several industrial and scientific sectors. In the context of this PhD research, the digital twin have the great advantage to help the structural and seismic assessment activities. At the end of this process, the updated model offers indications of the effective safety margin evolution of the structure and allows for “a posteriori” evaluations in the Bayesian sense, in order to possibly help “decision-making action” over time. It is highlighted that cost analysis models and estimations are necessary for a good management (Lee, et al., 2019). All the steps described in this process are intended to be carried out in accordance with the regulations and guidelines currently in force, which are mentioned in this thesis.

7.2 Early post-tensioned concrete structures

In this paragraph, following the experience acquired from the case study application, a methodology for the condition assessment and diagnosis of early post-tensioned concrete structures is presented. As mentioned for concrete structures, also for post-tensioned structures:

- experimentally corroborated models are proposed;
- a multidisciplinary team is required.

The methodological approach, describing the aspects of the condition assessment, is in fully constituency and in combination with:

- the conservation principles shown in Figure 100 (Macdonald & Arato Gonçalves, 2020);
- other current international documents and guidelines;
- the approach for the condition assessment of concrete structures shown in Figure 101.

Figure 102 shows the methodology for the condition assessment of early post-tensioned concrete structures.

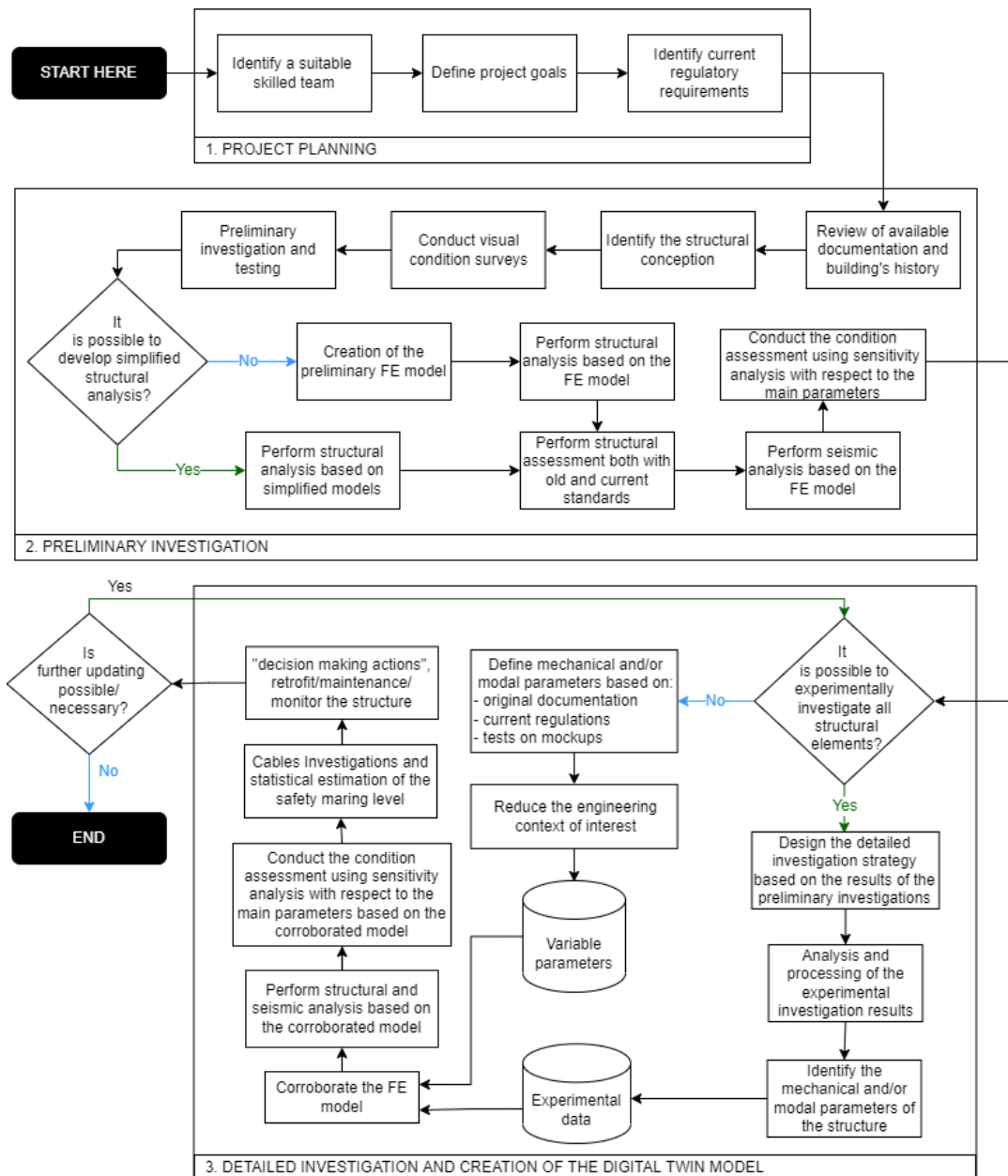


Figure 102: Flowchart illustrating the methodology for the condition assessment of early post-tensioned concrete structures

As can be observed from Figure 102, the process consists of the following phases:

1. Project planning phase: it emphasizes the most crucial general areas for the condition assessment of early post-tensioned concrete heritage structures.

- Identification of a suitable skilled team with appropriate technical knowledge;
 - Definition of project goals (refined and agreed early);
 - Identification of current regulatory requirements (codes, safety and accessibility relevant standards).
2. Preliminary investigation: it allows understanding the building.
- Review of available documentation and building's history (including past uses and maintenance executed);
 - Identification of the structural conception of the building;
 - Conduction of visual condition surveys;
 - Preliminary investigation and testing to identify some key structure characteristics;
 - Performing of structural analysis (based on a preliminary FE model or with a simplified model);
 - Perform structural assessment of the post-tensioned elements at the design stage with both the standards in force at the construction time and the current standards;
 - Conducting of condition assessment of the post-tensioned elements using sensitivity analysis with respect to the main parameters (percentage of corrosion in the wires or error in positioning the tendons);
 - Performing of seismic analysis based on a preliminary FE model.
3. Detailed investigation and creation of the digital twin model.
- Designing the detailed investigation strategy based on the results of the preliminary investigations;
 - Analysis and processing of the experimental investigation results;
 - Identify the mechanical and/or modal parameters of the structure;
 - For the structural that cannot be experimentally investigated, definition of mechanical and/or modal parameters based on original documentation, current regulations and tests on mock-ups, in order to reduce the engineering context of interest;
 - Determining the state of health of the structural elements, by means of both destructive and non-destructive tests (such as checks of ordinary and prestressing steel, concrete cover, the layout of post-tensioning cables, possible grouting defects, mechanical test on concrete, static load and ambient vibration tests);

- Corroboration of the FE model (obtaining a sort of digital twin) using experimental data and variable parameters for a better prediction of the response to imposed or seismic actions;
- Performing structural and seismic analysis based on the corroborated FE model (digital twin)
- Conducting of condition assessment of the post-tensioned elements using sensitivity analysis with respect to the main parameters on the corroborated FE model;
- Evaluate the safety level depending by the state of health of the structural elements;
- Cable investigations and statistical estimation of the safety margin level;
- “Decision making actions”, retrofit/maintenance/monitor the structure supported by the condition assessment with the digital twin;
- If further updating are possible and/or necessary, phase 3 can be repeated.

All the steps described in this process are intended to be carried out in accordance with the regulations and guidelines currently in force, which are mentioned in this thesis.

Conclusions

This thesis has dealt with the extremely topical aspects of the condition assessment of 20th century historic concrete structures. In fact, the main objective of the present research is, more specifically, the definition of methodological approaches for the static and seismic condition assessments, relied on experimentally calibrated models, of reinforced concrete architectural heritage. In particular, non-invasive monitoring techniques are of paramount interest in this context, especially those that exploit the natural vibration of the structure.

The condition assessment of reinforced concrete heritage structures represents a complex challenge also due to the continuous experimentation that has characterized the construction of these buildings, which causes difficulties of reaching out their accurate knowledge. Moreover, a part of this heritage has been built with the post-tensioned concrete technique, which is very sensitive to natural deterioration and excessive environmental attacks. Unfortunately, the partial rupture or corrosion of pre-stressing tendons may be particularly difficult to detect. Despite the increased recognition and the great amount of researches on these topics, the service life prolongation of 20th century historic concrete structures raises several unresolved issues, which require optimal strategies based on a correct maintenance, structural health monitoring and preferably non-destructive techniques to pursue the conservation principles.

Moreover, protection strategies have to take into account national and international principles and guidelines for the analysis, conservation and structural restoration of modern architectural heritage. A multidisciplinary approach and a shared effort between structural engineers and architects are required. This thesis showed the important role of a refined condition assessment, based on SHM and updated FE Models, in the preservation field of 20th century historic concrete structures.

The first part of the thesis introduced the main features of both reinforced concrete heritage and prestressed concrete systems. In addition to the first developments and the rapid spread of these systems, the construction possibilities, the durability problems and diagnostic techniques are reported. The central part

provided an overview of the main issues in the protection and analysis of the reinforced concrete architectural heritage, highlighting the multidisciplinary approach required for its conservation. The most relevant national and international documents are presented and discussed. Moreover, some examples of interdisciplinary approach to concrete heritage structures are reported. As a further step, this central part contains also a critical review of structural and seismic safety evaluations methods applied to modern architectural heritage, and the important role of experimentally corroborated models for its structural analysis and preservation. Finally, referring to the condition assessment for the preservation of the post-tensioned Pavilion V of Turin Exhibition Center, the case study application for this research is reported in order to show and validated the proposed approaches, which are summarized at the end of the last part.

Accordingly, for the Pavilion V an extensive investigation campaign was carried out to evaluate the health condition of the building. A model updating, considering static, mechanical and dynamic data from experimental campaign, is conducted on the numerical model of Pavilion V. Such a model is consequently used for the static and seismic condition assessment of the structure in order to help in identifying the appropriate strategies for lifetime extension of such post-tensioned concrete masterwork of one pioneering engineer of the 20th century. In the determination of modal parameters, particular attention was paid to the role of structural joints. The presence of joints introduced complexity in the modal response and high sensitivity of the stiffness parameters, as usually happens for the dynamics of many civil engineering structures with interacting bodies (e.g., multi-span bridges). This complexity also affects the design of the experimental setups. Consequently, some simplified models can be considered to aid in the modal identification process, which can become a difficult task, even if conducted in the linear field. A further problem in the operational modal analysis of the case study structure is related to its underground configuration and the presence of important slab spans, producing vertical modes relatively more amplified than horizontal ones.

Within the future research steps, the stiffness of the joints active in the non-linear field could be considered, giving rise to a more complex behavior of the case study. Non-linear behavior could be effectively possible in the presence of a strong excitation (e.g., seismic action).

The post-tensioned system is known to be very sensitive to corrosion phenomena and requires in-depth assessments to appropriately evaluate the safety

levels. In fact, although the particular structural conception of Pavilion V, with the intertwining of the ribs makes it robust with respect to local weakening, progressive corrosion and defects in post-tensioning wires are confirmed to be one of the main issues to be addressed for the preservation and reuse of this type of structure. In this context, sensitivity analyses can be a useful tool to evaluate the decreases in safety margin level due to the corrosion increase. Possible strategies for an appropriate conservation could be based on more extensive cables investigations in order to probabilistically update the safety levels with more reliability in the Bayesian sense. If safety levels are found to be insufficient, external structures with upper hanging systems for the roof of the Pavilion could be designed and built for a life extension of the building.

Regarding the dynamic response, the critical elements (shorter and longer strut beams) and the presence of effective joints constitute important factors of vulnerability for Pavilion V. In particular, any retrofitting interventions must consider that the seismic action is mainly entrusted to the shorter strut beams, which were not designed to withstand important horizontal shear actions, with the aggravating circumstance that many of these short elements are in an advanced degradation state. Retrofit strategies for the life prolongation of the building could be based on the preliminary repair and the consequent application of FRP composites as local interventions on the critical elements. Moreover, in a retrofitting project, the joints should be redesigned to guarantee an integral diaphragmatic behavior, for example by means of shock transmission devices, and to regularize the global longitudinal and transvers behavior of the roof.

The proposed methodological approach for the condition assessment of reinforced concrete architectural heritage is based on three main phases: i) the project planning; ii) the preliminary investigation; iii) the detailed investigation and creation of the digital twin model. The common purpose of the phases of this approach is to increase the level of knowledge of these structures from different point of view, in order to accomplish an appropriate condition assessment. In fact, the condition assessment plays a key role in the conservation of a modern heritage building, helping “decision-making action” over time. Certainly, this approach is not simple for practical use and quite time consuming also because implies the creation of a sophisticated model and a significant number of experimental tests. On the other hand, compared to other existing methodologies, this approach has the advantage of taking into account the complexity of the structures under investigation, following the conservation principles and the regulations prescriptions currently in force.

References

- Abbas, N., Calderini, C., Cattari, S., Lagomarsino, S., Rossi, M., Corradini, R., . . . Piovanello, V. (2010). Classification of the cultural heritage assets, description of the target performances and identification of damage measures. *Deliverable D4, WP No1, PERPETUATE Project (FP7), European Research Project on the Seismic Protection of Cultural Heritage*.
- ACI. (2014). Report on Corrosion of Prestressing Steels. *ACI Committee 222 Protection of Metals in Concrete against Corrosion*.
- Aktan, A. E., Lee, K. L., Chuntavan, C., & Aksel, T. (1994). Modal testing for structural identification and condition assessment of constructed facilities. *Proceedings-spie the International Society for Optical Engineering*, (p. 462-468).
- Allemang, R. J. (2003). The modal assurance criterion—twenty years of use and abuse. *Sound and vibration*, 37(8), pages 14-23.
- ANSYS.Inc. (2013). *ANSYS Mechanical APDL. Theory reference. Release15*.
- Appalla, A., ElBatanouny, M. K., Velez, W., & Ziehl, P. (2016). Assessing corrosion damage in posttensioned concrete structures using acoustic emission. *Journal of Materials in Civil Engineering*, 28(2), 04015128.
- Baldwin, R., & North, M. A. (1973). A stress-strain relationship for concrete at high temperatures. *Magazine of concrete research*, 25(85), pages 208-212.
- Bartoli, I., Salamone, S., Phillips, R., Lanza di Scalea, F., & Sikorsky, C. S. (2011). Use of interwire ultrasonic leakage to quantify loss of prestress in multiwire tendons. *Journal of Engineering Mechanics*, 137(5), pages 324-333.
- Beckmann, P., & Bowles, R. (2004). *Structural aspects of building conservation*. 2nd Edition, Oxford Elsevier.
- Berman, A., & Nagy, E. J. (1983). Improvement of a large analytical model using test data. *AIAA journal*, 21(8), pages 1168-1173.

- Bertolini, L., Elsener, B., Pedferri, P., Redaelli, E., & Polder, R. B. (2013). *Corrosion of steel in concrete: prevention, diagnosis, repair*. John Wiley & Sons.
- Blockley, D. I. (1992). *Engineering safety*. McGraw-Hill.
- Boaga, G. (1984). *Riccardo Morandi*. Bologna: Zanichelli.
- Boaga, G., & Boni, B. (1962). *Riccardo Morandi*. Milano: Edizioni di Comunità.
- Bonadè Bottino, V., & Morandi, R. (1959). Sistemazione area del galoppatoio a Torino. Roma: Studio Tecnico Riccardo Morandi.
- Botte, W., Vereecken, E., Taerwe, L., & Caspeele, R. (2021). Assessment of posttensioned concrete beams from the 1940s: Large-scale load testing, numerical analysis and Bayesian assessment of prestressing losses. *Structural Concrete*, 22, 1500-1522.
- Breysse, D. (2012). *Non-destructive assessment of concrete structures: Reliability and limits of single*. Springer Science & Business Media, (Ed.) 2012.
- Bruno, E. (2013). Riccardo Morandi per il Vpadiglione di Torino Esposizioni. *Olmo C., Pogacnik M., Sorace S., La concezione strutturale: Architettura e Ingegneria in Italia negli anni 50 e 60*, Umberto Allemandi & C., Torino, p. 229-240.
- Bunton, D. (2002). Generic moves in PhD thesis introductions. In J. Flowerdew, *Academic discourse* (p. 57-75). London: Pearson Education Limited.
- Capozucca, R. (2008). Detection of damage due to corrosion in prestressed RC beams by static and dynamic tests. *Construction and Building Materials*, 22(5), pages 738-746.
- Carbonara, G. (1996). *Trattato di restauro architettonico*. Utet, Torino.
- Casciati, F., & Roberts, B. (1996). *Mathematical models for structural reliability analysis*. CRC Press.
- Cassinello, P., Schlaich, M., & Torroja, J. A. (2010). *Félix Candela. En memoria (1910-1997). Del cascarón de hormigón a las estructuras ligeras del s. XXI*. Informes de la Construcción, Vol 62, No 519, p. 5-26.

- Cecchi, R., Calvi, M., & Lagormarsino, S. (2006). *Guidelines for the evaluation and reduction of seismic risk of cultural heritage with reference to the Technical Code for Constructions; (in Italian)*.
- CEN, EUROCODE 2. (2004). *Design of concrete structures*. European Standard EN, 2004.
- CEN, EUROCODE 8. (2005). *Design Provisions for Earthquake Resistance of Structures*. European Standard EN, 2005.
- Ceravolo, R. (2020). Condition assessment, monitoring and preservation of some iconic concrete structures of the 20th century. *(Keynote lecture) IABSE SYMPOSIUM Wroclaw 2020 - Synergy of Culture and Civil Engineering – History and Challenges*, (p. 58-82). Wroclaw, Poland.
- Ceravolo, R., & Abbiati, G. (2013). Time domain identification of structures: comparative analysis of output-only methods. *Journal of Engineering Mechanics*, 139(4), 537-544.
- Ceravolo, R., & Lenticchia, E. (2019). Diagnosis and preservation of 20th Century architectural Heritage: from the first thin shell solutions to the iconic structures built by Pier Luigi Nervi and Riccardo Morandi in Turin. *(Keynote lecture) 7th Structural Engineers World Congress*, (p. 165-179). Istanbul, Turkey.
- Ceravolo, R., Coletta, G., Lenticchia, E., Li, L., Quattrone, A., & Rollo, S. (2019). In-Operation Experimental Modal Analysis of a Three Span Open-Spandrel RC Arch Bridge. *International Conference on Arch Bridge* (p. 491-499). Springer, Cham.
- Ceravolo, R., Coletta, G., Lenticchia, E., Minervini, D., & Quattrone, A. (2020). Dynamic investigation on the health state and seismic vulnerability of Morandi's Pavilion V of Turin Exhibition Center. *Proceedings of the IABSE Symposium on Synergy of Culture and Civil Engineering - History and Challenges*. Wroclaw, Poland.
- Ceravolo, R., De Lucia, G., Lenticchia, E., & Miraglia, G. (2019). *Seismic Structural Monitoring of Cultural Heritage Structures*. Springer, 2019, p. 51-85.

- Ceravolo, R., De Lucia, G., Miraglia, G., & Pecorelli, M. L. (2020). Thermoelastic finite element model updating with application to monumental buildings. *Computer-Aided Civil and Infrastructure Engineering*, 35(6), 628-642.
- Ceravolo, R., Lenticchia, E., Miraglia, G., Oliva, V., & Scussolini, L. (2022). Modal Identification of Structures with Interacting Diaphragms. *Applied Sciences*, 12(8), 4030.
- Ceravolo, R., Pistone, G., Zanotti Fragonara, L., Massetto, S., & Abbiati, G. (2016). Vibration-based monitoring and diagnosis of cultural heritage: a methodological discussion in three examples. *International Journal of Architectural Heritage*, 10(4), pages 375-395.
- Cestari, C. B., Chiabrando, F., Invernizzi, S., Marzi, T., & Spanò, A. (2014). The thin concrete vault of the Paraboloid of Casale, Italy. Innovative methodologies for the survey, structural assessment and conservation interventions. *Structural Faults & Repair*. London, UK, 8-10.
- Chilton, J., & Isler, H. (2000). *Heinz Isler: the engineer's contribution to contemporary architecture*. Thomas Telford.
- Coppola, L. (2015). *Il restauro dell'architettura moderna in cemento armato*. HOEPLI EDITORE.
- Cornell, C. A. (1967). Bounds on the reliability of structural systems. *Journal of the Structural Division*, 93(1), pages 171-200.
- Cornell, C. A. (1969). A probability-based structural code. *Journal Proceedings*, 66(12), pages 974-985.
- Croft, C., & Macdonald, S. (2019). *Concrete: Case studies in conservation practice*. (Vol. 1). Getty Publications.
- Custance-Baker, A., & Macdonald, S. (2015). *Conserving Concrete Heritage Experts Meeting. The Getty Center, Los Angeles, California, June 9-11, 2014*. Los Angeles: The Getty Conservation Institute.
- Decreto Ministero per i lavori pubblici, 3 marzo 1975. (1975). *Disposizioni concernenti l'applicazione delle norme tecniche per le costruzioni in zone sismiche*. (in Italian).

- Ditlevsen, O., & Madsen, H. O. (1996). *Structural reliability methods*. New York: Wiley.
- El Saddik, A. (2018). Digital twins: The convergence of multimedia technologies. *IEEE multimedia*, 25(2), 87-92.
- Elefante, L. (2009). *Dealing with Uncertainties in the Assessment of Existing RC Buildings*. Doctoral dissertation, Università di Napoli Federico II.
- Farrar, C., & Worden, K. (2007). An introduction to Structural Health Monitoring. *Philosophical Transactions of the Royal Society A: Mathematical, Physical and Engineering Sciences*, 365.1851 (2007), pages 303-315.
- fib. (2010). Model Code for Concrete Structures. fib 2013. Lausanne.
- Friswell, M. I., Mottershead, J. E., & Ahmadian, H. (2001). Finite–element model updating using experimental test data: parametrization and regularization. *Philosophical Transactions of the Royal Society of London. Series A: Mathematical, Physical and Engineering Sciences*, 359(1778), pages 169-186.
- Gazzetta Ufficiale del Regno d'Italia. (1939). RDL n.2229/1939, Norme per l'esecuzione delle opere in conglomerato cementizio semplice od armato.
- Ghorbanpoor, A., Borchelt, R., Edwards, M., & Salam, E. A. (2000). Magnetic-Based NDE of Prestressed and Post-Tensioned Concrete Members: The MFL System.
- Gibson, E. J. (1982). *Working with the Performance Approach in Building*. Rotterdam CIB Report, Publication 64.
- Gilbert, R. I., Mickleborough, N. C., & Ranzi, G. (2017). *Design of prestressed concrete to Eurocode 2*. CRC Press.
- Giovannardi, F. (2008). Eugène Freyssinet, oltre il limite del cemento armato.
- Guidi, C. C. (1987). *Cemento armato precompresso*.
- ICOMOS, Australia. (2013). *The Burra Charter: The Australia ICOMOS charter for places of cultural significance*. Burra: ICOMOS.

- ICOMOS, International Committee on Twentieth Century Heritage. (2017). *Approaches to the conservation of twentieth century cultural heritage—Madrid-New Delhi Document*.
- ICOMOS, ISCARSAH Committee. (2003). ICOMOS Charter—Principles for the analysis, conservation and structural restoration of architectural heritage. *Proceedings of the ICOMOS 14th General Assembly and Scientific Symposium*. Victoria Falls, Zimbabwe (Vol. 2731).
- Ingold, L., & Erb, T. (2018). *Riccardo Morandi: formes sous contraintes*. Tracés 23-24/2018: 18-25.
- Invernizzi, S., Spanò, A., & Chiabrando, F. (2019). Survey, assessment and conservation of post-industrial cultural heritage: the case of the thin concrete vault in Casale, Italy. *Structural Analysis of Historical Constructions*, (p. 1401-1409).
- Iori, T. (2001). *Il cemento armato in Italia: dalle origini alla seconda guerra mondiale*. Rome: Edilstampa.
- Iori, T. (2003). Prestressed concrete: first developments in Italy. *Proceedings of the First International Congress on Construction History*. Vol. 20, Madrid.
- IRCC. (2008). *Architectural Heritage and Performance-Based Building Codes: Approaches and Experiences*. Madrid Report of the IRCC Workshop of 13 November 2008.
- Jeyasehar, C. A., & Sumangala, K. (2006). Damage assessment of prestressed concrete beams using artificial neural network (ANN) approach. *Computers & structures*, 84(26-27), pages 1709-1718.
- Joint Committee on Structural Safety. (2001). Probabilistic assessment of existing structures, RILEM Publ.
- Jones, B. E. (1920). *Cassell's Reinforced Concrete*. The Waverley Book Company, Ltd, London.
- Kim, J. T., Ryu, Y. S., Cho, H. M., & Stubbs, N. (2003). Damage identification in beam-type structures: frequency-based method vs mode-shape-based method. *Engineering structures*, 25(1), pages 57-67.

- Kotnik, T., & Schwartz, J. (2011). The architecture of heinz isler. *Journal of the international association for shell and spatial structures*, 52(3), pages 185-190.
- Kwan, B. S. (2009). Reading in preparation for writing a PhD thesis: Case studies of experiences. *Journal of English for Academic Purposes*, pages 180-191.
- Laboratorio di Dinamica e Sismica. (2019). *Relazione sulle prove di caratterizzazione dinamica del Padiglione Morandi di Torino Esposizioni*. Politecnico di Torino, Torino.
- Lagomarsino, S., Cattari, S., & Calderini, C. (2012). DELIVERABLE D41 European Guidelines for the seismic preservation of cultural heritage assets. *PERPETUATE PERFORMANCE-BASED APPROACH TO EARTHQUAKE PROTECTION OF CULTURAL HERITAGE IN EUROPEAN AND MEDITERRANEAN COUNTRIES*.
- Lagomarsino, S., Modaresi, H., Pitilakis, K., Bosiljkov, V., Calderini, C., D'ayala, D., . . . Cattari, S. (2010). PERPETUATE Project: The proposal of a performance-based approach to earthquake protection of cultural heritage. *Advanced Materials Research*, 133, 1119–1124, 1119-1124. Tratto da <https://doi.org/10.4028/www.scientific.net/AMR.133-134.1119>
- Lee, J. H., Choi, Y., Ann, H., Jin, S. Y., Lee, S. J., & Kong, J. S. (2019). Maintenance Cost Estimation in PSCI Girder Bridges Using Updating Probabilistic Deterioration Model. *Sustainability*, 11(23), 6593.
- Legge n. 64, 2 febbraio 1974. (1974). *Provvedimenti per le costruzioni con particolari prescrizioni per le zone sismiche*. (in Italian).
- Lenticchia, E. (2017). *Vibration-based monitoring of complex architectural heritage buildings*. Doctoral dissertation, Politecnico di Torino.
- Lenticchia, E., Ceravolo, R., & Chiorino, C. (2017). Damage scenario-driven strategies for the seismic monitoring of XX century spatial structures with application to Pier Luigi Nervi's Turin Exhibition Centre. *Engineering Structures*, 137, pages 256-67.
- Lenticchia, E., Miraglia, G., Quattrone, A., & Ceravolo, R. (2021). Condition Assessment of an Early Thin Reinforced Concrete Vaulted System. *International Journal of Architectural Heritage*, 1-19.

- Leonhardt, F. (1980). *CA & CAP Calcolo di progetto e tecniche costruttive (Volume 5 - Il precompresso)*. Edizioni Tecniche.
- Levi, F., & Chiorino, M. A. (2004). Concrete in Italy. A review of a century of concrete progress in Italy, Part 1: Technique and architecture. *ACI Concrete Int.*, 26(9), pages 55-61.
- Limongelli, M. P., Siegert, D., Merliot, E., Waeytens, J., Bourquin, F., Vidal, R., & Cottineau, L. M. (2016). Damage detection in a post tensioned concrete beam-Experimental investigation. *Engineering Structures*, 128, pages 15-25.
- Lorenzoni, F. (2013). Integrated methodologies based on structural health monitoring for the protection of cultural heritage buildings. Università degli Studi di Trento, PhD Thesis.
- Maas, S., Zürbes, A., Waldmann, D., Waltering, M., Bungard, V., & De Roeck, G. (2012). Damage assessment of concrete structures through dynamic testing methods. Part 1–Laboratory tests. *Engineering Structures*, 34, pages 351-362.
- Macdonald, S., & Arato Gonçalves, A. P. (2020). *Conservation Principles for Concrete of Cultural Significance*. Los Angeles: Getty Conservation Institute.
- Macdonald, S., & Ostergren, G. (2011). *Developing an Historic Thematic Framework to Assess the Significance of Twentieth-century Cultural Heritage*. Los Angeles: Getty Conservation Institute.
- Marrey, B., & Grote, J. (2003). The story of prestressed concrete from 1930 to 1945: A step towards the European Union. *Proceedings of the First International Congress on Construction History*. Madrid.
- MASTRLAB DISEG. (2019). *Prove di caratterizzazione meccanica dei materiali e prove di carico sulla struttura di copertura del Padiglione V Torino Esposizioni*. Politecnico di Torino, Torino.
- Merce, R. N., Doz, G. N., de Brito, J. L., Macdonald, J., & Friswell, M. I. (2007). Finite element model updating of a suspension bridge using ansys software.

Proceedings of the Inverse Problems, Design and Optimization Symposium, (p. 16-18). Miami, FL, USA.

- Ministero delle infrastrutture e dei trasporti. (2005). *Norme Tecniche per le costruzioni*. (in Italian). DECRETO 14 Settembre 2005. Approvazione Delle Norme Tecniche per Le Costruzioni.
- Ministero delle infrastrutture e dei trasporti. (2008). *Norme Tecniche per le Costruzioni*. (in Italian). DECRETO 14 Gennaio 2008. Approvazione Delle Nuove Norme Tecniche per Le Costruzioni.
- Ministero delle Infrastrutture e dei Trasporti. (2018). *Aggiornamento delle Norme tecniche per le costruzioni*. (in Italian). DECRETO 17 Gennaio 2018. Aggiornamento Delle «Norme Tecniche per Le Costruzioni».
- Ministero delle Infrastrutture e dei Trasporti. (2019). *Istruzioni per l'applicazione dell'«Aggiornamento delle “Norme tecniche per le costruzioni”»*. CIRCOLARE 21 Gennaio 2019, n. 7 C.S.LL.PP. Istruzioni per l'applicazione Dell'«Aggiornamento Delle “Norme Tecniche per Le Costruzioni”» Di Cui Al Decreto Ministeriale 17 Gennaio 2018.
- Ministero delle Infrastrutture e dei Trasporti, Consiglio Superiore dei Lavori Pubblici. (2020). *Linee guida per la classificazione e gestione del rischio, la valutazione della sicurezza ed il monitoraggio dei ponti esistenti*. Roma, Italy.
- Miraglia, G. (2019). *Hybrid simulation techniques in the structural analysis and testing of architectural heritage*. Doctoral dissertation, Politecnico di Torino.
- Modica, M., & Santarella, F. (2015). *Paraboloidi: un patrimonio dimenticato dell'architettura moderna*. EDIFIR, *Collana Spazi di Architettura*.
- Moller, P. W., & Friberg, O. (1998). Updating large finite element models in structural dynamics. *AIAA journal*, 36(10), pages 18681-1868.
- Morandi, R. (1959). *Sistemazione area del Galoppatoio in Torino*. Calcoli di stabilità. Roma, 2 Aprile 1959. Archivio Maire Tecnimont, Torino.
- Moustafa, A., Niri, E. D., Farhidzadeh, A., & Salamone, S. (2014). Corrosion monitoring of post-tensioned concrete structures using fractal analysis of

guided ultrasonic waves. *Structural Control and Health Monitoring*, 21(3), pages 438-448.

- Muttoni, A. (2014). Some innovative prestressed concrete structures in Switzerland. (*Keynote lecture*) 23rd Symposium on Developments in Prestressed Concrete, Japan Prestressed Concrete Institute. Morioka, Japan.
- Normandin, K. C., & Macdonald, S. (2013). *A Colloquium to Advance the Practice of Conserving Modern Heritage: the Getty Center, Los Angeles, California, March 6-7, 2013*. Los Angeles: Getty Conservation Institute.
- Ordinanza del Presidente del Consiglio dei Ministri n. 3431. (2005). *Ulteriori modifiche ed integrazioni all'ordinanza del Presidente del Consiglio dei Ministri n. 3274 del 20 marzo 2003*. Gazzetta Ufficiale della Repubblica Italiana n. 107 del 10-5-2005 (Suppl. Ordinario n.85). (in Italian).
- Pachón, P., Infantes, M., Cámara, M., Compán, V., García-Macias, E., Friswell, M. I., & Castro-Triguero, R. (2020). Evaluation of optimal sensor placement algorithms for the Structural Health Monitoring of architectural heritage. Application to the Monastery of San Jerónimo de Buenavista (Seville, Spain). *Engineering Structures*, 202, 109843.
- Pecorelli, M. L., Ceravolo, R., & Epicoco, R. (2018). An automatic modal identification procedure for the permanent dynamic monitoring of the sanctuary of Vicoforte. *International Journal of Architectural Heritage*.
- Peeters, B., & De Roeck, G. (2001). One-year monitoring of the Z24-Bridge: environmental effects versus damage events. *Earthquake engineering & structural dynamics*, 30(2), pages 149-171.
- Prudon, T. H. (2008). *Preservation of modern architecture*. Hoboken, NJ: John Wiley & Sons, Inc.
- Recommendations PCM. (2011). *Assessment and mitigation of seismic risk of cultural heritage with reference to the Italian Building Code (NTC2008)*. Directive of the Prime Minister, 9/02/2011. G.U. no. 47, 26/02/2011 (suppl. ord. no. 54) (in Italian).

- Ruocci, G. (2010). *Application of the SHM methodologies to the protection of masonry arch bridges from scour*. Doctoral dissertation, Politecnico di Torino.
- Salawu, O. S. (1997). Detection of structural damage through changes in frequency: a review. *Engineering structures*, 19(9), pages 718-723.
- Santarella, L. (1926). *Il cemento armato nelle costruzioni civili ed industriali*. Hoepli.
- Shull, P. J. (2002). *Nondestructive evaluation: theory, techniques, and applications*. CRC press.
- Sobester, A., Forrester, A., & Keane, A. (2008). *Engineering design via surrogate modelling: a practical guide*. John Wiley & Sons.
- Theryo, T. S., Hartt, W. H., & Paczkowski, P. (2013). *Guidelines for Sampling, Assessing, and Restoring Defective Grout in Prestressed Concrete Bridge Post-Tensioning Ducts*. (No. FHWA-HRT-13-028).
- Van Overschee, P., & De Moor, B. L. (2012). *Subspace identification for linear systems: Theory-Implementation-Applications*. Springer Science & Business Media.
- Wen, Y. K., Ellingwood, B. R., Veneziano, D., & Bracci, J. (2003). *Uncertainty modeling in earthquake engineering*.
- Xia, Y., Hao, H., Zanardo, G., & Deeks, A. (2006). Long term vibration monitoring of an RC slab: temperature and humidity effect. *Engineering structures*, 28(3), pages 441-452.
- Zanotti Fragonara, L. (2012). *Dynamic models for ancient heritage structures*. Doctoral dissertation, Politecnico di Torino.
- Zhou, X. Q., & Huang, W. (2013). Vibration-based structural damage detection under varying temperature conditions. *International Journal of Structural Stability and Dynamics*, 13(05), 1250082.